Fall 12-31-2018

Wireless coverage using unmanned aerial vehicles

Hazim Shakhatreh
New Jersey Institute of Technology

Copyright Warning & Restrictions

The copyright law of the United States (Title 17, United States Code) governs the making of photocopies or other reproductions of copyrighted material.

Under certain conditions specified in the law, libraries and archives are authorized to furnish a photocopy or other reproduction. One of these specified conditions is that the photocopy or reproduction is not to be "used for any purpose other than private study, scholarship, or research." If a, user makes a request for, or later uses, a photocopy or reproduction for purposes in excess of "fair use" that user may be liable for copyright infringement,

This institution reserves the right to refuse to accept a copying order if, in its judgment, fulfillment of the order would involve violation of copyright law.

Please Note: The author retains the copyright while the New Jersey Institute of Technology reserves the right to distribute this thesis or dissertation

Printing note: If you do not wish to print this page, then select "Pages from: first page # to: last page #" on the print dialog screen

ABSTRACT

WIRELESS COVERAGE USING UNMANNED AERIAL VEHICLES

by
Hazim Shakhatreh

The use of unmanned aerial vehicles (UAVs) is growing rapidly across many civilian application domains including real-time monitoring, search and rescue, and wireless coverage. UAVs can be used to provide wireless coverage during emergency cases where each UAV serves as an aerial wireless base station when the cellular network goes down. They can also be used to supplement the ground base station in order to provide better coverage and higher data rates for the users. During such situations, the UAVs need to return periodically to a charging station for recharging, due to their limited battery capacity. Given the recharging requirements, the problem of minimizing the number of UAVs required for a continuous coverage of a given area is first studied in this dissertation. Due to the intractability of the problem, partitioning the coverage graph into cycles that start at the charging station is proposed and the minimum number of UAVs to cover such a cycle is characterized based on the charging time, the traveling time and the number of subareas to be covered by a cycle. Based on this analysis, an efficient algorithm is proposed to solve the problem.

In the second part of this dissertation, the problem of optimal placement of a single UAV is studied, where the objective is to minimize the total transmit power required to provide wireless coverage for indoor users. Three cases of practical interest are considered and efficient solutions to the formulated problem under these cases are presented. Due to the limited transmit power of a UAV, the problem of minimizing the number of UAVs

required to provide wireless coverage to indoor users is studied and an efficient algorithm is proposed to solve the problem.

In the third part of this dissertation, the problem of maximizing the indoor wireless coverage using UAVs equipped with directional antennas is studied. The case that the UAVs are using one channel is considered, thus in order to maximize the total indoor wireless coverage, the overlapping in their coverage volumes is avoided. Two methods are presented to place the UAVs; providing wireless coverage from one building side and from two building sides. The results show that the upside-down arrangements of UAVs can improve the total coverage by 100% compared to providing wireless coverage from one building side.

In the fourth part of this dissertation, the placement problem of UAVs is studied, where the objective is to determine the locations of a set of UAVs that maximize the lifetime of wireless devices. Due to the intractability of the problem, the number of UAVs is restricted to be one. Under this special case, the problem is formulated as a convex optimization problem under a restriction on the coverage angle of the ground users and a gradient projection based algorithm is proposed to find the optimal location of the UAV. Based on this, an efficient algorithm is proposed for the general case of multiple UAVs. The problem of minimizing the number of UAVs required to serve the ground users such that the time duration of uplink transmission of each wireless device is greater than or equal to a threshold value is also studied. Two efficient methods are proposed to determine the minimum number of UAVs required to serve the wireless devices.

WIRELESS COVERAGE USING UNMANNED AERIAL VEHICLES

by
Hazim Shakhatreh

A Dissertation
Submitted to the Faculty of
New Jersey Institute of Technology
in Partial Fulfillment of the Requirements for the Degree of
Doctor of Philosophy in Electrical Engineering

Helen and John C. Hartmann Department of
Electrical and Computer Engineering

December 2018

APPROVAL PAGE

WIRELESS COVERAGE USING UNMANNED AERIAL VEHICLES

Hazim Shakhatreh

Dr. Abdallah Khreishah, Dissertation Advisor — Date
Associate Professor of Electrical and Computer Engineering, NJIT

Dr. Nirwan Ansari, Committee Member — Date
Distinguished Professor of Electrical and Computer Engineering, NJIT

Dr. Sui-Hoi Edwin Hou, Committee Member — Date
Professor of Electrical and Computer Engineering, NJIT

Dr. Roberto Rojas-Cessa, Committee Member — Date
Professor of Electrical and Computer Engineering, NJIT

Dr. Guiling Wang, Committee Member — Date
Professor of Computer Science, NJIT

BIOGRAPHICAL SKETCH

Author: Hazim Shakhatreh

Degree: Doctor of Philosophy

Date: December 2018

Undergraduate and Graduate Education:

- Doctor of Philosophy in Electrical Engineering,
  New Jersey Institute of Technology, Newark, NJ, 2018
- Master of Science in Wireless Communications Engineering,
  Yarmouk University, Irbid, Jordan, 2012
- Bachelor of Science in Telecommunications Engineering,
  Yarmouk University, Irbid, Jordan, 2008

Major: Electrical Engineering

Presentations and Publications:

H. Shakhatreh, A. Khreishah and I. Khalil, "Indoor Mobile Coverage Problem Using UAVs," *IEEE Systems Journal*, DOI: 10.1109/JSYST.2018.2824802, 2018.

H. Shakhatreh and A. Khreishah, "Optimal Placement of a UAV to Maximize the Lifetime of Wireless Devices," *IEEE International Wireless Communications and Mobile Computing Conference (IWCMC)*, Limassol, Cyprus, 2018.

H. Shakhatreh, A. Khreishah, N. Othman and A. Sawalmeh, "Maximizing Indoor Wireless Coverage Using UAVs Equipped with Directional Antennas," *IEEE Malaysia International Conference on Communications (MICC)*, Johor Bahru, Malaysia, 2017.

A. Sawalmeh, N. Othman, H. Shakhatreh and A. Khreishah, "Providing Wireless Coverage in Massively Crowded Events Using UAVs," *IEEE Malaysia International Conference on Communications (MICC)*, Johor Bahru, Malaysia, 2017.

H. Shakhatreh, A. Khreishah and B. Ji, "Providing Wireless Coverage to High-rise Buildings Using UAVs," *IEEE International Conference on Communications (ICC)*, Paris, France, 2017.

H. Shakhatreh, A. Khreishah, A. Alsarhan, I. Khalil, A. Sawalmeh and N. Othman, "Efficient 3D Placement of a UAV Using Particle Swarm Optimization," *IEEE International Conference on Information and Communication Systems (ICICS)*, Irbid, Jordan, 2017.

H. Shakhatreh, A. Khreishah, J. Chakareski, H. Bany Salameh and I. Khalil, "On the Continuous Coverage Problem for a Swarm of UAVs," *IEEE Sarnoff Symposium*, Newark, NJ, 2016.

To my parents, Mohammad and Mai; my siblings, Aya, Abdallah and Youmna; my aunt, Maqbouleh; my wife, Dina; and my son, Saif-Aldeen who always believed in me, encouraged me, and supported me through everything.

ACKNOWLEDGMENT

First of all, I thank Allah for all his blessings. I thank Allah for the gift of patience He gave me to do this research, and I thank Him for the opportunity to meet all kinds of people through the research process.

Second of all, I thank my advisor, Dr. Abdallah Khreishah for his guidance and patience in the last four years. It is been a pleasure working under such a great professor.

I also want to thank Dr. Nirwan Ansari, Dr. Sui-Hoi Edwin Hou, Dr. Roberto Rojas-Cessa and Dr. Guiling Wang for honoring me as members of my dissertation committee. I also thank them for their feedback on this research.

I would also like to thank all the professors who I have collaborated with to realize this research. I would especially like to thank Dr. Issa Khalil, Dr. Bo Ji, Dr. Ala Al-Fuqaha, and Dr. Jacob Chakareski for the useful discussions I had with them. These discussions opened my eyes on some important things both in life and this research.

Finally, I thank my parents, my brother, my sisters, my wife and my son for their support and faith in me. I am thankful for their prayers to Allah to help me throughout this research.

TABLE OF CONTENTS

Chapter **Page**

TABLE OF CONTENTS
(Continued)

Chapter **Page**

LIST OF TABLES

LIST OF FIGURES

Figure **Page**

LIST OF FIGURES
(Continued)

Figure **Page**

LIST OF FIGURES
(Continued)

Figure **Page**

CHAPTER 1

INTRODUCTION

UAVs can be used in many civilian applications due to their ease of deployment, low maintenance cost, high-mobility and ability to hover [2]. Such vehicles are being used for real-time monitoring of road traffic, remote sensing, search and rescue operations, delivery of goods, security and surveillance, precision agriculture, and civil infrastructure inspection. They can also be used as aerial wireless base stations to complement existing cellular network service by providing additional capacity to hotspot areas during special events [3] or to provide wireless coverage when cellular networks are not operational due to natural disasters [4]. Cell on wheels (COWs), is typically used to provide expanded wireless coverage for short-term demands, when cellular coverage is either minimal, never present or compromised by disaster, as shown in Figure 1.1. Compared to the COWs, the advantage of using UAV-based aerial base stations is their ability to quickly and easily move during emergency cases [5]. They can move to 3D efficient placements that optimize several objective functions of interest and update their placements based on users distribution changes. In Puerto Rico, AT&T have deployed LTE-equipped UAVs to provide wireless connectivity to customers who lost service after Hurricane Maria [6], as shown in Figure 1.2. They also look to utilize UAVs to enhance the wireless coverage at big events like music festivals [7].

Figure 1.1 Verizon COW used during the 2018 Spring Creek fire in Huerfano County, Colorado.
Source: [8].

1.1 UAV Classification

The authors in [9] classify the UAVs into four categories based on their altitudes and their wing types, each with its own strengths and weaknesses. The first category is the high altitude platforms (HAPs). HAPs are designed for long-duration flights counted in months at altitudes above 17 km. They are typically utilized to provide wide wireless coverage for remote geographic areas. However, they are costly and their deployment time is significantly long. The second category is the low altitude platforms (LAPs). LAPs are flexible and can fly at altitudes of up to a few kilometers. They are typically utilized to provide wireless coverage during emergency cases or to collect data from ground sensors. On the other hand, they need to return periodically to a charging station for recharging, due to their limited battery capacity. The third category is the fixed-wing UAVs. Fixed-wing UAVs have high speed and more payload, but they need to maintain a continuous forward motion in order to remain aloft, thus are not appropriate for stationary use cases. The fourth category is the rotary-wing UAVs. Rotary-wing UAVs can hover and stay stationary

Figure 1.2 AT&T UAV used after Hurricane Maria in Puerto Rico.
Source: [6].

in the air [10], but they have limited payload. In Table 1.1, we present the types of UAVs and their capabilities.

1.2 UAV Use Cases

The authors in [10–12] present the typical use cases of aerial wireless base stations. Some of the UAV use cases are as follows:

- UAVs to enhance the wireless coverage: UAVs can be utilized to supplement the ground base station in order to provide high probability line of sight channels when the location of user has a high blockage probability or low data rate due the high path loss as shown in Figure 1.3.a.
- UAVs as network gateways: In remote geographic areas or disaster-stricken areas, UAVs can be used as gateway nodes to provide connectivity to backbone networks, communication infrastructure, or the Internet as shown in Figure 1.3.b.
- UAVs as relay nodes: UAVs can be utilized as relay nodes to provide wireless connectivity between two or more distant wireless devices without reliable direct communication links as shown in Figure 1.3.c.
- UAVs for data collection: UAVs can be utilized to gather delay-tolerant information from a large number of distributed wireless devices. An example is to collect data from wireless sensors in precision agriculture applications as shown in Figure 1.3.d.

Table 1.1 UAV Classification

UAV Classification	Altitude	High altitude platform (HAP)	- Long endurance. - Wide coverage. - Altitude above 17 km.
		Low altitude platform (LAP)	- Fast deployment. - High Mobility. - Low cost. - Limited flight time .
	Wing type	Fixed-wing	- High speed. - Cannot hover. - High payload. - Fly for several hours.
		Rotary-wing	- Can hover. - Low speed. - Fly less than one hour.

Source: [9].

1.3 Dissertations Outline

We start by studying the continuous coverage problem in Chapter 3. In the continuous coverage problem, we aim to minimize the number of UAVs required for a continuous coverage of a given area, given the recharging requirements. Due to the intractability of the problem, we study partitioning the coverage graph into cycles that start at the charging station. We first characterize the minimum number of UAVs to cover such a cycle based on the charging time, the traveling time, and the number of subareas to be

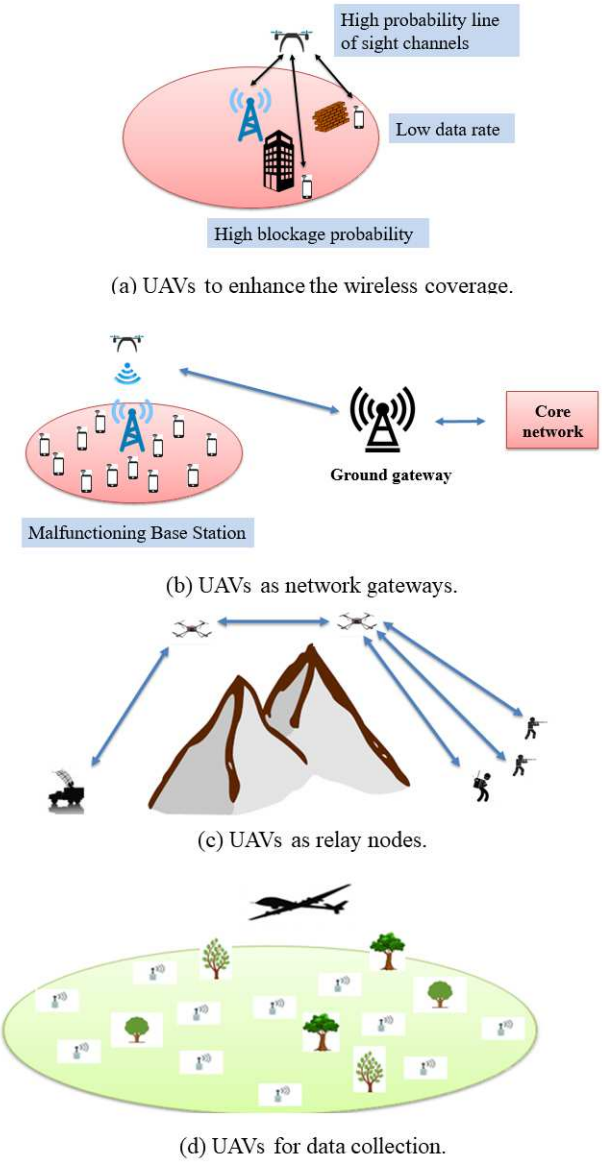

Figure 1.3 Typical use cases of aerial base stations.

covered by the cycle. Based on this analysis, we then develop an efficient algorithm, the cycles with limited energy algorithm. The straightforward method to continuously cover a given area is to split it into N subareas and cover it by N cycles using N additional UAVs. We demonstrate that the cycles with limited energy algorithm requires 69%-94% fewer additional UAVs relative to the straightforward method, as the energy capacity of

the UAVs is increased, and 67%-71% fewer additional UAVs, as the number of subareas is increased.

In Chapter 4, we study the problem of efficient placement of a single UAV, where the objective is to minimize the total transmit power required to cover the indoor users. The formulated problem is generally difficult to solve. To that end, we consider three cases of practical interest and provide efficient solutions to the formulated problem under these cases. Then, we study the problem of minimizing the number of UAVs required to provide wireless coverage to the indoor users and prove that this problem is NP-complete. Due to the intractability of the problem, we use clustering to minimize the number of UAVs required to cover the indoor users. In our proposed algorithm, we check if the maximum transmit power of a UAV is sufficient to cover each cluster. If not, the number of clusters is incremented by one, and the problem is solved again. In the uniform split method, we split the building into k regular structures and utilize k UAVs to provide wireless coverage for indoor users regardless of user distribution. We demonstrate through simulations that the method that splits the building into regular structures requires 80% more number of UAVs relative to our proposed algorithm.

In Chapter 5, we aim to maximize the indoor wireless coverage using UAVs equipped with directional antennas. We study the case that the UAVs are using one channel, thus in order to maximize the total indoor wireless coverage, we avoid any overlapping in their coverage volumes. We present two methods to place the UAVs; providing wireless coverage from one building side and from two building sides. Our results show that the upside-down arrangements of UAVs, can improve the maximum total coverage by 100% compared to providing wireless coverage from one building side

when the UAVs use one channel. In order to provide full wireless coverage, we use UAVs with multiple channels and show that the upside-down arrangements of UAVs required 20%-33% fewer number of UAVs.

In Chapter 6, we formulate the placement problem of UAVs, where the objective is to determine the locations of a set of UAVs that maximize the time duration of uplink transmission until the first wireless device runs out of energy. We prove that this problem is NP-complete. Due to its intractability, we start by restricting the number of UAVs to be one. We show that under this special case the problem can be formulated as a convex optimization problem under a restriction on the coverage angle of the ground users. After that, we propose a gradient projection-based algorithm to find the optimal location of the UAV. Based on this, we then develop an efficient algorithm for the general case of multiple UAVs. The proposed algorithm starts by clustering the wireless devices into several clusters where each cluster being served by one UAV. After it finishes clustering the wireless devices, it applies the gradient projection-based algorithm in each cluster. We also formulate the problem of minimizing the number of UAVs required to serve the ground users such that the time duration of uplink transmission of each wireless device is greater than or equal to a threshold value. We prove that this problem is NP-complete and propose to use two efficient methods to determine the minimum number of UAVs required to serve the wireless devices.

The dissertation is finally concluded in Chapter 7.

CHAPTER 2

RELATED WORK

UAVs deployment problem is gaining significant importance in UAV-based wireless communications where the performance of the aerial wireless network depends on the deployment strategy and the 3D placements of UAVs. In this chapter, we classify the related work based on the UAV deployment strategies.

The first deployment strategies are used for minimizing the transmit power of UAVs. The authors in [13] propose an efficient deployment framework for deploying the aerial base stations, where the goal is to minimize the total transmit power of UAVs while satisfying the user rate requirements. They apply the optimal transport theory to obtain the optimal cell association. After that, they derive the optimal locations of the UAVs using the facility location framework. The authors in [14] investigate the downlink coverage performance of a UAV, where the objective is to find the optimal UAV altitude which leads to the maximum ground coverage and the minimum transmit power. In [15], the authors propose an optimal placement algorithm for a UAV to maximize the number of covered users using the minimum transmit power. The algorithm decouples the UAV deployment problem in the vertical and horizontal dimensions without any loss of optimality. The authors in [16] consider two types of users in the network; the downlink users served by a UAV and device-to-device users that communicate directly with one another. Using the disk covering problem, the authors show that the entire target geographical area can be completely covered by a UAV in a shortest time with a minimum required transmit power. They also derive the overall outage probability for the device-to-device users, and show

that the outage probability increases as the number of stop points that a UAV needs to completely cover the area increases.

The second deployment strategies are used for maximizing the wireless coverage of UAVs. In [17], the authors study the placement problem with an objective of maximizing the number of users covered by a UAV. They formulate a quadratically-constrained mixed integer non-linear optimization problem and propose a computationally efficient numerical solution for the problem. The authors in [18] study the optimal deployment of UAVs equipped with directional antennas, using circle packing theory. The 3D locations of the UAVs are determined in a way that the total coverage area is maximized. In [19], the authors introduce the network-centric and user-centric approaches. In the network-centric approach, the network tries to serve as many users as possible, regardless of their rate requirements. In the user-centric approach, the users are determined based on the priority. The optimal 3D backhaul-aware placement of a UAV that maximizes the total number of served users is found for each approach. The authors in [20] study the UAV placement problem with an objective of maximizing the number of covered users with different Quality-of-Service requirements. They model the placement problem as a multiple circles placement problem and propose an optimal placement algorithm that utilizes an exhaustive search over a one-dimensional parameter in a closed region. They also propose a low-complexity algorithm, maximal weighted area algorithm, to tackle this problem. The authors in [21] utilize UAVs-hubs to provide connectivity to small-cell base stations with the core network. The goal is to find the best possible association of the small cell base stations with the UAVs-hubs such that the sum-rate of the overall network

is maximized. They present an efficient algorithm, distributed maximal demand minimum servers, to maximize the sum rate of the overall network.

The third deployment strategies are used for minimizing the number of UAVs required to perform a task. The authors in [22] propose the particle swarm optimization algorithm to find the minimum number of UAVs and their 3D placements so that all the ground users are served. In [23], the authors study the problem of deploying the minimum number of UAVs required to maintain the connectivity of ground mobile ad hoc networks under the condition that some UAVs have already been deployed in the air. They formulate this problem as a minimum steiner tree problem with existing mobile steiner points under edge length bound constraints. They prove the NP-completeness of the problem and propose an efficient algorithm, existing UAVs aware algorithm, to tackle this problem. The proposed algorithm uses a maximum match heuristic to compute the new positions for existing UAVs. The authors in [24] aim to minimize the number of UAVs required to provide wireless coverage for a group of distributed ground terminals such that each ground terminal is within the communication range of at least one UAV. They propose a polynomial-time algorithm, spiral UAV placement algorithm, to place the UAVs sequentially starting from the area perimeter of the uncovered ground terminals along a spiral path towards the center, until all ground terminals are covered.

The fourth deployment strategies are used for collecting data using UAVs. The authors in [5] propose an efficient framework for deploying UAVs to collect data from ground internet of things devices. They minimize the total transmit power of these devices by properly clustering them where each cluster being served by one UAV. The optimal trajectories of the UAVs are determined by exploiting the framework of optimal transport

theory. In [25], the authors present a UAV enabled data collection system, where a UAV is dispatched to collect a given amount of data from ground terminals at fixed location. They aim to find the optimal ground terminal transmit power and UAV trajectory that achieve different Pareto optimal energy trade-offs between the ground terminal and the UAV. The authors in [26] study the problem of UAV trajectory planning for wireless sensor network deployed in remote areas. The missions are given by a set of ground points which define the wireless sensor network gathering zones. The UAVs should pass through the gathering zone to collect the data while avoiding passing over forbidden areas to avoid collisions. The proposed UAV trajectory planners, rapidly-exploring random trees and optimal rapidly-exploring random trees, are based on the genetic algorithm. The authors in [27] design a basic framework for UAV data collection, which includes the following five components: deployment of networks, nodes positioning, anchor points searching, fast path planning for UAV, and data collection from network. They identify the key challenges for each component and propose an efficient algorithm, fast path planning with rules algorithm, to increase the efficiency of path planning, while guaranteeing the length of the path to be relatively short. In [28], the authors jointly optimize the sensor nodes wake-up schedule and the trajectory of a UAV to minimize the maximum energy consumption of all sensor nodes such that the required amount of data is collected reliably from each sensor node. They formulate a mixed-integer non-convex optimization problem and propose an efficient iterative algorithm to find a sub-optimal solution. Table 2.1 summarizes the related work.

Table 2.1 Summary of the Related Work

Reference	Objective Function	Deployment Strategy
[13]	Minimizing the transmit power	Optimal transport theory
[14]	Minimizing the transmit power	Closed-form expression
[15]	Minimizing the transmit power	Optimal 3D placement algorithm
[16]	Minimizing the transmit power	Disk covering problem
[17]	Maximizing the wireless coverage	Bisection search algorithm
[18]	Maximizing the wireless coverage	Circle packing theory
[19]	Maximizing the wireless coverage	Branch and bound algorithm
[20]	Maximizing the wireless coverage	Exhaustive search algorithm
[21]	Maximizing the wireless coverage	Branch and bound algorithm
[22]	Minimizing the number of UAVs	Particle swarm optimization
[23]	Minimizing the number of UAVs	Polynomial time algorithm
[24]	Minimizing the number of UAVs	Polynomial time algorithm
[5]	Collecting data using UAVs	Optimal transport theory
[25]	Collecting data using UAVs	Circular and straight UAV trajectories
[26]	Collecting data using UAVs	Genetic algorithm
[27]	Collecting data using UAVs	Polynomial time algorithm
[28]	Collecting data using UAVs	Polynomial time algorithm

CHAPTER 3

PROVIDING CONTINUOUS WIRELESS COVERAGE USING UAVS

3.1 Introduction

In 2005[1], Hurricane Katrina in the United States caused over 1,900 deaths, 3 million land-line phone interruptions, and more than 2,000 base stations going out of service [4,30,31]. Another example of a large-scale interruption of telecommunications service is the World Trade Center attack in 2001, when it took just minutes for the nearby base stations to be overloaded. The attacks caused the disturbance of a phone switch with over 200,000 lines, 20 cell sites, and 9 TV broadcast stations [4, 32]. These incidents demonstrate the need for quick/efficient deployment networks for emergency cases.

The authors in [33] propose a UAV-based replacement network during disasters, where the UAVs serve as aerial wireless base stations. However, this study does not consider how the UAVs will guarantee a continuous coverage when they need to return to the charging station for recharging. Though a UAV has limited energy capacity and needs to recharge its battery before running out of energy during the coverage process, only few studies have considered this constraint in the UAV coverage problem. Concretely, the author in [34] determines the minimum number of UAVs that can provide continuous coverage for a single area using identical and non-identical UAVs. However, no consideration has been made for the case when there are multiple subareas that need to be covered, which is the typical scenario during disasters. The author in [35] formulates the mobile charging problem, in which multiple mobile chargers collaborate to charge

[1]The work of this chapter has been published in [29].

static sensors with minimum number of mobile chargers subject to speed and energy limits of the mobile chargers. In this problem, the chargers will not cover the sensors continuously. The mobile charger will visit the sensor and stay for a specific time to charge the sensor. After finishing the charging process, it will visit the other sensors. In [36], the authors study the continuous coverage problem for mobile targets. During the coverage process, a UAV that runs out of energy is replaced by a new one.

Many studies [13,14,37,38] focus on minimizing the total transmission power of the UAVs during the coverage of a geographical area, however, no limits on the UAV energy capacity and the need for recharging have not been considered. The work in [39] report that the energy consumption during data transmission and reception is much smaller than the energy consumption during the UAV hovering, i.e., it only constitutes 10%-20% of the UAV energy capacity. Thus, it is important to conduct studies that take into account the energy consumption during the UAV hovering rather than focusing on minimizing the energy consumption during data transmission and reception.

Contrary to the related work above, we integrate the recharging requirements into the coverage problem and examine the minimum number of required UAVs for enabling continuous coverage under that setting, as shown in Figure 3.1.

3.2 System Model

Consider a geographical area G=$\{g_1,...,g_N\}$, where g_i represents a subarea i, the subarea $g_1 \in G$ includes the charging station and all subareas except subarea g_1 need to be covered G_0=$G \setminus g_1$. We aim to find the minimum number of UAVs that can provide a continuous coverage over G_0 by placing the UAVs at locations where each UAV will provide full

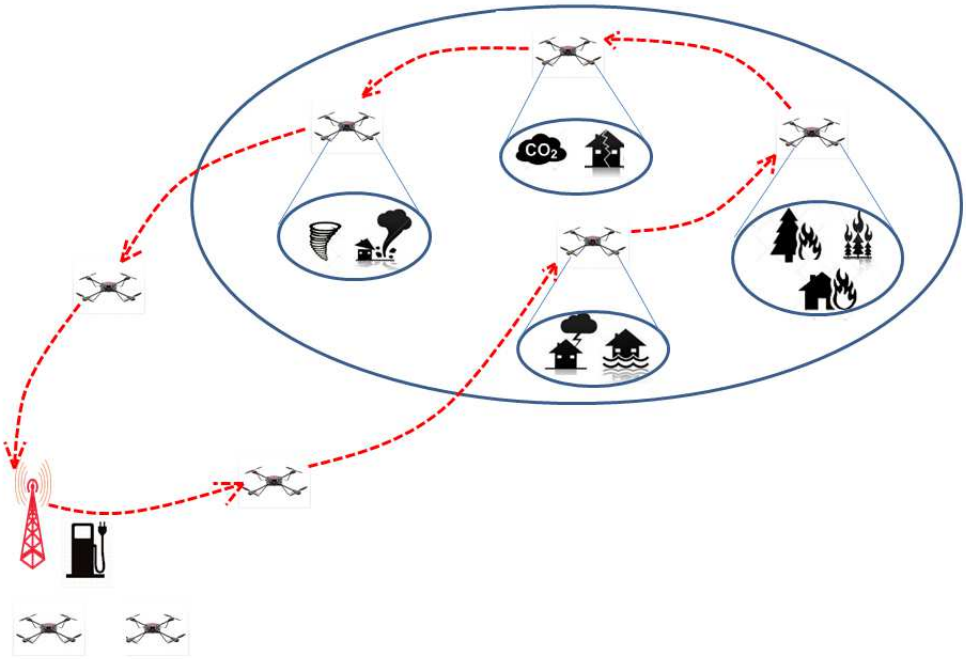

Figure 3.1 Providing continuous wireless coverage.

coverage for one subarea. In the continuous coverage problem, we assume: (1) Time slotted system in which the slot duration is 1 time unit and the total coverage duration is T. (2) All UAVs start the coverage process from the charging station and they need to return to the charging station after they complete the coverage process. (3) Each UAV has limited energy capacity E and it needs to return to the charging station to recharge the battery before running out of energy during the coverage process. (4) Each UAV can move (from the charging station to location i), (from location i to location j) or (from location j to the charging station) and this process will take one time slot. (5) Each UAV covers a given subarea for one or multiple time slots. (6) At each time slot, each subarea will be covered by only one UAV. (7) The UAV cannot travel to the charging station or to any other location until the handoff process is completed in which another UAV arrives

Table 3.1 List of Notations

M	The set of fully charged UAVs available at the charging station.
E	The energy capacity of each UAV.
T	The total coverage duration.
E_{ij}^{Travel}	The energy consumed by a UAV when it travels from subarea i to subarea j, where $i, j \in G$.
E_{j}^{Cover}	The energy consumed by a UAV when it covers the subarea j for one time slot, where $j \in G_0$ (constant).
T_{charge}	The time that a UAV needs to recharge the battery at the charging station.

to cover the subarea such that the continuous coverage is guaranteed. (8) The recharging process takes T_{charge} at the charging station.

3.3 The Continuous Coverage Problem

3.3.1 Problem Formulation

In order to present the problem formulation, we introduce the binary variable x_m that takes the value of 1 if the UAV m visits any subarea from charging station during the coverage duration T and equals 0 otherwise; the binary variable $y_{ij,m}^{t}$ that takes the value of 1 if the UAV m moves through edge ij during the time slot t and equals 0 otherwise; the binary variable $z_{j,m}^{t}$ that takes the value of 1 if the UAV m covers the subarea j at time slot t and equals 0 otherwise. Table 3.1 lists the notations used in this chapter.

$$\min \sum_{m \in M} x_m$$

subject to

$$y^t_{ij,m} \leq x_m \qquad \forall i,j \in G, \forall t \in [0,T], \forall m \in M \tag{3.1}$$

$$z^t_{j,m} \leq x_m \qquad \forall j \in G_0, \forall t \in (0,T), \forall m \in M \tag{3.2}$$

$$\sum_{m \in M} y^0_{1j,m} = 1 \qquad \forall j \in G_0 \tag{3.3}$$

$$\sum_{m \in M} z^t_{j,m} = 1 \qquad \forall j \in G_0, \forall t \in (0,T) \tag{3.4}$$

$$\sum_{i \in G, i \neq j} \sum_{m \in M} y^t_{ij,m} \leq 1 \qquad \forall j \in G_0, \forall t \in [0,T] \tag{3.5}$$

$$\sum_{i_1 \in G} y^t_{i_1 j,m_1} = \sum_{i_2 \in G} y^{t+1}_{j i_2,m_2} \qquad \forall j \in G_0, \forall t \in (0,T), m_1 \neq m_2 \tag{3.6}$$

$$\sum_{m \in M} \sum_{t \in [0,T)} \sum_{i \in G} y^t_{ij,m} \leq \sum_{m \in M} \sum_{t \in (0,T)} z^t_{j,m} \qquad \forall j \in G_0 \tag{3.7}$$

$$\sum_{j \in G_0} \sum_{\tau \in T_{charge}} [y^t_{j1,m} + y^{t+\tau}_{1j,m}] \leq 1 \qquad \forall m \in M, \forall t \in (0,T) \tag{3.8}$$

$$\sum_{m \in M} \sum_{t \in [0,T]} \sum_{j \in G_0} y^t_{1j,m} = \sum_{m \in M} \sum_{t \in [0,T]} \sum_{i \in G_0} y^t_{i1,m} \tag{3.9}$$

$$\sum_{t\in[t_1,t_2]}\sum_{i,j\in G} E_{ij}^{Travel} y_{ij,m}^{t} + \sum_{t\in[t_1,t_2]}\sum_{j\in G} E_{j}^{Cover} z_{j,m}^{t} \leq E \quad \forall m \in M,$$
$$\forall [t_1,t_2] \in [0,T], t_1 = arg\ y_{1j,m}^{t}, t_2 = arg\ y_{i1,m}^{t}, t_2 > t_1. \tag{3.10}$$

The objective is to minimize the number of UAVs that are needed to provide a continuous coverage during the coverage duration T. Constraint sets (3.1) and (3.2) ensure that a UAV can travel and cover the subareas only if we select it to participate in the coverage process. Constraint set (3.3) ensures that all subareas will be covered at the first time slot. Constraint set (3.4) guarantees the continuous coverage for each subarea. Constraint set (3.5) allows the UAV to visit a new subarea (when $y_{ij,m}^{t}$=1) or to continue covering the current subarea (when $y_{ij,m}^{t}$=0). Constraint set (3.6) characterizes the handoff process between the UAVs, when the UAV m_1 wants to visit the subarea j from subarea i_1 at time t ($y_{i_1 j,m_1}^{t}$=1), the UAV m_2 that covers the subarea j will travel to subarea i_2 at time $t+1$ (y_{ji_2,m_2}^{t+1}=1). Constraint set (3.7) describes the relation between the traveling process and the covering process, where the number of times that the subarea j is covered will be greater than or equal the number of times that it is visited. Constraint set (3.8) shows that the recharging process will take T_{charge} at the charging station. Constraint (3.9) ensures that the number of UAVs outgoing from the charging station and the number of UAVs incoming to charging station are the same after we complete the coverage process. Constraint set (3.10) shows that the energy capacity of a UAV can cover the wasted energy during the traveling and the covering processes in each cycle where t_1 represents the time that a UAV travels from the charging station with full energy capacity and t_2 represents the time that a UAV arrives to the charging station to charge the battery. Next, we prove that the continuous coverage problem is an NP-complete.

3.3.2 NP Completeness

Theorem 1. *The Continuous Coverage Problem is NP-complete.*

Proof. The number of constraints is polynomial in terms of the number of subareas, the number of UAVs and the number of time slots. Given any solution for our problem, we can check the solution's feasibility in polynomial time, then the problem is NP.

To prove that the problem is NP-hard, we reduce the Bin Packing Problem which is NP-hard [40] to a special case of our problem. The special case of our problem is the discrete coverage problem. In this problem, each subarea will be visited one time by one UAV during the coverage process. In the Bin Packing Problem, we have a set of items $U = \{1, 2, ..., W\}$, in which each item has volume z_w, where $w \in U$. All items must be packed into a finite number of bins (b_1, b,...,b_B), each of volume V in a way that minimizes the number of bins used. The reduction steps are: 1) The b-th bin in the Bin Packing Problem is mapped to the m-th UAV in our problem, where the volume V for each bin is mapped to the energy capacity of the UAV E. 2) The w-th item is mapped to the n-th subarea, where the volume for each item w is mapped to the energy consumed when a UAV visits and covers subarea n. 3) All UAVs have the same energy capacity E. 4) The energy consumed during the traveling and the covering processes when a UAV visits subarea j from any subarea $i \in G \setminus \{j\}$ will be constant. 5) The energy required for a UAV to return to the charging station from any subarea i will be zero (E_{i1}^{Travel}=0). 6) The time that a UAV needs to recharge a battery at the charging station will be infinity. 7) Each subarea will be visited one time by one UAV during the coverage process. If there exists a solution to the bin packing problem with cost C, then the selected bins will

represent the UAVs and the items in each bin will represent the subareas that a UAV must visit and the total cost of our problem is C. □

3.4 Heuristic Algorithm

Due to the intractability of the problem, we study partitioning the coverage graph into cycles that start at the charging station. We first characterize the minimum number of UAVs required to cover each cycle based on the charging time, the traveling time, and the number of subareas to be covered by the cycle. Our analysis based on the uniform coverage in which a UAV covers each subarea in a given cycle for a constant time. Based on this analysis, we then develop an efficient algorithm, the cycles with limited energy algorithm, that minimizes the required number of UAVs that guarantees a continues coverage.

3.4.1 Analysis

It is obvious that we need N UAVs to cover N subareas at any given time, but the question here is how many additional UAVs are needed to guarantee a continuous coverage. In this subsection, we assume that a UAV visits the subareas based on a cycle that starts from the charging station and ends at the charging station for charging process. We also assume that a given UAV covers the subareas in the cycle uniformly, in which a UAV covers each subarea in a given cycle for a constant time. In Theorem 2, we find the minimum number of additional UAVs that are needed to guarantee a continuous coverage for a cycle, which will help us while developing Algorithm 1.

Theorem 2. *The minimum number of additional UAVs k that are required to provide continuous and uniform coverage for a cycle that contains n subareas must satisfy this inequality:*

$$k\frac{T_{Coverage}}{n} \geq (n+1)T + T_{Charge},$$

where $T_{Coverage}$ is the time that a UAV allocates to cover all subareas in the cycle, T is the time that a UAV needs to travel from subarea i to subarea j and T_{charge} is the time that a UAV needs to recharge the battery at the charging station.

Proof. Consider that all n subareas in the cycle are covered by n UAVs and the UAV that covers the last subarea want to return to the charging station to recharge its battery. The handoff process needs to begin between one of the additional UAVs from the charging station and the UAV that covers the first subarea in the cycle.

The UAV that covers the last subarea needs to wait $(n-1)\ T$ to do the handoff process, during this time the additional UAVs are covering the first subarea. After the handoff process is completed, the UAV needs T time units to return to the charging station, T_{charge} to recharge the battery and T to visit the first subarea in the cycle again. Then, we have:

$$k\frac{T_{Coverage}}{n} \geq (n-1)T + T + T_{Charge} + T$$

□

Example: Given $n = 3$, $T_{Coverage} = T_C = 9T$ and $T_{Charge} = T$, we want to find the minimum number of the additional UAVs k that guarantees the continuous coverage for

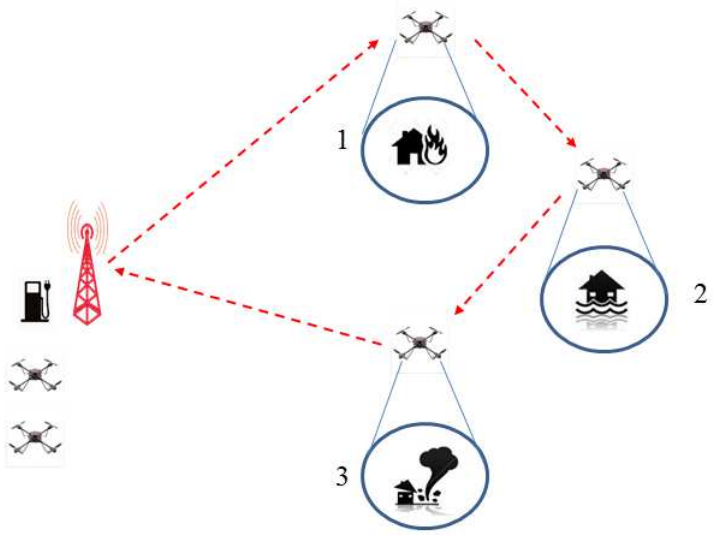

Figure 3.2 Minimum number of additional UAVs.

a given subareas (see Figure 3.2). Tables 3.2-3.6 show the paths of UAVs. It is obvious that the first UAV will be ready to cover the first subarea in the cycle again at $4T + T_C + T_{charge} = 14T$. After the second additional UAV covered the first subarea in the cycle, it needs to do the handoff with one of the UAVs from the charging station at $T + \frac{5}{3}T_C = T + \frac{5}{3}(9T) = T + 15T = 16T$. The first UAV is ready to do that, it will wait T at the charging station and it needs T to arrive to the first subarea. We only need two additional UAVs to continuously cover this cycle. Now, Let us check our solution by applying Theorem 2, we have $k\frac{T_{Coverage}}{n} \geq (n+1)T + T_{Charge} \Rightarrow 2\frac{9T}{3} \geq (3+1)T + T \Rightarrow 6T \geq 5T$.

3.4.2 The Cycles with Limited Energy Algorithm

The straightforward method (SM) to continuously cover N subareas is to allocate two UAVs for each subarea. At the first time slot, N UAVs cover the N subareas. Then, any UAV wants to return to the charging station to recharge the battery will do the handoff

Table 3.2 Path of the UAV1

Time	0	T	T+$\frac{1}{3}$ T_C
Subarea Index	Charging station	1	1
Coverage Time	0	0	$\frac{1}{3}$ T_C
Time	2T+$\frac{1}{3}$ T_C	2T+$\frac{2}{3}$ T_C	3T+$\frac{2}{3}$ T_C
Subarea Index	2	2	3
Coverage Time	0	$\frac{1}{3}$ T_C	0
Time	3T+T_C	4T+T_C	4T+T_C+T_{Charge}
Subarea Index	3	Charging station	Charging station
Coverage Time	$\frac{1}{3}$ T_C	0	0

Table 3.3 Path of the UAV2

Time	0	T+$\frac{1}{3}$ T_C	T+$\frac{2}{3}$ T_C
Subarea Index	Charging station	1	1
Coverage Time	0	0	$\frac{1}{3}$ T_C
Time	2T+$\frac{2}{3}$ T_C	2T+T_C	3T+ T_C
Subarea Index	2	2	3
Coverage Time	0	$\frac{1}{3}$ T_C	0
Time	3T+$\frac{4}{3}T_C$	4T+$\frac{4}{3}T_C$	4T + $\frac{4}{3}$ T_C+T_{Charge}
Subarea Index	3	Charging station	Charging station
Coverage Time	$\frac{1}{3}$ T_C	0	0

Table 3.4 Path of the UAV3

Time	0	T+$\frac{2}{3}$ T_C	T+T_C
Subarea Index	Charging station	1	1
Coverage Time	0	0	$\frac{1}{3}$ T_C
Time	2T+T_C	2T+$\frac{4}{3}T_C$	3T+ $\frac{4}{3}T_C$
Subarea Index	2	2	3
Coverage Time	0	$\frac{1}{3}$ T_C	0
Time	3T+$\frac{5}{3}T_C$	4T+$\frac{5}{3}T_C$	4T + $\frac{5}{3}$ T_C+T_{Charge}
Subarea Index	3	Charging station	Charging station
Coverage Time	$\frac{1}{3}$ T_C	0	0

Table 3.5 Path of the First Additional UAV

Time	0	T+T_C	T+$\frac{4}{3}T_C$
Subarea Index	Charging station	1	1
Coverage Time	0	0	$\frac{1}{3}$ T_C
Time	2T+$\frac{4}{3}T_C$	2T+$\frac{5}{3}T_C$	3T+ $\frac{5}{3}T_C$
Subarea Index	2	2	3
Coverage Time	0	$\frac{1}{3}$ T_C	0
Time	3T+2T_C	4T+2T_C	4T + 2T_C+T_{Charge}
Subarea Index	3	Charging station	Charging station
Coverage Time	$\frac{1}{3}$ T_C	0	0

Table 3.6 Path of the Second Additional UAV

Time	0	T+$\frac{4}{3}T_C$	T+$\frac{5}{3}T_C$
Subarea Index	Charging station	1	1
Coverage Time	0	0	$\frac{1}{3}\ T_C$
Time	$2T$+$\frac{5}{3}T_C$	$2T$+$2T_C$	$3T$+ $2T_C$
Subarea Index	2	2	3
Coverage Time	0	$\frac{1}{3}\ T_C$	0
Time	$3T$+$\frac{7}{3}T_C$	$4T$+$\frac{7}{3}T_C$	$4T$ + $\frac{7}{3}T_C$+T_{Charge}
Subarea Index	3	Charging station	Charging station
Coverage Time	$\frac{1}{3}\ T_C$	0	0

process with one of the additional UAVs that are available at the charging station. By applying SM, we need N additional UAVs to cover all subareas.

Our proposed algorithm, the cycles with limited energy algorithm (CLE), is inspired by the nearest neighbor algorithm, the nearest neighbor algorithm is used to solve the Traveling Salesman Problem [41], in which the salesman keeps visiting the nearest unvisited vertex until all the vertices are visited. In our algorithm, the UAV (salesman) has limited energy capacity and before visiting any new subarea, we must check if the remaining energy is enough to return to the charging station from the new location or not. In Theorem 2, we show how to find the minimum number of additional UAVs that are required to guarantee the continuous coverage for a given cycle, we use the Theorem 2 to find the minimum number of additional UAVs that are required to provide the continuous

Algorithm 1 The Cycles with Limited Energy Algorithm

1: **Input:**
2: The geografical area G=$\{g_1$,...,$g_N\}$,
3: The required time to travel between two subareas T,
4: The energy capacity of UAV E,
5: The time that a UAV needs to recharge the battery at the charging station T_{Charge},
6: The energy consumed by a UAV when it covers the subarea for one second e,
7: The index of the cycle i=1.
8: **Start:**
9: **While** G not empty
10: c_i=$\{g_1\}$
11: **Do:**
12: v= most recently added subarea to cycle c_i
13: Find $\{g\}$= $argmin_{b \in G-\{v\}}\ distance(v, b)$
14: Calculate $E_{Coverage}$=E-E_{Travel}-$E_{ReturntoBS}$
15: Calculate $T_{Coverage} = \frac{E_{Coverage}}{e}$
16: **If** $\frac{T_{Coverage}}{|c_i|} \geq (|c_i| + 1)T + T_{Charge}$ **then**
17: $c_i \longleftarrow c_i \cup \{g\}$
18: $G \longleftarrow G \setminus \{g\}$
19: **while** ($\frac{T_{Coverage}}{|c_i|} \geq (|c_i| + 1)T + T_{Charge}$)
20: $c_i \longleftarrow c_i \cup \{g_1\}$
21: **C** $\longleftarrow$ **C** $\cup\ c_i$
22: i=i+1
23: **EndWhile**
24: **Output: C**

coverage for a given area, by finding the cycles that need only one additional UAV. The pseudo code of this algorithm is shown in Algorithm 1.

3.5 Performance Evaluation

We quantify the power consumption by UAV when it is hovering, traveling and transmitting data. The power consumption in watt by a UAV during hovering can be given

by [42]:

$$P = 4\frac{T_h^{3/2}}{\sqrt{2QS}} + p,$$

where T_h is the fourth of the quadcopter total weight in newton, Q is the density of the air in kg/m^3, S is the rotor swept area in m^2 and p is the power consumption of electronics in watt.

The power consumption in kW by a UAV during traveling can be given by [43]:

$$P = \frac{(m_p + m_v)v}{370\eta r} + p,$$

where m_p is the payload mass in kg, m_v is the vehicle mass in kg, r is the lift-to-drag ratio (equals 3 for the vehicle that is capable of vertical takeoff and landing), η is the power transfer efficiency for motor and propeller, p is the power consumption of electronics in kW and v is the velocity in km/h.

The power consumption in dB by a UAV during data transmission can be given by [14]:

$$P_t(dB) = P_r(dB) + \bar{L}(R, h) \tag{3.11}$$

$$\bar{L}(R, h) = P(LOS) \times L_{LOS} + P(NLOS) \times L_{NLOS} \tag{3.12}$$

$$P(LOS) = \frac{1}{1 + \alpha.exp(-\beta[\frac{180}{\pi}\theta - \alpha])} \tag{3.13}$$

$$L_{LOS}(dB) = 20log(\frac{4\pi f_c d}{c}) + \xi_{LOS} \tag{3.14}$$

$$L_{NLOS}(dB) = 20log(\frac{4\pi f_c d}{c}) + \xi_{NLOS} \tag{3.15}$$

In equation (3.11), P_t is the transmit power, P_r is the required received power to achieve a SNR greater than threshold γ_{th}, $\bar{L}(R,h)$ is the average path loss as a function of the altitude h and coverage radius R. In equation (3.12), $P(LOS)$ is the probability of having line of sight (LOS) connection at an evaluation angle of θ, $P(NLOS)$ is the probability of having non LOS connection and equals (1-$P(LOS)$), L_{LOS} and L_{NLOS} are the average path loss for LOS and NLOS paths. In equations (3.13-3.15), α and β are constant values which depend on the environment, f_c is the carrier frequency, d is the distance between the UAV and user, c is the speed of the light , ξ_{LOS} and ξ_{NLOS} are the average additional losses which depend on the environment. In this chapter, we assume that the power wasted during data transmission is constant, where the power consumed by a UAV during data transmission and reception is much smaller than the power consumed during hovering or traveling [39].

Given a geographical area G , the number of the subareas that we need to cover and the density of the users, the question here is how to find the optimal boundaries of the subareas that will be covered by the UAVs. To answer this question, the authors of [13] utilize the transport theory to find the optimal boundaries of the subareas. Unfortunately, this approach needs to solve $\binom{N}{2}$ non-linear equations at each iteration, where N is the number of subareas. In this chapter, we divide the geographical area uniformly and apply the SM and CLE algorithms to find the minimum number of additional UAVs that provides the continuous coverage. We study the effect of the UAV energy capacity, the grid size of the geographical area, the charging time and the traveling time on the number of the additional UAVs. Table 3.7 lists the parameters used in the numerical analysis [44].

Table 3.7 Parameters in Numerical Analysis

UAV energy capacity	0.88kW.h
Power consumption by the electronics	0.15kW
Grid size	4x4
Area of the graph	1kmx1km
Traveling time through edge	2.5 min
Charging station location (x,y)	(0,0)
Charging time	5 min
UAV weight with battery	8.5 k.g
Maximum payload weight	2 k.g
Maximum forward speed	12 m/s

In Figure 3.3, we uniformly divide the geographical area into 16 subareas and apply the CLE algorithm to find the cycles with minimum number of additional UAVs. From the figure, we notice that 5 cycles are needed to cover all subareas with 5 additional UAVs. Also, we note that the paths of the cycles are intersected in many locations. To avoid the collisions between the UAVs, we operate the paths (cycles) at different altitudes with small altitude differences.

In Figure 3.4, we study the effect of the UAV energy capacity on the number of additional UAVs needed to cover the subareas. When we increase the energy capacity of a UAV and apply SM, the number of additional UAVs needed will not change because each subarea is covered by one cycle and two UAVs, only the coverage time of each UAV increases. On the other hand, increasing the energy capacity of each UAV results

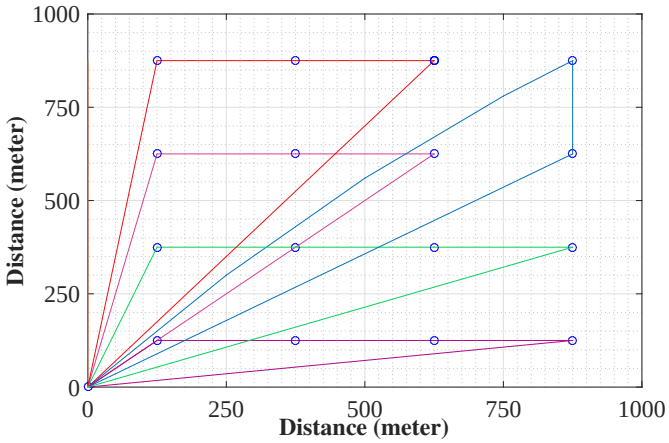

Figure 3.3 Cycles that cover the subareas using the CLE algorithm.

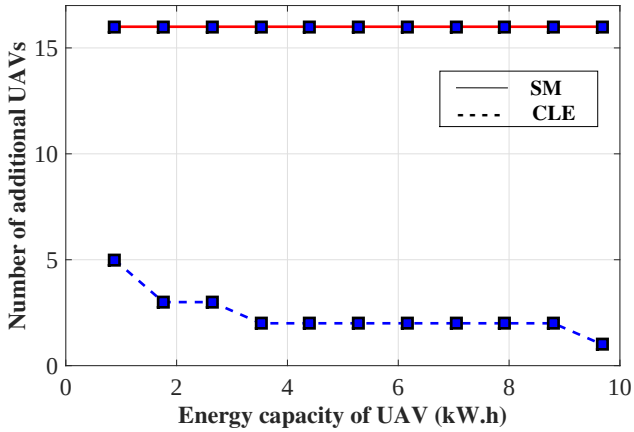

Figure 3.4 Energy capacity vs. the number of additional UAVs.

in minimizing the number of additional UAVs that needed using CLE. This is because increasing the energy capacity of each UAV gives a UAV a chance to visit and to cover more subareas, which minimizes the number of the cycles that are needed to cover the subareas.

In Figure 3.5, the slope of the line produced by SM is greater than the curve of CLE. When applying SM, the number of additional UAVs increases linearly with the grid size. This is because the number of additional UAVs equals the grid size. Also, when applying

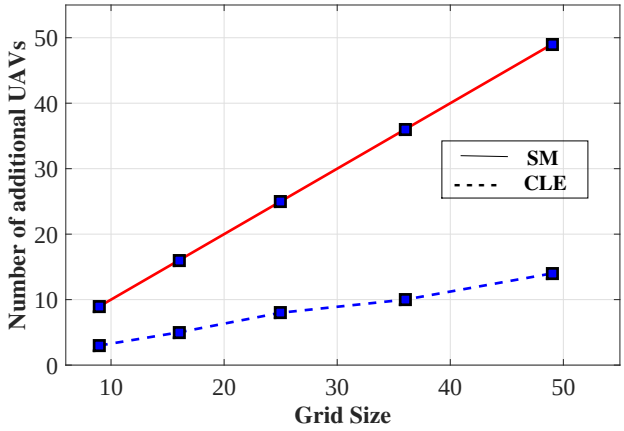

Figure 3.5 Grid size vs. the number of additional UAVs.

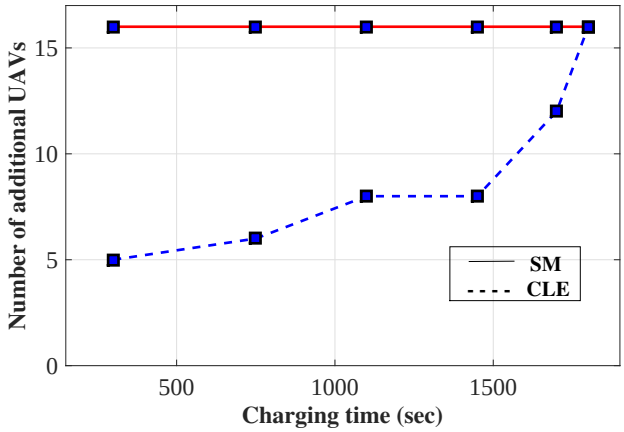

Figure 3.6 Charging time vs. the number of additional UAVs.

the CLE, the number of additional UAVs increases with the grid size. This is because more cycles are needed to cover more subareas, and each cycle needs one additional UAV.

In Figure 3.6, we study the effect of the charging time on the number of additional UAVs needed. Changing the charging time will not affect the number of additional UAVs needed when applying SM. This is because the coverage time of each UAV will cover the time that the UAV needs to return to the charging station to recharge the battery and to visit the subarea again. On the other hand, when applying CLE, it will be a critical issue (see Theorem 2). Actually, charging the battery of a UAV takes long time. For this

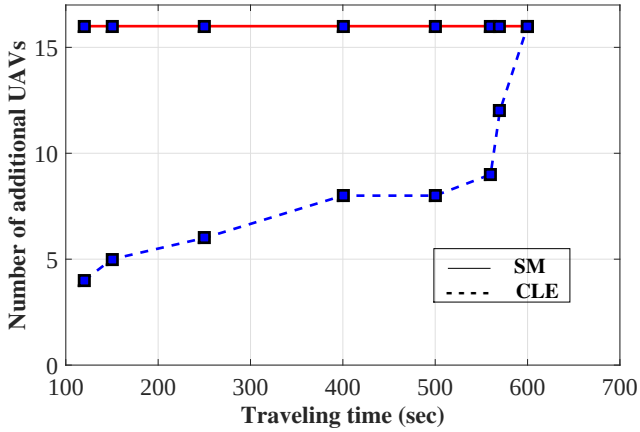

Figure 3.7 Traveling time vs. the number of additional UAVs.

reason, each UAV has a replacement battery [44]. We assume the time needed to replace the battery for each UAV is 5 minutes.

In Figure 3.7, we study the effect of the traveling time on the number of additional UAVs. Changing the traveling time will not affect the number of additional UAVs when applying SM. On the other hand, it will be a critical issue to choose the appropriate traveling time when applying CLE. When increasing the traveling time, the wasted energy during traveling will increase and the coverage time will decrease. Hence, the chance to visit other subareas will decrease.

CHAPTER 4

PROVIDING INDOOR WIRELESS COVERAGE USING UAVS

4.1 Introduction

In order to use UAV as an aerial wireless base station[1], the authors in [48] presented an Air-to-Ground path loss model that helped academic researchers to formulate many important UAV-based coverage problems. The authors in [14] utilized this model to evaluate the impact of a UAV altitude on the downlink ground coverage and to determine the optimal values for altitude which lead to maximum coverage and minimum required transmit power. In [13], the authors used the path loss model to propose a power-efficient deployment for UAVs under the constraint of satisfying the rate requirement for all ground users. The authors in [18] utilized the path loss model to study the optimal deployment of multiple UAVs equipped with directional antennas, using circle packing theory. The 3D locations of the UAVs are determined in a way that the total coverage area is maximized. In [22], the authors used the path loss model to find the minimum number of UAVs and their 3D locations so that all outdoor ground users are served. However, it is assumed that all users are outdoor and the location of each user can be represented by an outdoor 2D point. These assumptions limit the applicability of this model when one needs to consider indoor users.

Providing good wireless coverage for indoor users is very important. According to Ericsson report [49], 90% of the time people are indoor and 80% of the mobile Internet access traffic also happens indoors [50, 51]. To guarantee wireless coverage, service

[1]The work of this chapter has been published in [45–47].

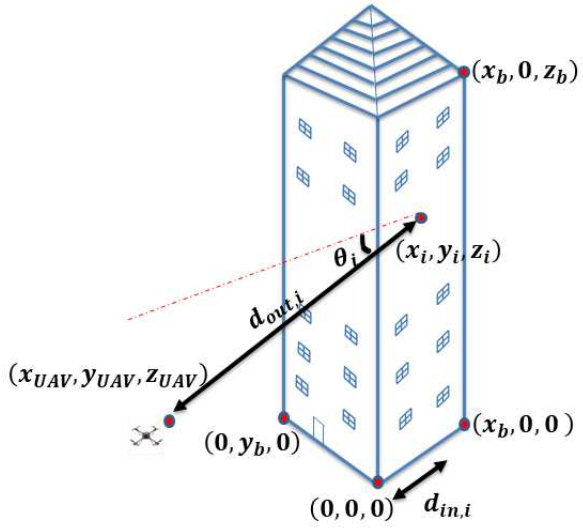

Figure 4.1 Parameters of the path loss model.

providers are faced with several key challenges, including providing service to a large number of indoor users and the ping pong effect due to interference from near-by macro cells [52–54]. In this chapter, we propose using UAVs to provide a wireless coverage for users inside a high-rise building after partial or complete infrastructure damage due to natural disasters or after base station offloading in extremely crowded events [10] (such as concerts, indoor sporting events, etc.), when the cellular network service is not available or unable to serve all indoor users.

4.2 System Model

4.2.1 System Settings

Let (x_{UAV},y_{UAV},z_{UAV}) denote the 3D location of the UAV. We assume that all users are located inside a high-rise building as shown in Figure 4.1, and use (x_i,y_i,z_i) to denote the location of user i. The dimensions of the high-rise building, in the shape of a rectangular prism, are $[0, x_b] \times [0, y_b] \times [0, z_b]$. Also, let $d_{out,i}$ be the distance between the UAV and indoor user i, let θ_i be the incident angle that represents the angle between the line of sight

path and a unit vector normal to the building wall, and let $d_{in,i}$ be the distance between the building wall and indoor user i.

4.2.2 Outdoor-Indoor Path Loss Models

The Air-to-Ground path loss model presented in [48] is not appropriate when we consider wireless coverage for indoor users, because this model assumes that all users are outdoor and located at 2D points. In this work, we adopt the Outdoor-Indoor path loss model, certified by the ITU [55], for the lower part of Super High Frequency band (low-SHF) (450 MHz to 6 GHz). The path loss is given as follows:

$$L_i = L_F + L_B + L_I = (w \log_{10} d_{out,i} + w \log_{10} f_{Ghz} + g_1) \\ +(g_2 + g_3(1 - \cos\theta_i)^2) + (g_4 d_{in,i})$$

where L_F is the free space path loss, L_B is the building penetration loss, and L_I is the indoor loss. In this model, we also have w=20, g_1=32.4, g_2=14, g_3=15,g_4=0.5 [55] and f_{Ghz} is the carrier frequency.

In [56], the authors clarify the Outdoor-to-Indoor path loss characteristics based on the measurement for 0.8 to 37 GHz frequency band. We adopt this path loss model for the high-SHF operating frequency (over 6 GHz). The path loss is given as follows:

$$L_i = L_F + L_B + L_I = (\alpha_1 + \alpha_2 \log_{10} d_{out,i} + \alpha_3 \log_{10} f_{Ghz}) + \\ (\beta_1 + \frac{\beta_2 - \beta_1}{1 + exp(-\beta_3(\theta_i - \beta_4))}) + (\gamma_1 d_{in,i})$$

In this model, we have α_1=31.4, α_2=20, α_3=21.5, β_1=6.8, β_2=21.8, β_3=0.453, β_4=19.7 and γ_1=0.49.

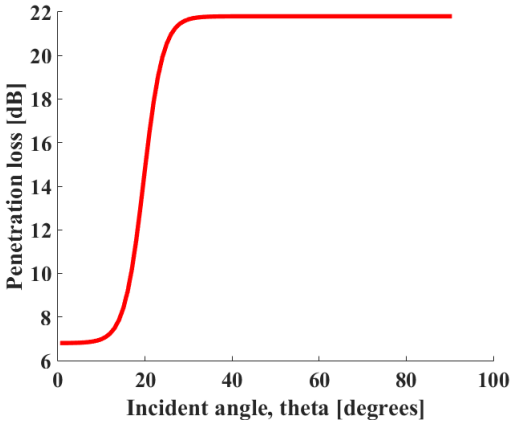

Figure 4.2 Building penetration loss for high-SHF.

Note that there is a key tradeoff in the path loss models when the horizontal distance between the UAV and a user changes. When this horizontal distance increases, the free space path loss (i.e., L_F) increases as $d_{out,i}$ increases, while the building penetration loss (i.e., L_B) decreases as the incident angle (i.e., θ_i) decreases as shown in Figure 4.2.

4.3 Providing Wireless Coverage Using a Single UAV

4.3.1 Problem Formulation

Consider a transmission between a UAV located at (x_{UAV},y_{UAV},z_{UAV}) and an indoor user i located at (x_i,y_i,z_i). The date rate for user i is given by:

$$C_i = Blog_2(1 + \frac{P_{t,i}/L_i}{N})$$

where B is the transmission bandwidth of the UAV, $P_{t,i}$ is the UAV transmit power to indoor user i, L_i is the path loss between the UAV and an indoor user i and N is the noise power. In this work, we do not explicitly model interference, and instead, implicitly model it as noise.

Let us assume that each indoor user has a channel with bandwidth equals B/M, where M is the number of users inside the building and the rate requirement for each user is v. Then the minimum power required to satisfy this rate for each user is given by:

$$P_{t,i,min} = (2^{\frac{v.M}{B}} - 1) \times N \times L_i$$

Our goal is to find the optimal location of UAV such that the total transmit power required to satisfy the downlink rate requirement of each indoor user is minimized. The objective function can be represented as:

$$P = \sum_{i=1}^{M} (2^{\frac{v.M}{B}} - 1) \times N \times L_i,$$

where P is the UAV total transmit power. Since $(2^{\frac{v.M}{B}} - 1) \times N$ is constant, our problem can be formulated as:

$$\min_{x_{UAV}, y_{UAV}, z_{UAV}} L_{Total} = \sum_{i=1}^{M} L_i$$

$$subject\ to$$

$$x_{min} \leq x_{UAV} \leq x_{max},$$

$$y_{min} \leq y_{UAV} \leq y_{max},$$

$$z_{min} \leq z_{UAV} \leq z_{max},$$

$$L_{Total} \leq L_{max}$$

where the first three constraints represent the minimum and maximum allowed values for x_{UAV}, y_{UAV} and z_{UAV}. In the fourth constraint, L_{max} is the maximum allowable path loss and equals $P_{t,max}/((2^{\frac{v.M}{B}} - 1) \times N)$, where $P_{t,max}$ is the maximum transmit power of UAV.

Finding the optimal placement of UAV is generally difficult because the problem is non-convex. Therefore, in the next subsection, we consider three special cases of practical interest and derive efficient solutions under these cases.

4.3.2 Efficient Placement of a Single UAV

Case 1. *The worst location in building:* In this case, we find the minimum transmit power required to cover the building based on the location that has the maximum path loss inside the building. The locations that have the maximum path loss are located at the corners of the highest and lowest floors, where these locations have the maximum $d_{out,i}$, maximum θ_i, and maximum $d_{in,i}$. Since the locations that have the maximum path loss inside the building are the corners of the highest and lowest floors, we place the UAV at the middle of the building (y_{UAV}= 0.5y_b and z_{UAV}=0.5z_b). Here, the corners of the highest and lowest floors represent the cell edges and the middle of the building represents the center of the cell. Then, given Outdoor-to-Indoor path loss models for low-SHF and high-SHF bands, we need to find an efficient horizontal point x_{UAV} for the UAV such that the total transmit power required to cover the building is minimized.

Now, when the horizontal distance between the UAV and this location increases, the free space path loss also increases as $d_{out,i}$ increases, while the building penetration loss decreases because we decrease the incident angle θ_i. In Figure 4.3, we demonstrate the minimum transmit power required to cover a building of different heights, where the minimum transmit power required to cover the building is given by:

$$P_{t,min}(dB) = P_{r,th} + L_i$$

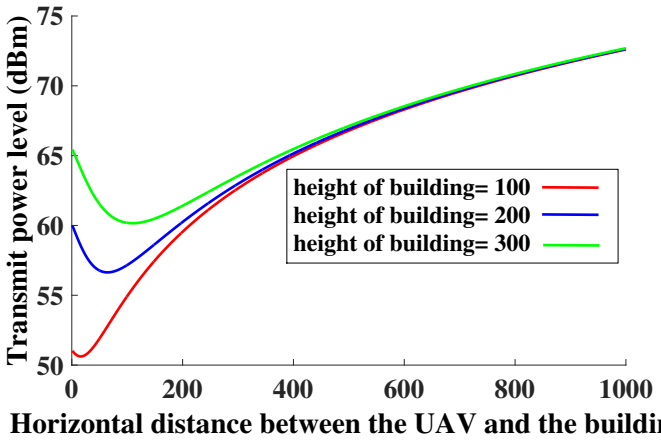

Figure 4.3 Transmit power required to cover the building.

$$P_{r,th}(dB) = N + \gamma_{th}$$

where $P_{r,th}$ is the minimum received power, N is the noise power (equals -120dBm), γ_{th} is the threshold SNR (equals 10dB), y_b=50 meters , x_b=20 meters and the carrier frequency is 2Ghz. The numerical results show that there is an optimal horizontal point that minimizes the total transmit power required to cover a building. Also, we note that when the height of the building increases, the optimal horizontal distance increases. This is to compensate for the increased building penetration loss due to an increased incident angle.

In Theorem 3, we characterize the optimal incident angle θ for low-SHF band that minimizes the transmit power required to cover the building. This helps us finding the optimal horizontal distance between the UAV and the building.

Theorem 3. *For the low-SHF operating frequency case, when we place the UAV at the middle of building , the optimal incident angle θ that minimizes the transmit power required to cover the building will be equal to 48.654^o and the optimal horizontal distance between the UAV and the building will be equal to* $((\frac{0.5z_b}{tan(48.654^o)})^2 - (0.5y_b)^2)^{0.5} - x_b$.

Proof. In order to find the optimal horizontal point, we rewrite the equation that represents the path loss in terms of the incident angle (θ_i) and the altitude difference between the UAV and the user i (Δh_i):

$$L_i(\Delta h_i, \theta_i) = w \log_{10} \frac{\Delta h_i}{\sin \theta_i} + w \log_{10} f_{Ghz} + g_1 \\ + g_2 + g_3(1 - \cos \theta_i)^2 + g_4 d_{in,i}$$

Since we place the UAV at the middle of the building and the locations that have the maximum path loss are located at the corners of the highest and lowest floors, the altitude difference between the UAV and the location that has the maximum path loss is constant for a given building. Now, when we take the first derivative with respect to θ and assign it to zero, we get:

$$\begin{aligned} \frac{dL(\theta)}{d\theta} &= \frac{w}{ln10} \frac{\frac{-\Delta h. \cos \theta}{\sin^2 \theta}}{\frac{\Delta h}{\sin \theta}} + 2g_3 \sin \theta (1 - \cos \theta) = 0 \\ \frac{dL(\theta)}{d\theta} &= \frac{-w}{ln10} \frac{\cos \theta}{\sin \theta} + 2g_3 \sin \theta (1 - \cos \theta) = 0 \\ \frac{w}{ln10} \cos \theta &= 2g_3 sin^2 \theta (1 - \cos \theta) \\ \frac{w}{ln10} \cos \theta &= 2g_3 (1 - \cos^2 \theta)(1 - \cos \theta) \\ 2g_3 \cos^3 \theta - 2g_3 \cos^2 \theta &- (\frac{w}{ln10} + 2g_3) \cos \theta + 2g_3 = 0 \end{aligned} \tag{4.1}$$

To prove that the function is convex, we take the second derivative and we get:

$$\frac{d^2 L}{d\theta^2} = \frac{w}{ln10} \frac{1}{\sin^2 \theta} + 2g_3 \cos \theta (1 - \cos \theta) + 2g_3 \sin^2 \theta > 0 \quad for\ 0 < \theta \leq 90$$

Equation (4.1) has only one valid solution which is $\cos \theta$=0.6606. Therefore, the optimal incident angle between the UAV and the location that has the maximum path loss inside the building will be 48.654^o.

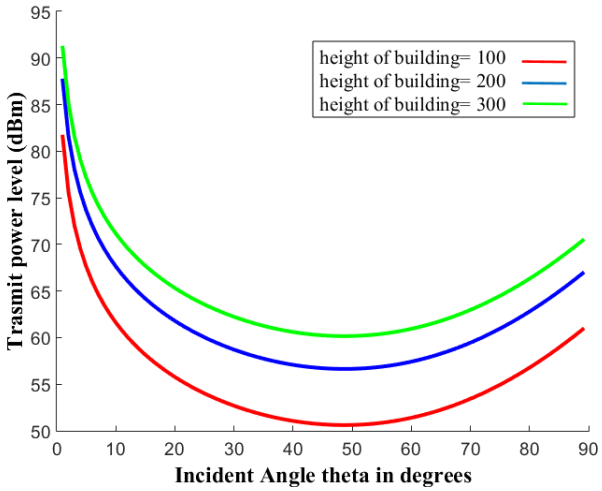

Figure 4.4 Transmit power required to cover the building, f_c=2 GHz.

In order to find the optimal horizontal distance between the UAV and the building, we apply the pythagorean's theorem. This gives us:

$$d_H = ((\frac{0.5z_b}{tan(48.654^o)})^2 - (0.5y_b)^2)^{0.5}$$

Therefore, the optimal horizontal distance between the UAV and the building is given by:

$$d_{opt} = ((\frac{0.5z_b}{tan(48.654^o)})^2 - (0.5y_b)^2)^{0.5} - x_b$$

□

In Figure 4.4, we demonstrate the transmit power required to cover the building as a function of the incident angle, we notice that the optimal angle that we characterize in Theorem 3 gives us the minimum transmit power.

Now, we find an efficient incident angle θ for high-SHF band that minimizes the transmit power required to cover the building. In order to find an efficient angle, we rewrite the equation that represents the path loss in terms of the incident angle (θ) and the

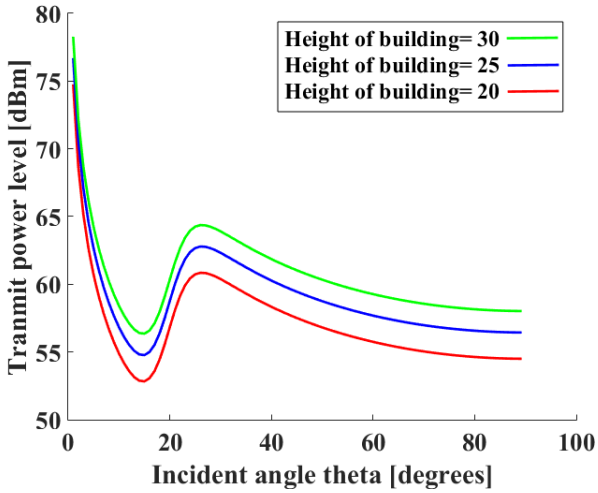

Figure 4.5 Transmit power required to cover the building, f_c=10 GHz.

altitude difference between the UAV and location that has the maximum path loss inside the building (Δh), we get:

$$L(\Delta h, \theta) = (\alpha_1 + \alpha_2 \log_{10} \frac{\Delta h}{\sin \theta} + \alpha_3 \log_{10} f_{Ghz}) + (\beta_1 + \frac{\beta_2 - \beta_1}{1 + exp(-\beta_3(\theta_i - \beta_4))}) + (\gamma_1 d_{in,i})$$

By numerically plotting the transmit power required to cover the location that has the maximum path loss inside the building (see Figures 4.5 and 4.6), where y_b=50 meters and x_b=20 meters, we show that for different building heights and different operating frequencies there exists only one global minimum value. As can be seen from the figures, to provide wireless coverage to small buildings, the UAV transmit power must be very high, due to the high free space path loss, this demonstrates the need for multiple UAVs to cover the high rise building when we use high-SHF operating frequency. To find an efficient incident angle that could give us the global minimum value, we use the ternary search algorithm [57]. The pseudo code of this algorithm is shown in Algorithm 2. A ternary search algorithm is a method for finding the minimum of a unimodal function, it

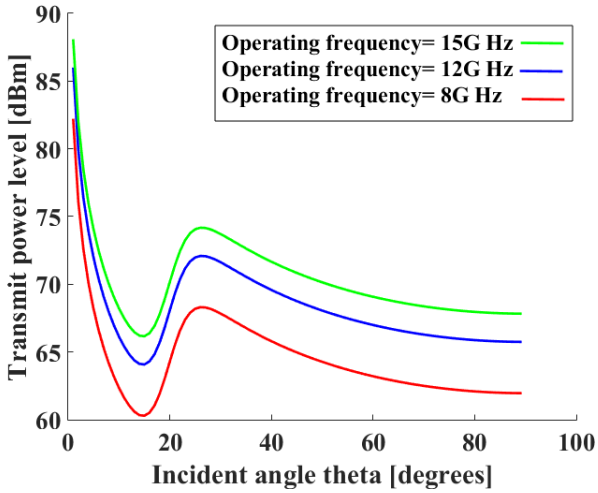

Figure 4.6 Transmit power required to cover 30 meters building height.

iteratively splits the domain into three separate regions (steps 6-7) and discards the one where the minimum does not belong to (steps 8-11). The ternary search algorithm is known to have a time complexity of $O(logn)$, where n is the input data size. From our numerical results, we found that the angle that minimizes the power is always 15^o. This is because the building penetration loss will be minimized at this angle (see Figure 4.2). The angles less than 15^o will also give us minimum building penetration loss but the free space path loss will increase as the incident angle θ_i decreases. Note that for the high-SHF case the incident angle that results in the minimum path loss is smaller than that for low-SHF case. This is due to the fact that the building penetration loss at high operating frequency will be higher than that at low operating frequency.

Case 2. *The locations of indoor users are symmetric across the xy and xz planes:* In this case, we assume that the locations of indoor users are symmetric across the xy plane and the xz plane (such as office buildings or hotels). Under the assumption that the $z = 0$ plane divides the building into two equal halves as shown in Figure 4.7, the locations of indoor users are symmetric across the xy plane when each user i at location

Algorithm 2 Ternary search algorithm

1: **Input:**
2: The interval [a,b] of unimodal function that contains the efficient incident angle.
3: The absolute precision $=\mu$.
4: **If** $|b\text{-}a| < \mu$:
5: **Return** $\frac{(a+b)}{2}$
6: $l = a + \frac{(b-a)}{3}$
7: $r = b - \frac{(b-a)}{3}$
8: **If** $f(l) > f(r)$
9: **Return** ternary_search(f, l, b, μ)
10: **Else**
11: **Return** ternary_search(f, a, r, μ)

(x_i, y_i, z_i) has a symmetric point with user j at location (x_i, y_i, -z_i). Similarly, under the assumption that the $y = 0$ plane divides the building into two equal halves, the locations of indoor users are symmetric across the xz plane when each user i at location (x_i, y_i, z_i) has a symmetric point with user j at location (x_i, -y_i, z_i), where $i, j \in M$. First, we prove that z_{UAV}=$0.5z_b$ and y_{UAV}=$0.5y_b$ when the locations of indoor users are symmetric across the xy and xz planes and the operating frequency is low-SHF (Theorem 4) or high-SHF (Theorem 5). Then we use the gradient descent algorithm [58] to find an efficient x_{UAV} that minimizes the transmit power required to cover the building.

Theorem 4. *For the low-SHF operating frequency case, when the locations of indoor users are symmetric across the xy and xz planes, the optimal (y_{UAV},z_{UAV}) that minimizes the power required to cover the indoor users will be equal ($0.5y_b$,$0.5z_b$).*

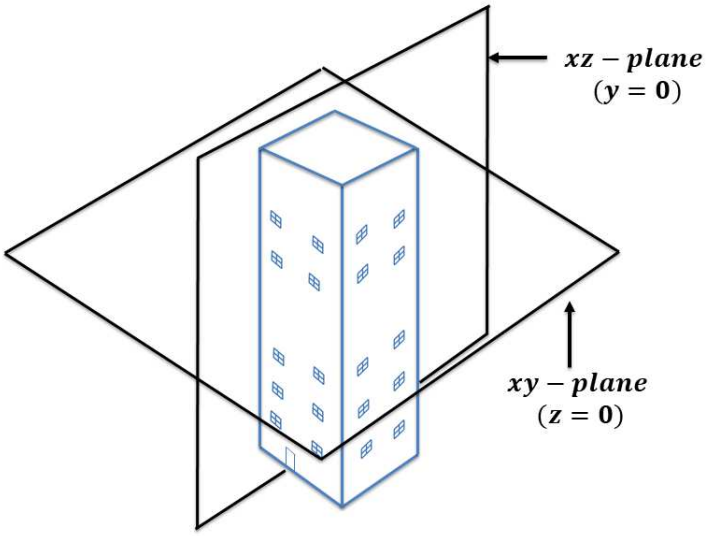

Figure 4.7 xy-plane and xz-plane.

Proof. Consider that m_1 represents the users that have altitude lower than the UAV altitude and m_2 represents the users that have altitude higher than the UAV altitude, then:

$$d_{out,i} = ((x_{UAV} - x_i)^2 + (y_{UAV} - y_i)^2 + (z_{UAV} - z_i)^2)^{0.5}, \ \ \forall z_{UAV} > z_i$$

$$d_{out,i} = ((x_{UAV} - x_i)^2 + (y_{UAV} - y_i)^2 + (z_i - z_{UAV})^2)^{0.5}, \ \ \forall z_{UAV} < z_i$$

Also,

$$cos_{\theta_i} = \frac{((x_{UAV} - x_i)^2 + (y_{UAV} - y_i)^2)^{0.5}}{((x_{UAV} - x_i)^2 + (y_{UAV} - y_i)^2 + (z_{UAV} - z_i)^2)^{0.5}}, \ \ \forall z_{UAV} > z_i$$

$$cos_{\theta_i} = \frac{((x_{UAV} - x_i)^2 + (y_{UAV} - y_i)^2)^{0.5}}{((x_{UAV} - x_i)^2 + (y_{UAV} - y_i)^2 + (z_i - z_{UAV})^2)^{0.5}}, \ \ \forall z_{UAV} < z_i$$

Rewrite the total path loss:

$$L_{Total} = \sum_{i=1}^{m_1}(wlog_{10}(d_{out,i}) + g_3(1 - \cos\theta_i)^2) + \sum_{i=1}^{m_2}(wlog_{10}(d_{out,i}) + g_3(1 - \cos\theta_i)^2) + K$$

Where:

$$K = \sum_{i=1}^{M}(wlog_{10}f_{Ghz} + g_1 + g_2 + g_4 d_{in,i})$$

Now, take the derivative with respect to z_{UAV}, we get:

$$\frac{dL_{Total}}{dz_{UAV}} = \sum_{i=1}^{m_1} \frac{w}{ln10} \frac{(z_{UAV} - z_i)}{((x_{UAV} - x_i)^2 + (y_{UAV} - y_i)^2 + (z_{UAV} - z_i)^2)} + 2g_3.(1 - \frac{((x_{UAV} - x_i)^2 + (y_{UAV} - y_i)^2)^{0.5}}{((x_{UAV} - x_i)^2 + (y_{UAV} - y_i)^2 + (z_{UAV} - z_i)^2)^{0.5}}). (\frac{((x_{UAV} - x_i)^2 + (y_{UAV} - y_i)^2)^{0.5}(z_{UAV} - z_i)}{((x_{UAV} - x_i)^2 + (y_{UAV} - y_i)^2 + (z_{UAV} - z_i)^2)^{\frac{3}{2}}}) + \sum_{i=1}^{m_2} \frac{w}{ln10} \frac{-(z_i - z_{UAV})}{((x_{UAV} - x_i)^2 + (y_{UAV} - y_i)^2 + (z_i - z_{UAV})^2)} + 2g_3.(1 - \frac{((x_{UAV} - x_i)^2 + (y_{UAV} - y_i)^2)^{0.5}}{((x_{UAV} - x_i)^2 + (y_{UAV} - y_i)^2 + (z_i - z_{UAV})^2)^{0.5}}). (\frac{-((x_{UAV} - x_i)^2 + (y_{UAV} - y_i)^2)^{0.5}(z_i - z_{UAV})}{((x_{UAV} - x_i)^2 + (y_{UAV} - y_i)^2 + (z_i - z_{UAV})^2)^{\frac{3}{2}}})$$

Rewrite the $\frac{dL_{Total}}{dz_{UAV}}$ again, we have:

$$\frac{dL_{Total}}{dz_{UAV}} = \sum_{i=1}^{m_1} \frac{w}{ln10} \frac{(z_{UAV} - z_i)}{d_{out,i}^2} + 2g_3.(1 - \frac{((x_{UAV} - x_i)^2 + (y_{UAV} - y_i)^2)^{0.5}}{d_{out,i}}). (\frac{((x_{UAV} - x_i)^2 + (y_{UAV} - y_i)^2)^{0.5}(z_{UAV} - z_i)}{d_{out,i}^3}) + \sum_{i=1}^{m_2} \frac{w}{ln10} \frac{-(z_i - z_{UAV})}{d_{out,i}^2} + 2g_3.(1 - \frac{((x_{UAV} - x_i)^2 + (y_{UAV} - y_i)^2)^{0.5}}{d_{out,i}}). (\frac{-((x_{UAV} - x_i)^2 + (y_{UAV} - y_i)^2)^{0.5}(zi - z_{UAV})}{d_{out,i}^3})$$

The equation above equals zero when the UAV altitude equals the half of the building height, where the locations of indoor users are symmetric across the xy and xz planes.

□

The question now is how to find an efficient horizontal point x_{UAV} that minimizes the total transmit power. In order to find this point, we use the gradient descent algorithm:

$$x_{UAV,n+1} = x_{UAV,n} - a\frac{dL_{Total}}{dx_{UAV,n}}$$

Algorithm 3 Efficient x_{UAV} using gradient descent algorithm

1: **Input:**
2: The 3D locations of the users inside the building.
3: The step size a, the step tolerance ϵ.
4: The dimensions of the building $[0, x_b] \times [0, y_b] \times [0, z_b]$.
5: The maximum number of iterations N_{max}.
6: **Initialize** x_{UAV}
7: **For** n=1,2,..., N_{max}
8: $x_{UAV,n+1} \leftarrow x_{UAV,n} - a\frac{dL_{Total}}{dx_{UAV,n}}$
9: **If** $\| x_{UAV,n} - x_{UAV,n+1} \| < \epsilon$
10: **Return:** $x_{UAV,opt} = x_{UAV,n+1}$
11: **End for**

Where:

$$\frac{dL_{Total}}{dx_{UAV}} = \sum_{i=1}^{M} \frac{w}{ln10} \frac{-(x_i - x_{UAV})}{d_{out,i}^2} + 2g_3.(1 - \frac{((x_i - x_{UAV})^2 + (y_i - y_{UAV})^2)^{0.5}}{d_{out,i}}).$$
$$(\frac{(x_i - x_{UAV}) d_{out,i} ((x_i - x_{UAV})^2 + (y_i - y_{UAV})^2)^{-0.5}}{d_{out,i}^2} -$$
$$\frac{((x_i - x_{UAV})^2 + (y_i - y_{UAV})^2)^{0.5} (x_i - x_{UAV}) d_{out,i}^{-1}}{d_{out,i}^2})$$

a: the step size.

$d_{out,i}$=$((x_i - x_{UAV})^2 + (y_i - y_{UAV})^2 + (z_i - z_{UAV})^2)^{0.5}$

The pseudo code of this algorithm is shown in Algorithm 3. The algorithm uses the gradient of the function to find the nearest local minimum. The algorithm begins with an initial guess of the solution x_{UAV} (step 6). Then, it takes the gradient of the function at that point and generates the next iteration by taking a step along the negative gradient direction (step 8). The algorithm will converge when the gradient is zero (steps 9-11). Now, we prove that $z_{UAV} = 0.5z_b$ and $y_{UAV} = 0.5y_b$ when the locations of indoor users are symmetric across the xy and xz planes and the operating frequency is high-SHF.

Theorem 5. *For the high-SHF operating frequency case, when the locations of indoor users are symmetric across the xy and xz planes, the optimal (y_{UAV}, z_{UAV}) that minimizes the power required to cover the indoor users will be equal ($0.5y_b$,$0.5z_b$).*

Proof. Consider that m_1 represents the users that have altitude lower than the UAV altitude and m_2 represents the users that have altitude higher than the UAV altitude, then:

$$d_{out,i} = ((x_{UAV} - x_i)^2 + (y_{UAV} - y_i)^2 + (z_{UAV} - z_i)^2)^{0.5}, \quad \forall z_{UAV} > z_i$$

$$d_{out,i} = ((x_{UAV} - x_i)^2 + (y_{UAV} - y_i)^2 + (z_i - z_{UAV})^2)^{0.5}, \quad \forall z_{UAV} < z_i$$

Also,

$$\theta_i = sin^{-1}(\frac{(z_{UAV} - z_i)}{((x_{UAV} - x_i)^2 + (y_{UAV} - y_i)^2 + (z_{UAV} - z_i)^2)^{0.5}}), \quad \forall z_{UAV} > z_i$$

$$\theta_i = sin^{-1}(\frac{(z_i - z_{UAV})}{((x_{UAV} - x_i)^2 + (y_{UAV} - y_i)^2 + (z_i - z_{UAV})^2)^{0.5}}), \quad \forall z_{UAV} < z_i$$

Rewrite the total path loss:

$$L_{Total} = \sum_{i=1}^{m_1} \alpha_2 log_{10}(d_{out,i}) + \frac{(\beta_2 - \beta_1)}{(1 + exp(-\beta_3(sin^{-1}(u) - \beta_4)))} + \sum_{i=1}^{m_2} \alpha_2 log_{10}(d_{out,i}) + \frac{(\beta_2 - \beta_1)}{(1 + exp(-\beta_3(sin^{-1}(u) - \beta_4)))} + K$$

Where:

$$u = (\frac{(z_{UAV} - z_i)}{((x_{UAV} - x_i)^2 + (y_{UAV} - y_i)^2 + (z_{UAV} - z_i)^2)^{0.5}}), \quad \forall z_{UAV} > z_i$$

$$u = (\frac{(z_i - z_{UAV})}{((x_{UAV} - x_i)^2 + (y_{UAV} - y_i)^2 + (z_i - z_{UAV})^2)^{0.5}}), \quad \forall z_{UAV} < z_i$$

$$K = \sum_{i=1}^{M} (\alpha_1 + \alpha_3 log_{10} f_{Ghz} + \beta_1 + \gamma_1 d_{in,i})$$

Now, take the derivative with respect to z_{UAV}, we get:

$$\frac{dL_{Total}}{dz_{UAV}} = \sum_{i=1}^{m_1} \frac{\alpha_2}{ln10} \frac{(z_{UAV} - z_i)}{((x_{UAV} - x_i)^2 + (y_{UAV} - y_i)^2 + (z_{UAV} - z_i)^2)}$$
$$+(\frac{-(\beta_2 - \beta_1)(\frac{-\beta_3}{\sqrt{1-u^2}})(\frac{d_{out,i} - (z_{UAV} - z_i)^2 d_{out,i}^{-1}}{d_{out,i}^2})}{(1 + exp(-\beta_3(sin^{-1}u - \beta_4)))} . \frac{exp(-\beta_3(sin^{-1}u - \beta_4))}{(1 + exp(-\beta_3(sin^{-1}u - \beta_4)))}) +$$
$$\sum_{i=1}^{m_2} \frac{\alpha_2}{ln10} \frac{-(z_i - z_{UAV})}{((x_{UAV} - x_i)^2 + (y_{UAV} - y_i)^2 + (z_i - z_{UAV})^2)}$$
$$+(\frac{-(\beta_2 - \beta_1)(\frac{-\beta_3}{\sqrt{1-u^2}})(\frac{-d_{out,i} + (z_{UAV} - z_i)^2 d_{out,i}^{-1}}{d_{out,i}^2})}{(1 + exp(-\beta_3(sin^{-1}u - \beta_4)))} . \frac{exp(-\beta_3(sin^{-1}u - \beta_4))}{(1 + exp(-\beta_3(sin^{-1}u - \beta_4)))})$$

The equation above equals zero when the UAV altitude equals the half of the building height, where the locations of indoor users are symmetric across the xy and xz planes. □

To find an efficient horizontal point x_{UAV} that minimizes the total transmit power, we use the gradient descent algorithm, where:

$$\frac{dL_{Total}}{dx_{UAV}} = \sum_{i=1}^{M} \frac{\alpha_2}{ln10} \frac{(x_{UAV} - x_i)}{d_{out,i}^2} + (\frac{-(\beta_2 - \beta_1)(\frac{-\beta_3}{\sqrt{1-u^2}})(\frac{-(z_{UAV} - z_i)(x_{UAV} - x_i)}{d_{out,i}^3})}{(1 + exp(-\beta_3(sin^{-1}u - \beta_4)))} .$$
$$\frac{exp(-\beta_3(sin^{-1}u - \beta_4))}{(1 + exp(-\beta_3(sin^{-1}u - \beta_4)))})$$

$d_{out,i}$=$((x_i - x_{UAV})^2 + (y_i - y_{UAV})^2 + (z_i - z_{UAV})^2)^{0.5}$

u=$(\frac{(z_{UAV} - z_i)}{((x_{UAV} - x_i)^2 + (y_{UAV} - y_i)^2 + (z_{UAV} - z_i)^2)^{0.5}})$

Case 3. *The locations of indoor users are uniformly distributed in each floor:* In this case, we propose the Particle Swarm Optimization (PSO) [59] to find an efficient 3D placement of the UAV, when the locations of indoor users are uniformly distributed in each floor. In general, the PSO algorithm can be used for any type of distribution as done in [22]. The pseudo code of the PSO algorithm is shown in Algorithm 4.

Algorithm 4 Efficient UAV placement using PSO algorithm

Input:

The lower and upper bounds of decision variable (v_{min}, v_{max}), Construction coefficients (κ,ϕ_1,ϕ_2), Maximum number of iterations (t_{max}), Population size (W)

Initialiaztion:

ϕ=ϕ_1+ϕ_1, χ = $2\kappa/|2-\phi-(\phi^2-4\phi)^{0.5}|$

w=χ, c_1=$\chi\phi_1$, c_2=$\chi\phi_2$, $C_{global.best} = inf$

for i=1:W

  Each particle i starts at a random initial position:

  $Q(i) = uniformrandom(v_{min}, v_{max}, v_{size})$

  Each particle i starts with zero velocity:

  $V(i) = zeros(v_{size})$

  Find the cost of particle i:

  $C(i) = costfunction(Q(i))$

  Let the best location of particle i equals the current location:

  $Q(i)_{best} = Q(i)$

  Let the best cost of particle i equals the current cost:

  $C(i)_{best} = C(i)$

  if $C(i)_{best} < C_{global.best}$

    $C_{global.best} = C(i)_{best}$

  end if

end

PSO Loop:

for $t = 1 : t_{max}$

  for i=1:W

    Find the velocity, position and cost for particle i:

    $V(i) = w * V(i) + c_1 * rand(v_{size}). * (Q(i)_{best} - Q(i))$
    $+c_2 * rand(v_{size}). * (Q_{global.best} - Q(i))$

    $Q(i) = Q(i) + V(i)$

    $C(i) = costfunction(Q(i))$

    if $C(i) < C(i)_{best}$

      $Q(i)_{best} = Q(i)$

      $C(i)_{best} = C(i)$

      Find an efficient placement of a UAV:

      if $C(i)_{best} < C_{global.best}$

        $Q_{global.best} = Q(i)_{best}$

      end if

    end if

  end

end

The particle swarm optimization algorithm starts with (W) random solutions (steps 6-15) and iteratively tries to improve the candidate solutions based on the best experience of each candidate ($Q(i)_{best}$) and the best global experience ($Q_{global.best}$). In each iteration (steps 17-29), the best location for each particle ($Q(i)_{best}$) and the best global location ($Q_{global.best}$) are updated and the velocities and locations of the particles are calculated based on them [22]. The velocity value indicates how much the location can be changed. The velocity is given by:

$$V(i) = w * V(i) + c_1 * rand(v_{size}). * (Q(i)_{best} - Q(i))$$

$$+c_2 * rand(v_{size}). * (Q_{global.best} - Q(i))$$

where w is the inertia weight, c_1 and c_2 are the personal and global learning coefficients, and $rand(v_{size})$ is a random positive number. Also, the location of each particle is updated as:

$$Q(i) = Q(i) + V(i)$$

The time complexity of PSO algorithm will depend on the number of candidate solutions (W) and the number of iterations (t_{max}). Convergence of the candidate solutions has been investigated for PSO [60]. This analyses has resulted in guidelines for selecting a set of coefficients (κ,ϕ_1,ϕ_2) that are believed to cause convergence to a point and prevent divergence of the swarms particles. We selected our parameters according to this analysis (see Table 4.1 and Algorithm 4 (steps 4-5)).

4.4 Providing Wireless Coverage Using Multiple UAVs

Providing wireless coverage to High-rise building using a single UAV can be impractical, due to the limited transmit power of a UAV. The transmit power required to cover the building is too high. It is in the range of 50 dBm to 65 dBm (see Figures 4.3-4.6), which corresponds to 100-3000 watts. In this section, the UAVs adopt a frequency division multiple access (FDMA) technique to provide wireless coverage for the indoor users in which the total bandwidth B is divided to multiple subchannels, and we allocate one subchannel to each indoor user. Therefore, there is no interference between UAVs. Furthermore, the authors in [61] show that significant power gains are attainable for indoor users even in rich indoor scattering conditions, if the indoor users use directional antennas. Our problem can be formulated as:

$$
\begin{aligned}
&\min |k| \\
&\text{subject to} \\
&\sum_{j=1}^{|k|} y_{ij} = 1 && \forall i \in m \quad (4.2.a) \\
&\sum_{i=1}^{|m|} (2^{\frac{v.|m|}{B}} - 1).N.L_{ij}.y_{ij} \leq P && \forall j \in k \quad (4.2.b) \\
&x_{min} \leq x_j \leq x_{max} && \forall j \in k \quad (4.2.c) \\
&y_{min} \leq y_j \leq y_{max} && \forall j \in k \quad (4.2.d) \\
&z_{min} \leq z_j \leq z_{max} && \forall j \in k \quad (4.2.e)
\end{aligned}
\tag{4.2}
$$

where k is the set of UAVs required to provide wireless coverage for indoor users, m is the set of indoor users that requests a wireless coverage, v is the rate requirement for each user (constant), N is the noise power (constant), B is the transmission bandwidth (constant), L_{ij} is the total path loss between UAV j and user i and P is the maximum transmit power

of UAV (constant). We also introduce the binary variable y_{ij} that takes the value of 1 if the indoor user i is connected to the UAV j and equals 0 otherwise. The objective is to minimize the number of UAVs that are needed to provide a wireless coverage for indoor users. Constraint set (4.2.a) ensure that each indoor user should be connected to one UAV. Constraint set (4.2.b) ensure that the total power consumed by a UAV should not exceed its maximum power consumption limit. Constraints (4.2.c-4.2.e) represent the minimum and maximum allowed values for x_j, y_j and z_j.

Theorem 6. *The problem represented by (4.2) is NP-complete.*

Proof. The number of constraints is polynomial in terms of the number of indoor users, UAVs and 3D locations. Given any solution for our problem, we can check the solutions feasibility in polynomial time, then the problem is NP.

To prove that the problem is NP-hard, we reduce the Bin Packing Problem which is NP-hard [40] to a special case of our problem. In the Bin Packing Problem, we have a set of items $G = \{1, 2, .., N\}$ in which each item has volume z_n where $n \in G$. All items must be packed into a finite number of bins (b_1, b,...,b_B), each of volume V in a way that minimizes the number of bins used. The reduction steps are: 1) The b-th bin in the Bin Packing Problem is mapped to the j-th UAV in our problem, where the volume V for each bin is mapped to the maximum transmit power of the UAV P. 2) The n-th item is mapped to the indoor i-th user, where the volume for each item n is mapped to the power required to cover the i-th indoor user. 3) All UAVs have the same maximum transmit power P. 4) The power required to cover the i-th indoor user from any 3D location will be constant. If there exists a solution to the bin packing problem with cost C, then the selected bins will

represent the UAVs that are selected and the items in each bin will represent the indoor users that the UAV must cover and the total cost of our problem is C. □

Due to the intractability of the problem, we consider clustering of indoor users. The pseudo code of clustering indoor users is shown in Algorithm 5. In the k-means clustering algorithm [62], we are given a set of points m, and want to group the points into k clusters such that each point belongs to the cluster with the nearest mean. The first step in the algorithm is to choose the number of clusters k. Then, randomly initialize k clusters centroids (step 6). In each iteration, the algorithm will do two things:1) Cluster assignment step. 2) Move centroids step (step 7). In cluster assignment step, the algorithm goes through each point and chooses the closest centroids and assigns the point to it. In move centroids step, the algorithm calculates the average for each group and moves the centroids there. The algorithm will repeat these two steps until it converges. The algorithm will converge when the assignments no longer change. The k-means clustering algorithm is known to have a time complexity of $O(km)$, where k is the number of clusters and m is the number of points. To find the minimum number of UAVs required to cover the indoor users, we utilize this algorithm to cluster the indoor users. In our algorithm, we assume that each cluster will be covered by only one UAV. We start the algorithm with $k = 2$ (step 4) and after it finishes clustering the indoor users, it applies the particle swarm optimization [59] to find the UAV 3D location and UAV transmit power needed to cover each cluster. Then, it checks if the maximum transmit power is sufficient to cover each cluster, if not, the number of clusters k is incremented by one and the problem is solved again (steps 8-9).

Algorithm 5 Clustering Indoor Users

1: **Input:**

2: The maximum transmit power of UAV (P).

3: The 3D locations of m indoor users (x_i, y_i, z_i).

4: Number of clusters $(|k| = 2)$.

5: **START:**

6: Initialize cluster centroids $\gamma_1, \gamma_2, ..., \gamma_k \in R^n$ randomly.

7: Repeat until convergence:

For every indoor user $i \in m$, set

$$c^{(i)} = arg \min_{j \in k} ||(x_i, y_i, z_i) - \gamma_j||^2$$

For each cluster $j \in k$, set

$$\gamma_j = \frac{\sum_{i \in m, c^{(i)} = j} (x_i, y_i, z_i)}{\sum_{i \in m, c^{(i)} = j} 1}$$

8: Using particle swarm optimization algorithm, calculate the UAV efficient 3D location and the transmit power for each cluster $j \in k$:

$$P(j) = \sum_{i \in m, c^{(i)} = j} (2^{\frac{v.|m|}{B}} - 1) \star N \star L_i$$

9: **For** $j = 1\ to\ |k|$

If $(P(j) > P)$

$|k| = |k| + 1$

go to START

End

10: **Output:**

11: $|k|$ Clusters.

12: The transmit Power of each UAV.

13: The 3D locations of UAVs.

4.5 Numerical Results

4.5.1 Simulation Results for Single UAV

First, we verify our results for the second case, when the locations of indoor users are symmetric across the xy and xz planes, using different operating frequencies, 2GHz for

Table 4.1 Parameters in Numerical Analysis for Single UAV

Vertical width of building y_b	50 meters
Hight of each floor	5 meters
Step size a "GD algorithm"	0.01
Maximum number of iterations N_{max} "GD algorithm"	500
The carrier frequency f_{Ghz}, low-SHF	2Ghz
The carrier frequency f_{Ghz}, high-SHF	15Ghz
Number of users in each floor	20 users
(varmin,varmax) "PSO algorithm"	(0,1000)
(κ,ϕ_1,ϕ_2) "PSO algorithm"	(1,2.05,2.05)

low-SHF band and 15GHz for high-SHF. We assume that each floor contains 20 users. Then we apply the gradient descent (GD) algorithm to find the optimal horizontal point x_{UAV} that minimizes the transmit power required to cover the indoor users. Table 4.1 lists the parameters used in the numerical analysis for single UAV cases.

In Figures 4.8 and 4.9, we find the optimal horizontal points for a building of different heights. In the upper part of the figures, we find the total path loss at different locations (x_{UAV},0.5y_b,z_{UAV}) and the optimal horizontal point x_{UAV} that results in the minimum total path loss using the GD algorithm. In the lower part of the figures, we show the convergence speed of the GD algorithm. As can be seen from the figures, when the height of the building increases, the optimal horizontal point x_{UAV} increases. This is to compensate the increased building penetration loss due to an increased incident angle.

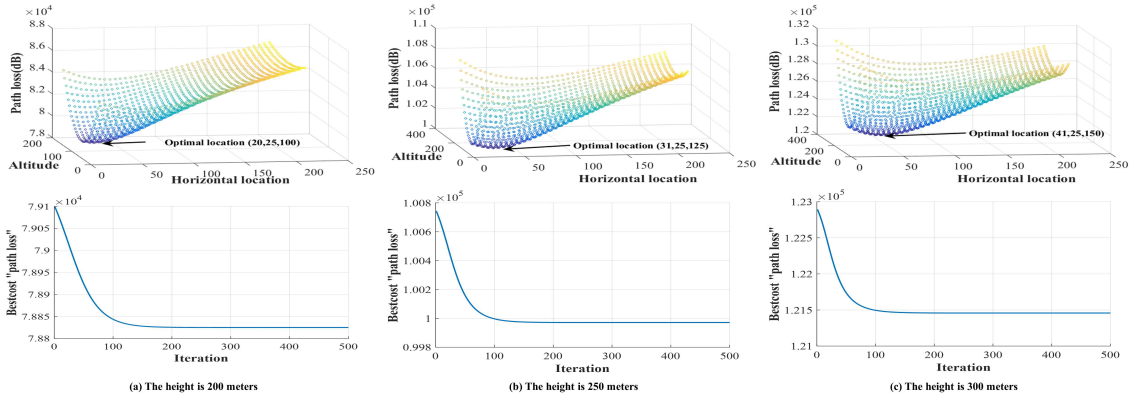

Figure 4.8 UAV optimal placement and convergence speed of the GD algorithm for different building heights, $f_c = 2G\ Hz$.

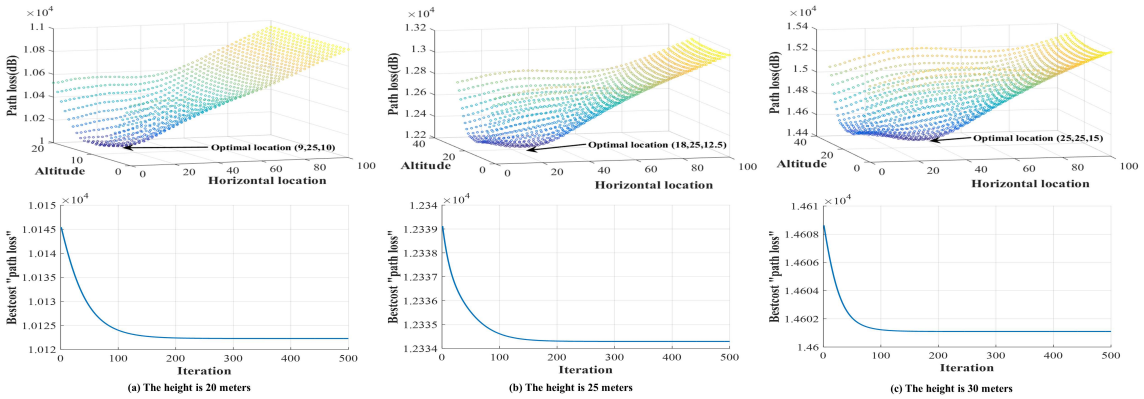

Figure 4.9 UAV optimal placement and convergence speed of the GD algorithm for different building heights, $f_c = 15G\ Hz$.

In Figures 4.10 and 4.11, we investigate the impact of different building widths (i.e., x_b). We fix the building height to be 250 meters for low-SHF operating frequency and 25 meters for high-SHF, then we vary the building width. As can be seen from the figures, when the building width increases, the optimal horizontal distance decreases. This is to compensate for the increased indoor path loss due to an increased building width.

Now, we validate the simulation results for low-SHF operating frequency by using the particle swarm optimization (PSO) algorithm and verify our result for the third case, when the locations of indoor users are uniformly distributed in each floor, using low-SHF operating frequency. As can be seen from the simulation results in Table 4.2, both

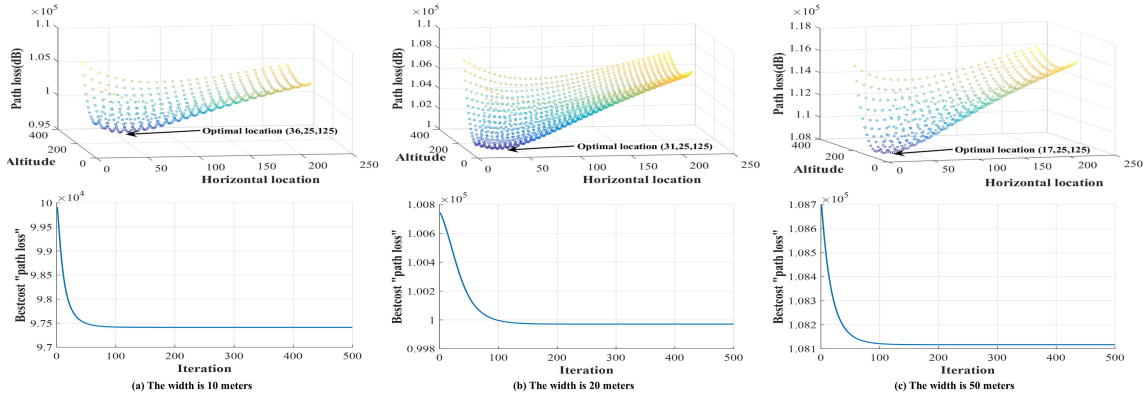

Figure 4.10 UAV optimal placement and convergence speed of the GD algorithm for different building widths, $f_c = 2G\ Hz$.

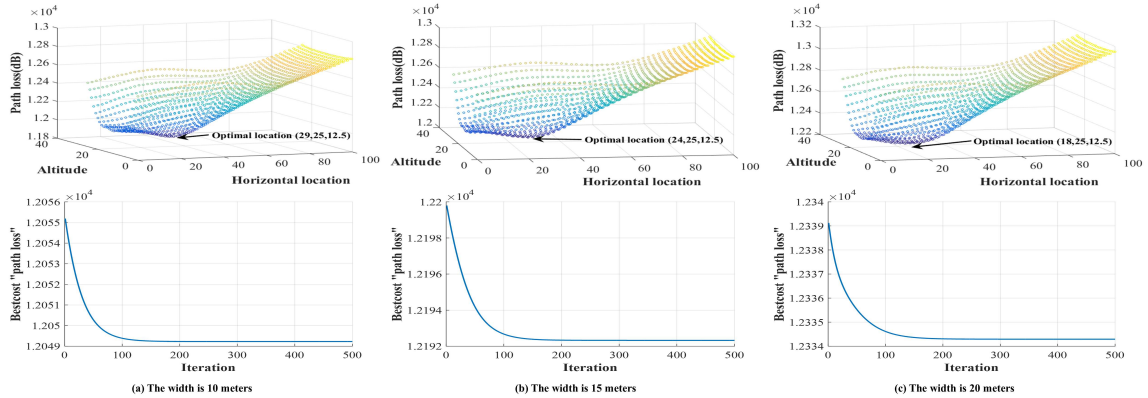

Figure 4.11 UAV optimal placement and convergence speed of the GD algorithm for different building widths, $f_c = 15G\ Hz$.

algorithms converge to the same 3D placement, when the locations of indoor users are symmetric across the xy and xz planes.

After that, we assume that each floor contains 20 users and the locations of these users are uniformly distributed in each floor. When we apply the GD algorithm, the 3D efficient placements and the total costs for 200 meter, 250 meter and 300 meter buildings are (24.7254, 25, 100) ($7.8853 * 10^4$), (33.8180, 25, 125) ($9.9855 * 10^4$) and (43.1170, 25, 150)($1.2154 * 10^5$), respectively. UAV efficient placement and the convergence speed of the PSO algorithm for different building heights is shown in Figure 4.12. The 3D efficient placements and the total costs for 200 meter, 250 meter and 300 meter buildings are

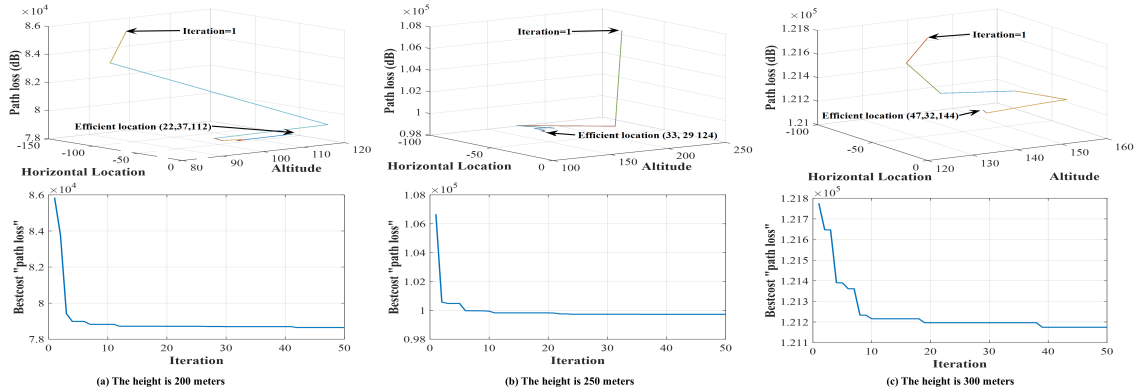

Figure 4.12 UAV efficient placement and convergence speed of the PSO algorithm for different building heights.

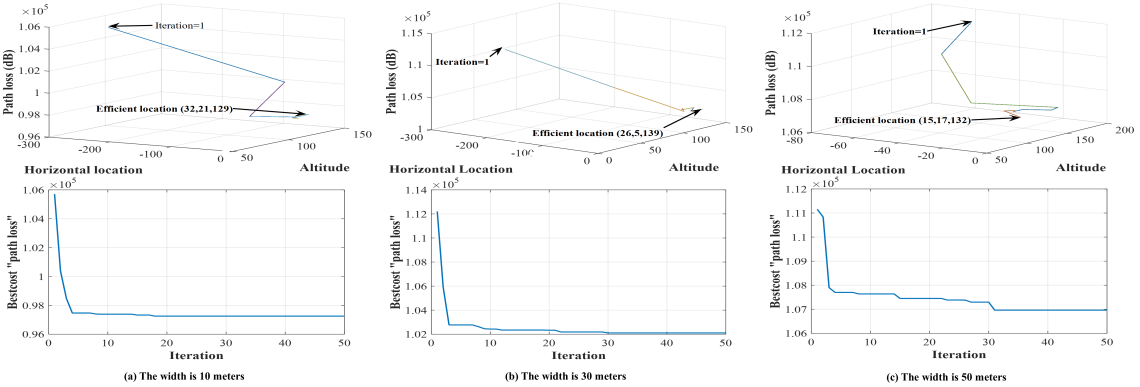

Figure 4.13 UAV efficient placement and convergence speed of the PSO algorithm for different building widths.

(21.7995, 37.3891, 111.7901) ($7.8645 * 10^4$), (32.9212, 28.7125, 124.0291) ($9.9725 * 10^4$) and (46.5898, 31.5061 ,143.8588)($1.2117 * 10^5$), respectively. As can be seen from the simulation results in Table 4.3, the PSO algorithm provides better results. It provides total cost less than the cost that the GD algorithm provides by (37dB-208dB). This is because the PSO algorithm is designed for the case in which the locations of indoor users are uniformly distributed in each floor. On the other hand, the GD algorithm is designed for the case in which the locations of indoor users are symmetric across the dimensions of each floor.

Table 4.2 Simulation Results: Validate the Simulation Results for the Second Case

Algorithm	z_b	x_b	y_b	Efficient 3D placement	Efficient total path loss(dB)
GD	200	20	50	(20.025, 25, 100)	$7.8825 * 10^4$
PSO	200	20	50	(20.040, 25.0130, 100.0015)	$7.8825 * 10^4$
GD	250	20	50	(30.809, 25, 125)	$9.9971 * 10^4$
PSO	250	20	50	(30.736 , 24.960, 124.956)	$9.9971 * 10^4$
GD	300	20	50	(40.746, 25, 150)	$1.2146 * 10^5$
PSO	300	20	50	(40.758, 25.048, 150.054)	$1.2146 * 10^5$

We also investigate the impact of different building widths (i.e., x_b) using the GD and PSO algorithms (see Figure 4.13). We fix the building height to be 250 meters and vary the building width. As can be seen from the simulation results, the PSO algorithm provides better results. It provides total cost less than the cost that the GD algorithm provides by (57dB-161dB).

We can notice that the tradeoff in case three is similar to that in case two, when the height of the building increases, the efficient horizontal point x_{UAV} computed by our algorithm increases. This is to compensate the increased building penetration loss due to an increased incident angle. Also, when the building width increases, the efficient horizontal distance computed by our algorithm decreases. This is to compensate the increased indoor path loss due to an increased building width.

Table 4.3 Simulation Results: Verify the Results for the Third Case

Algorithm	z_b	x_b	y_b	Efficient 3D placement	Efficient total path loss(dB)
GD	200	20	50	(24.725, 25, 100)	$7.8853 * 10^4$
PSO	200	20	50	(21.799, 37.389, 111.790)	$7.8645 * 10^4$
GD	250	20	50	(33.818, 25, 125)	$9.9855 * 10^4$
PSO	250	20	50	(32.921, 28.712, 124.029)	$9.9725 * 10^4$
GD	300	20	50	(43.117, 25, 150)	$1.2154 * 10^5$
PSO	300	20	50	(46.589, 31.506 ,143.858)	$1.2117 * 10^5$
GD	250	10	50	(38.521, 25, 125)	$9.7413 * 10^4$
PSO	250	10	50	(32.104, 21.017, 129.266)	$9.7252 * 10^4$
GD	250	30	50	(29.393, 25, 125)	$1.0275 * 10^5$
PSO	250	30	50	(25.529, 4.938, 138.765)	$1.0211 * 10^5$
GD	250	50	50	(22.711, 25, 125)	$1.0753 * 10^5$
PSO	250	50	50	(14.548, 17.308 ,131.8940)	$1.0696 * 10^5$

4.5.2 Simulation Results for Multiple UAVs

In this section, we verify our results for multiple UAVs scenario. First, we assume that a building will host a special event (such as concert, conference, etc.), the dimensions of the building are $[0, 20] \times [0, 50] \times [0, 100]$. The organizers of the event reserve all floors higher than 75 meters and they expect that 200 people will attend the event. Due to interference from near-by macro cells, the organizers decide to use UAVs to provide wireless coverage to the indoor users. We assume that 200 indoor users are uniformly

Table 4.4 Parameters in Numerical Analysis for Multiple UAVs

Maximum transmit power of UAV (P)	5 Watt
Operating frequency (f)	2Ghz
Transmission bandwidth (B)	50M Hz
Rate requirement for each user (υ)	2.2Mbps
Noise power (N)	-150 dBm
Min and Max allowed values for x_j,$[x_{min}, x_{max}]$	[25,1000]
Min and Max allowed values for y_j, $[y_{min}, y_{max}]$	[0,50]
Min and Max allowed values for z_j, $[z_{min}, z_{max}]$	[0,1000]

distributed in upper part of the building (higher than 75 meters) and 200 indoor users are uniformly distributed in the lower part (less than 75 meters). Then, we apply the clustering indoor users algorithm to find the minimum number of UAVs required to cover the indoor users. Table 4.4 lists the parameters used in the numerical analysis for multiple UAVs.

The algorithm starts with $k = 2$ and after it finishes clustering the indoor users, it applies the particle swarm optimization to find the UAV 3D location and UAV transmit power needed to cover each cluster. Then, it checks if the maximum transmit power is sufficient to cover each cluster, if not, the number of clusters k is incremented by one and the problem is solved again. As can be seen from the simulation results in Figure 4.14, we need 5 UAVs to cover the indoor users. We can notice that an efficient horizontal point x_{UAV} for all UAVs 3D locations is the same $x_{UAV} = 25$, the minimum allowed value for x_{UAV}, this is because the tradeoff (shown in Figure 4.3) disappears when a UAV covers small height of building.

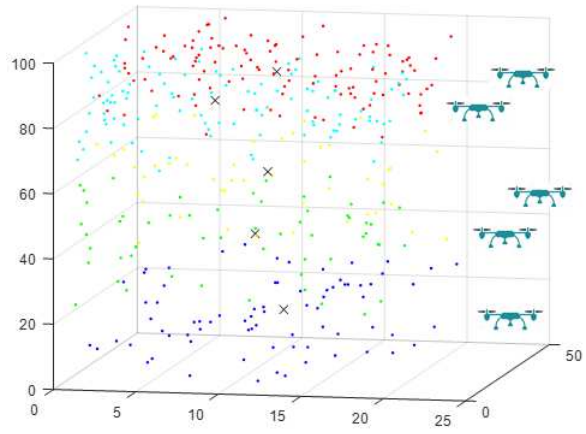

Figure 4.14 UAVs efficient placements using clustering algorithm.

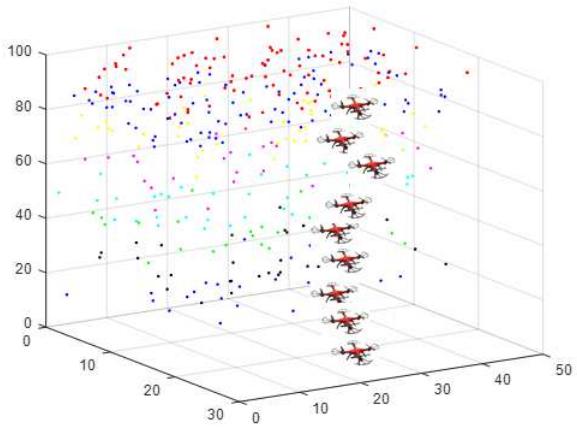

Figure 4.15 UAVs efficient placements using uniform split method.

In Figure 4.15, we uniformly split the building into k parts and cover it by k UAVs. As can be seen from the simulation results, we need 9 UAVs to cover the indoor users. The clustering algorithm provides better results, this is because it utilizes the distribution of indoor users to divide them into clusters. On the other hand, the uniformly split method is designed for the case in which the locations of indoor users uniformly distributed in the building.

CHAPTER 5

MAXIMIZING THE INDOOR WIRELESS COVERAGE USING UAVS

5.1 Introduction

In this chapter[1], we aim to maximize the indoor wireless coverage using UAVs equipped with directional antennas. We study the case that the UAVs are using one channel, thus in order to maximize the total indoor wireless coverage, we avoid any overlapping in their coverage volumes. We present two methods to place the UAVs; providing wireless coverage from one building side and from two building sides. In the first method, we utilize the circle packing theory to determine the 3-D locations of the UAVs in a way that the total coverage area is maximized. In the second method, we place the UAVs in front of two building sides and efficiently arrange the UAVs in alternating upside-down arrangements. Our results show that the upside-down arrangements of UAVs, can improve the total coverage by 100% compared to providing wireless coverage from one building side.

5.2 System Model

5.2.1 System Settings

Consider a $3D$ building, as shown in Figure 5.1, where N UAVs must be deployed to maximize the wireless coverage to indoor users located within the building. Let the dimensions of the high-rise building, in the shape of a rectangular prism, be $[0, x_b] \times [0, y_b] \times [0, z_b]$. Let ($x_k$, y_k, z_k) denote the 3D location of k-th UAV, and let (X_i, Y_i,

[1]The work of this chapter has been published in [63].

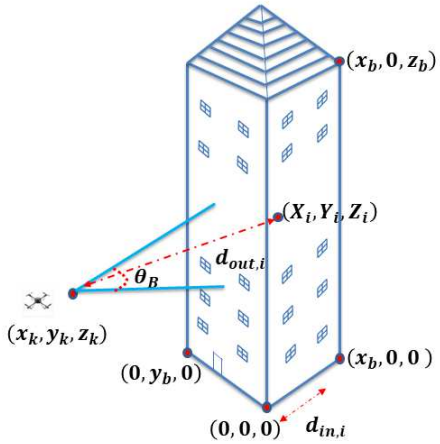

Figure 5.1 System model.

Z_i) denote the location of user i. Also, let $d_{out,i}$ be the distance between the UAV and indoor user i, and let $d_{in,i}$ be the distance between the building wall and indoor user i. Each UAV uses a directional antenna to provide wireless coverage where the antenna half power beamwidth is θ_B. The authors in [64] use an outdoor directional antenna to provide wireless coverage for indoor users. They show that the highest RSRP (Reference Signal Received Power) and throughput values are measured along the main beam direction, thus the radiation pattern of a directional antenna is a cone and the indoor volume covered by a UAV is a truncated cone, as shown in Figure 5.2. Here, r_i is the radius of the circle that is located at yz-rectangular side ((0,0,0), (0,0,z_b), (0,y_b,z_b), (0,y_b,0))), r_j is the radius of the circle that is located at yz-rectangular side ((x_b,0,0), (x_b,0,z_b), (x_b,y_b,z_b), (x_b,y_b,0)) and x_b is the horizontal width of the building. The volume of a truncated cone is given by:

$$V = \frac{1}{3}\pi x_b(r_i^2 + r_j^2 + r_i r_j) \tag{5.1}$$

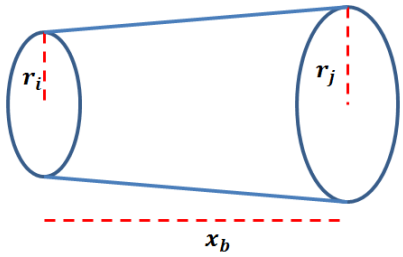

Figure 5.2 Three dimensions of a truncated cone.

5.2.2 User Received Power

In [61], the authors show that significant power gains are attainable for indoor users even in rich indoor scattering conditions, if the indoor users use directional antennas. Now, consider a transmission between k-th UAV located at (x_k, y_k, z_k) and i-th indoor user located at (X_i, Y_i, Z_i). The received signal power at i-th indoor user location can be given by:

$$P_{r,ik}(dB) = P_t + G_t + G_r - L_i \tag{5.2}$$

where $P_{r,ik}$ is the received signal power, P_t is the transmit power of UAV, G_t is the antenna gain of the UAV. It can be approximated by $G_t \approx \frac{29000}{\theta_B^2}$ with θ_B in degrees [18] and G_r is the antenna gain of indoor user i, which is given by [61]:

$$G_r(dB) = G_{r,dir} - G_{r,omni} - GRF \tag{5.3}$$

where $G_{r,dir}$ and $G_{r,omni}$ are free-space antenna gains of a directive and an omnidirectional antenna respectively and GRF is the decrease in gain advantage of a directive over an omnidirectional antenna, due to the presence of clutter.

Also, L_i is the path loss for the Outdoor-Indoor communication which can be represented by [55]:

$$L_i = L_F + L_B + L_I = (w \log_{10} d_{out,i} + w \log_{10} f_{Ghz} + g_1) + (g_2 + g_3(1 - \cos\theta_i)^2) + (g_4 d_{in,i}) \tag{5.4}$$

where L_F is the free space path loss, L_B is the building penetration loss, and L_I is the indoor loss. In the path loss model, we also have w=20, g_1=32.4, g_2=14, g_3=15, g_4=0.5 and f_{Ghz} is the carrier frequency.

5.3 Maximizing Indoor Wireless Coverage

In this section, the UAVs are assumed to be homogeneous having the same transmit power, the same horizontal location x_k, the same channel and the same antenna half power beamwidth θ_B. We show two methods to place the UAVs in a way that tries to maximize the total coverage and avoids any overlapping in their coverage volumes.

5.3.1 Providing Wireless Coverage from One Building Side

In this method, we place all UAVs in front of one building side (side A, side B or side C), see Figure 5.3. The objective is to determine the three-dimensional location of each UAV in a way that the total covered volume is maximized. Now, consider that we place the UAVs in front of building side A, then the projection of UAV's coverage on the building

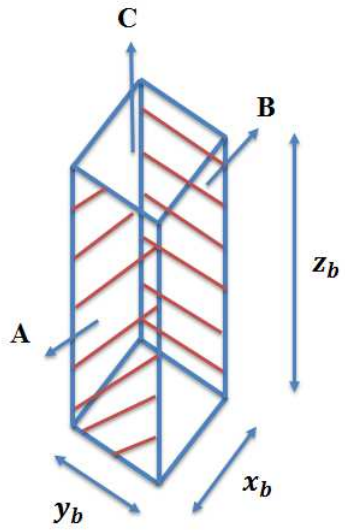

Figure 5.3 Building sides.

side B is a circle as shown in Figure 5.4. Our problem can be formulated as:

$$\max \ \ |N| \times \frac{1}{3}\pi x_b(r_i^2 + r_j^2 + r_i r_j)$$

$$subject\ to$$

$$\sqrt{(y_k - y_q)^2 + (z_k - z_q)^2} \geq 2r_j, \ \ k \neq q \in N \ \ (5.5.a)$$

$$z_b - (z_k + r_j) \geq 0, \ \ k \in N \qquad (5.5.b) \qquad (5.5)$$

$$(z_k - r_j) \geq 0, \ \ k \in N \qquad (5.5.c)$$

$$y_b - (y_k + r_j) \geq 0, \ \ k \in N \qquad (5.5.d)$$

$$(y_k - r_j) \geq 0, \ \ k \in N \qquad (5.5.e)$$

The objective is to maximize the indoor wireless coverage (covered volume), where $|N|$ is the number of UAVs. Constraint set (5.5.a) guarantees that truncated cones cannot overlap. Constraint sets (5.5.b-5.5.e) ensure that UAV should not cover outside the $3D$ building, see Figure 5.4. We model this problem by utilizing the well-known circle packing problem [65]. In this problem, N circles should be packed inside a given surface

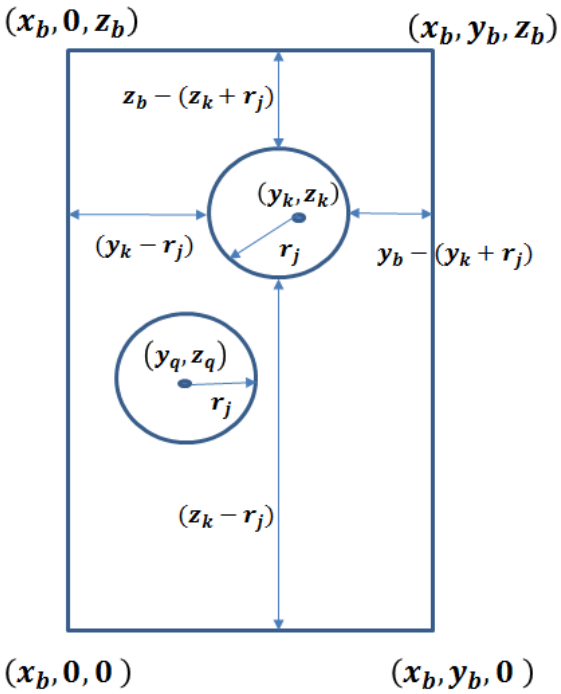

Figure 5.4 Circle packing in a rectangle.

such that the packing density is maximized and no overlapping occurs, note that the surface in our problem is a rectangle. The authors of [65] tackle this problem by solving a number of decision problems. The decision problem is:

Given N circles of radius r_j and a rectangle of dimension $y_b \times z_b$, whether is it possible to locate all the circles into the rectangle or not.

They introduce a nonlinear model for this problem. Finding the answer for the decision problem will depend on finding the global minimizer of a nonconvex and nonlinear optimization problem. In each decision problem, they investigate the feasibility of packing N identical circles. If this is feasible, N is incremented by one and the decision problem is solved again. The algorithm will stop when the decision problem yields an infeasible packing [66]. The pseudo code of the algorithm is shown in Algorithm 6. In the next section, we utilize the two building sides to maximize the indoor wireless coverage. This

Algorithm 6 Circle packing in a rectangle

1: $N \longleftarrow 1$
2: Solve the decision problem for N circles
3: If Answer $=$ YES
4: **Then** $N \longleftarrow N + 1$
5: **Return** to step 2
6: If Answer $=$ NO
7: $N \longleftarrow N - 1$
8: **End**
9: **Output** N

will allow us to extend the indoor wireless coverage compared with providing wireless coverage from one building side, because the holes induced by the cones of the UAVs of one side can be filled by the cones induced by the UAVs of the other side without causing overlap among the two sets of cones.

5.3.2 Providing Wireless Coverage from Two Building Sides

In this method, we place the UAVs in front of two building sides (side A and side B) and efficiently arrange the UAVs in alternating upside-down arrangements. In Theorem 7, we find the horizontal location of the UAV x_{UAV} that guarantees the upside-down arrangements of the truncated cones. In Theorem 8, we prove that if the truncated cones do not intersect in 3D, then the circles do not intersect in building sides (A and B), and vice versa. In Theorem 9, we prove that if we maximize the percentage of covered area of building sides (A and B), then we maximize the percentage of covered volume of building, and vice versa. These theorems enable us to transform the geometric problem from 3D to 2D and present an efficient algorithm to maximize the indoor wireless coverage.

Theorem 7. *The horizontal location of the UAV x_{UAV} that guarantees the upside-down arrangements of the truncated cones will be equal to $0.7071x_b$ regardless of the antenna half power beamwidth angle θ_B.*

Proof. The radius of the smaller circular face r_i is given by:

$$r_i = r_j \frac{x_{UAV}}{x_b + x_{UAV}} \tag{5.6}$$

Now, we divide the building sides A and B to square cells (as shown in Figures 5.5 and 5.6), the large circle in Figure 5.5 and the small circle in Figure 5.6 will represent the projections of UAV's coverage on building sides A and B when the UAV is placed in front of building side B. Similarly, the four small circle quarters in Figure 5.5 and the four large circle quarters in Figure 5.6 will represent the projections of UAVs coverage on building sides A and B when the UAVs are placed in front of building side A. From Figures 5.5 and 5.6, the diagonal of the square cell is given by $D = 2r_j + 2r_i$, where r_j is the radius of the larger circular face and r_i is the radius of the smaller circular face. By applying the pythagoreans theorem, we get:

$$r_i = \frac{\sqrt{8} - 2}{2} r_j = \gamma r_j \tag{5.7}$$

From equations (5.6) and (5.7), we get:

$$\frac{x_{UAV}}{x_b + x_{UAV}} = \frac{\sqrt{8}-2}{2} \Longrightarrow x_{UAV} = x_b \frac{(\sqrt{8}-2)}{(4-\sqrt{8})} = 0.7071 x_b \qquad \square$$

Thus, to guarantee the upside-down arrangements of the truncated cones, we must place the UAVs at horizontal distance equals to $0.7071x_b$. Theorems 8 and 9 enable us to transform the geometric problem from 3D to 2D.

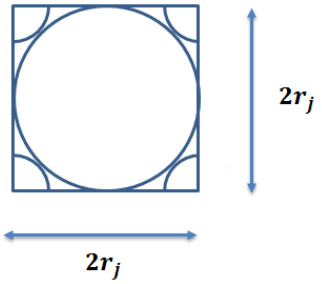

Figure 5.5 Square cell in side A.

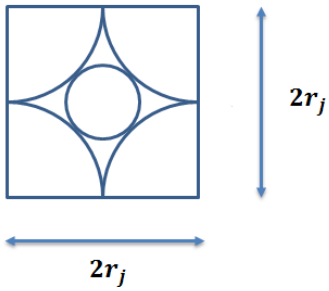

Figure 5.6 Square cell in side B.

Theorem 8. *The truncated cones do not intersect in 3D iff The circles do not intersect in building sides (A and B).*

Proof. First, we prove that if the truncated cones do not intersect in $3D$, then the circles do not intersect in building sides (A and B). Assume that we have a set of truncated cones $G = \{1, 2, ..., N\}$ and they do not intersect in 3D space. Each truncated cone $n \in G$ can be represented by a number of $2D$ circles $\{c_{1n}, c_{2n}, ..., c_{|h|n}\}$, where $|h|$ is the height of the truncated cone, c_{1n} is the smaller circular face and $c_{|h|n}$ is the larger circular face. It is obvious that if the $|G|$ truncated cones do not intersect in $3D$ space then the smaller and larger circular faces do not intersect in building sides (A and B).

Second, we prove that if the circles do not intersect in building sides (A and B), then the truncated cones do not intersect in $3D$. Assume that four circles (with large radius r_j) not intersect in building side A (see Figure 5.7), then the circles (with small radius r_i) in building side B will appear as shown Figure 5.8. Now, we need to do two steps: 1) Connect the lines between these points ($A_{|h|}$ with A_1, $B_{|h|}$ with B_1, $C_{|h|}$ with C_1 and $D_{|h|}$ with D_1). 2) Draw circles that pass through four points A_k, B_k, C_k and D_k where $k \in h$. After these two steps, the circles that have been drawn in step two will represent

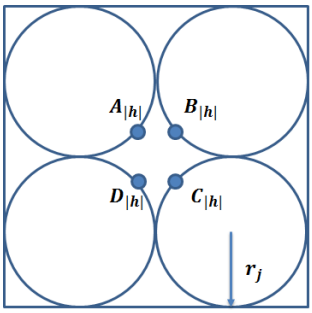

Figure 5.7 Four circles (with radius r_j) in building side A.

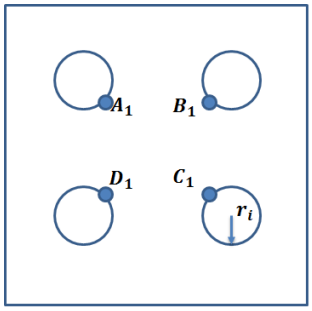

Figure 5.8 Four circles (with radius r_i) in building side B.

a truncated cone that his circular bases do not intersect with the four circles in building sides (A and B). Also, the truncated cones do not intersect in 3D space. □

Theorem 9. *We maximize the percentage of covered area of building sides (A and B) iff We maximize the percentage of covered volume of building.*

Proof. First, we divide the building sides A and B to square cells (as shown in Figures 5.5 and 5.6). The percentage of covered volume is given by:

$$V = \frac{\lfloor \frac{(y_b z_b)}{4r_j^2} \rfloor 2(\frac{\pi}{3} x_b(r_i^2 + r_i r_j + r_j^2))}{(x_b y_b z_b)} \tag{5.8}$$

Where:

$\lfloor \frac{(y_b z_b)}{4r_j^2} \rfloor$: the number of square cells in the building side.

2: the number of truncated cones in the square cell (see Figures 5.5 and 5.6).

$\frac{\pi}{3} x_b(r_i^2 + r_i r_j + r_j^2)$: the volume of truncated cone.

$(x_b y_b z_b)$: the volume of the building. Now, from equations (5.7) and (5.8), we get:

$$V = \frac{\lfloor \frac{(y_b z_b)}{4r_j^2} \rfloor (\frac{2\pi}{3})(\gamma^2 + \gamma + 1) r_j^2}{(y_b z_b)} = K_1 \lfloor \frac{(y_b z_b)}{4r_j^2} \rfloor r_j^2, \tag{5.9}$$

The percentage of covered area of building sides (A and B) is given by:

$$W = \frac{\lfloor \frac{(y_b z_b)}{4r_j^2} \rfloor (\pi r_i^2 + \pi r_j^2)}{(y_b z_b)} + \frac{\lfloor \frac{(y_b z_b)}{4r_j^2} \rfloor (\pi r_i^2 + \pi r_j^2)}{(y_b z_b)} = \frac{\lfloor \frac{(y_b z_b)}{4r_j^2} \rfloor 2\pi (r_i^2 + r_j^2)}{(y_b z_b)} \tag{5.10}$$

Now, from equations (5.7) and (5.10), we get:

$$W = \frac{\lfloor \frac{(y_b z_b)}{4r_j^2} \rfloor 2\pi(\gamma^2 + 1) r_j^2}{(y_b z_b)} = K_2 \lfloor \frac{(y_b z_b)}{4r_j^2} \rfloor r_j^2, \tag{5.11}$$

where $K_1 = \frac{(\frac{2\pi}{3})(\gamma^2+\gamma+1)}{(y_b z_b)}$, $K_2 = \frac{(2\pi)(\gamma^2+1)}{(y_b z_b)}$. From equations (5.9) and (5.11), maximizing the percentage of covered volume of building V is equivalent to maximizing the percentage of covered area of building sides (A and B) W, and vice versa, where K_1 and K_2 are constants. □

In Algorithm 7, we maximize the covered volume by placing the UAVs in alternating upside-down arrangements. First, we find the horizontal distance between the building and the UAVs $x_{UAV} = 0.7071 x_b$ (see Theorem 7) that guarantees the alternating upside-down arrangements. Then, we divide the building sides A and B to square cells and place one UAV in front of the square cell. In steps (8-16), we find the $3D$ locations of UAVs that cover the building from side B. On the other hand, steps (17-25) find the $3D$ locations of UAVs that cover the building from side A. Finally, the algorithm will output the total number of UAVs and the total covered volume.

5.4 Simulation Results

Let the dimensions of the building, in the shape of a rectangular prism, be $[0, x_b = 30] \times [0, y_b = 40] \times [0, zb = 60]$. We use three methods to cover the building using UAVs. In the first method, we place all UAVs in front of one building side (A or B) (FOBS). In the

Algorithm 7 Maximizing Indoor Wireless Coverage

Input:
The dimensions of building x_b, y_b and z_b
The radius of the larger circular face r_j
Initialization:
$r_i = \dfrac{\sqrt{8}-2}{2} r_j$
$x_{UAV} = 0.7071 x_b$
$u = q = 0$
The $3D$ locations of UAVs that cover the building from side B are given by:
For $k_1 = 1 : \lfloor \dfrac{y_b}{2r_j} \rfloor$
    For $s_1 = 1 : \lfloor \dfrac{z_b}{2r_j} \rfloor$
        $u = u + 1$
        $x_q = x_{UAV} + x_b$
        $y_u = (2k_1 - 1) r_j$
        $z_u = (2s_1 - 1) r_j$
    End
End
The $3D$ locations of UAVs that cover the building from side A are given by:
For $k_2 = 1 : \lfloor \dfrac{y_b}{3r_j} \rfloor$
    For $s_2 = 1 : \lfloor \dfrac{z_b}{3r_j} \rfloor$
        $q = q + 1$
        $x_q = -x_{UAV}$
        $y_q = (2k_2) r_j$
        $z_q = (2s_2) r_j$
    End
End
Output:
The number of UAVs$= u + q$
The covered volume$=(u+q)(\frac{\pi}{3} x_b (r_i^2 + r_i r_j + r_j^2))$

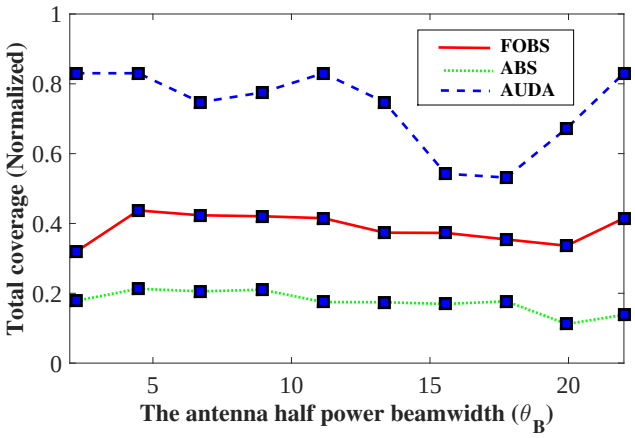

Figure 5.9 Total coverage vs. θ_B.

second method, we place all UAVs above the building (C) (ABS). In the third method, we arrange the UAVs in alternating upside-down arrangements (AUDA). In Figure 5.9, we find the maximum total coverage for different antenna half power beamwidth angles θ_B. As can be seen from the simulation results, the maximum total coverage is less than half for the FOBS and ABS methods, this is because providing wireless coverage from one building side will only maximize the covered area of the building side. On the other hand, we improve the maximum total coverage by applying the AUDA, this is because AUDA will allow us to use a higher number of UAVs to provide wireless coverage compared with providing wireless coverage from one building side, as shown in Figure 5.10.

In order to provide full wireless coverage, we utilize multiple channels to cover the holes. We start the coverage process with one channel and then we fill the holes using UAVs with multiple channels until we cover the whole building. In Figure 5.11, we find the total number of UAVs required to provide full coverage. As can be seen from the figure, FOBS and ABS need high number of UAVs to guarantee full wireless coverage, due to the irregular shapes of the holes in the building. Here, we can easily specify the number of UAVs required to cover each hole, due to the small projections of the holes

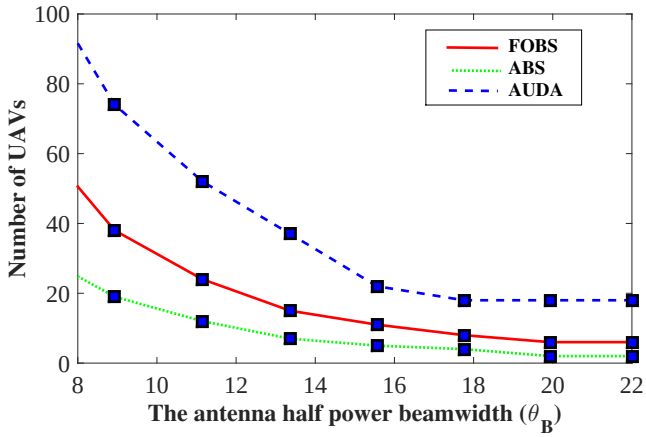

Figure 5.10 Number of UAVs vs. θ_B.

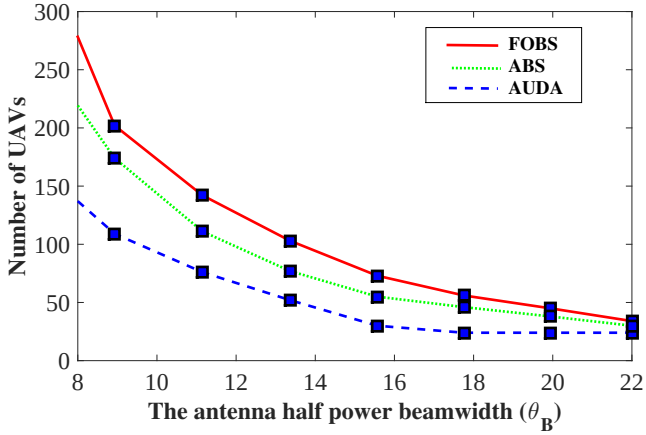

Figure 5.11 Number of UAVs vs. θ_B.

in the building side. On the other hand, AUDA needs fewer number of UAVs to provide full wireless coverage, due to the small-regular shapes of the uncovered spaces inside the building. Here, we need only one UAV to cover each hole. In Figure 5.12, we find the total transmit power consumed by UAVs when the building is fully covered. Here, we assume that the threshold SNR equals 25dB, the noise power equals -120dBm, the frequency of the channel is 2GHz and the antenna gain of each indoor user is 14.4 dB [61]. As can be seen from the figure, the total transmit power in all methods is very small, due to the high gain of the directional antennas. Also, we can notice that the total power consumed

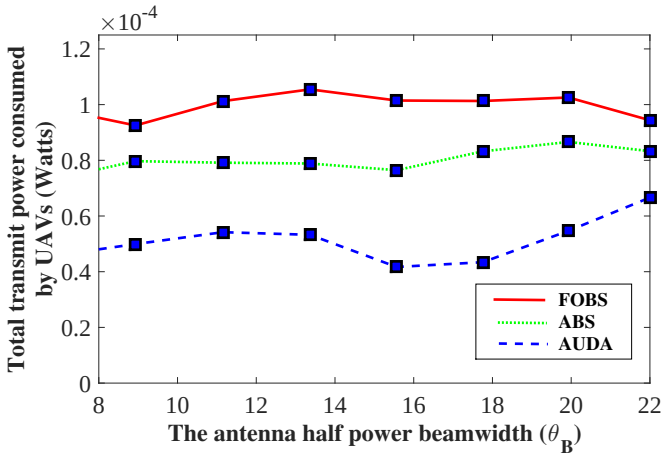

Figure 5.12 Total transmit power vs. θ_B.

in FOBS and ABS is higher than that of AUDA. This is because the number of UAVs required to fully cover the building in AUDA is fewer than that for FOBS and ABS.

CHAPTER 6

MAXIMIZING THE LIFETIME OF WIRELESS DEVICES USING UAVS

6.1 Introduction

Prior studies on UAV-based wireless coverage typically consider downlink scenarios from a UAV to ground users[1]. The authors in [14] investigate the downlink coverage performance of a UAV, where the objective is to find the optimal UAV altitude which leads to the maximum ground coverage and the minimum transmit power. In [13], the authors consider the downlink scenario, where the goal is to minimize the total required transmit power of UAVs while satisfying the users rate requirements. In [46] and [47], the authors propose using a UAV to provide wireless coverage for indoor users during emergency cases and special events, where the objective is to find an efficient placement of a single UAV that minimizes the total transmit power required to cover the indoor users. Due to the limited transmit power of the UAV, the authors in [45] study the problem of minimizing the number of UAVs required to cover the indoor users.

Only few studies consider the uplink scenario in which the ground wireless devices transmit data to a UAV. The authors in [68] study the throughput maximization problem in UAV relaying systems by optimizing the source/relay transmit power along with the UAV trajectory, subject to practical mobility constraints. In [25], the authors present a UAV enabled data collection system, where a UAV is dispatched to collect a given amount of data from ground terminals at fixed location. They aim to find the optimal ground terminal

[1]The work of this chapter has been published in [67].

transmit power and UAV trajectory that achieve different Pareto optimal energy trade-offs between the ground terminal and the UAV.

Under disaster situations (such as earthquakes or floods), users may not be able to communicate with remote-undamaged terrestrial ground stations due to the limited transmit power of wireless devices. They are also not able to recharge their wireless devices due to physical damage to energy infrastructure. In the case of Hurricane Katrina, about 700,000 customers in Louisiana and almost 200,000 in Mississippi lost power [69]. In such situations, providing wireless coverage becomes more important, since people in the disaster area seek to learn about the emergency event, locate their family and friends, and receive commands to flee the disaster-affected area [70, 71]. In this chapter, we are motivated to explore how the placements of UAVs can enhance the time durations of uplink transmissions of wireless devices when the UAVs are used to provide wireless coverage for the users utilizing these devices under disaster situations.

6.2 System Model

We assume that a set of ground users I is located within a 2D geographical area, where each user $i \in I$ has a wireless device with residual energy E_i. We consider an uplink scenario in which the ground users adopt a frequency division multiple access (FDMA) technique to transmit data to a set of UAVs U at a desired data rate R as done in [72] and [73], where the UAVs are supported by backhaul links that interconnect them to together and connect them to the core of the Internet. To realize these links, we could use free space optics. FDMA allocates one subchannel to each user for communications and hence the channels do not interfere with one another [72]. Notice that the equal

bandwidth division in FDMA ensures fairness among the ground users [74]. We also assume that each user $i \in I$ is served by a UAV for a time duration τ_{iu} seconds and this time duration depends on the residual energy of wireless device represented by the battery level E_i and the placement of UAV u, where $u \in U$. Received Signal Strength Indicator (RSSI) sensors on board the UAVs measure the strength of RF signals across a range of frequencies. The received signals, although noisy due to the radio-propagation environment and sensor noise, can be used to determine the approximate locations of wireless devices using Bayesian filters [75] and Kalman filters [76], where running the localization algorithm has minimal effect on the power consumptions of wireless devices. We also assume that the ground wireless devices can send the values of residual energies to the UAVs using control messages [39].

In this chapter, we assume that the wireless channel between ground user i and UAV u is line of sight dominated, so that the free space path loss model is adopted similar to [68] and [25], where $i \in I$ and $u \in U$. In Section 6.4, we show that this assumption is realistic. The path loss is given as follows:

$$L_{iu} = \left(\frac{4\pi d_{iu} F}{c}\right)^2 \tag{6.1}$$

where $d_{iu} = \sqrt{(X_u - x_i)^2 + (Y_u - y_i)^2 + (Z_u)^2}$ is the distance between ground user i and UAV u, (x_i, y_i) is the 2D location of ground user i, (X_u, Y_u, Z_u) is the 3D location of UAV u, F is frequency (in Hz) and c is the speed of light (in m/s). Note that when the distance between a ground user and UAV (i.e., d_{iu}) increases, the required transmit power (i.e., p_{iu}) to satisfy a given data rate increases.

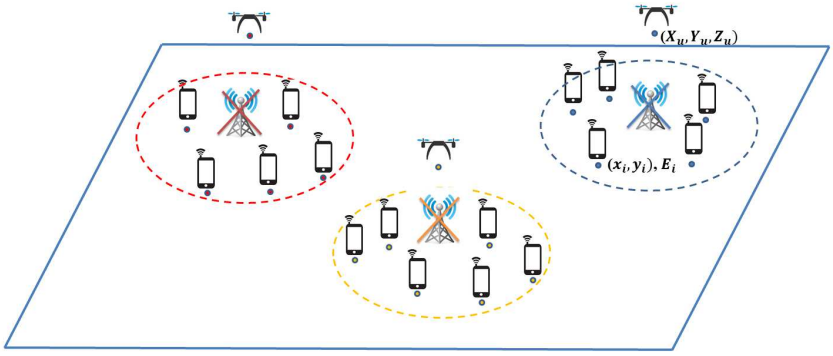

Figure 6.1 Ground users transmitting data to UAVs.

6.3 Problem Formulation

Consider a transmission between a user located at (x_i, y_i) and a UAV located at (X_u, Y_u, Z_u) that acts as an aerial base station to collect data from users as shown in Figure 6.1. The rate for user i is given by:

$$C_{iu} = B_i \log_2 \left(1 + \frac{p_{iu}/L_{iu}}{N}\right) \tag{6.2}$$

where B_i is the transmission bandwidth of user i, p_{iu} is the transmit power from user i to UAV u, L_{iu} is the path loss between user i and UAV u, and N is the noise power.

Let us assume that all users have the same data rate R and each user has a channel with bandwidth equals $B/|I|$, where B is the total available bandwidth in the system and $|I|$ is the number of ground users. FDMA allocates one subchannel to each user for communications and hence the user's transmissions do not interfere with one another. The minimum power required to satisfy the data rate R for each user is given by:

$$p_{iu} = \left(2^{\frac{R.|I|}{B}} - 1\right) N L_{iu} \tag{6.3}$$

In this chapter, the lifetime is defined as the time duration of uplink transmission until the first wireless device runs out of energy. Our goal is to find the optimal placements

of the $|U|$ UAVs such that the lifetime of wireless devices is maximized. Our problem can be formulated as:

$$\max_{(X_u,Y_u,Z_u),w_{iu},\tau_{iu}} \min_{i\in I,u\in U} \tau_{iu}$$

$$subject\ to$$

$$\begin{aligned}
&\sum_{u=1}^{|U|} w_{iu} = 1 && \forall i \in I && (6.4.a)\\
&w_{iu}\left(2^{\frac{R.|I|}{B}} - 1\right) NL_{iu} \leq P_{max} && \forall i \in I, \forall u \in U && (6.4.b)\\
&w_{iu}(\tau_{iu} - \tau_{th}) \geq 0 && \forall i \in I, \forall u \in U && (6.4.c)\\
&w_{iu}\tau_{iu}\left(2^{\frac{R.|I|}{B}} - 1\right) NL_{iu} \leq E_i && \forall i \in I, \forall u \in U && (6.4.d)\\
&x_{\min} \leq X_u \leq x_{\max} && \forall u \in U && (6.4.e)\\
&y_{\min} \leq Y_u \leq y_{\max} && \forall u \in U && (6.4.f)\\
&z_{\min} \leq Z_u \leq z_{\max} && \forall u \in U && (6.4.g)
\end{aligned} \tag{6.4}$$

where U is the set of UAVs that are utilized to serve the set of ground users I. We also introduce the binary variable w_{iu} that takes the value of 1 if the ground user i is connected to UAV u and equals 0 otherwise. The objective is to determine the locations of the UAVs such that the time duration of uplink transmission until the first wireless device runs out of energy is maximized. In order to maximize the duration of uplink transmission, each user will be connected to the nearest UAV. Constraint set (6.4.a) guarantees that each ground user should be connected to one UAV. Constraint set (6.4.b) ensures that the transmit power of each wireless device should not exceed its maximum transmit power P_{max}. Constraint set (6.4.c) guarantees that each ground user $i \in I$ is served by UAV for a time greater than τ_{th} seconds. Constraint set (6.4.d) ensures that the total energy

consumed by user's device should not exceed its battery energy level E_i. Constraint sets (6.4.e-6.4.g) represent the minimum and maximum allowable values for X_u, Y_u and Z_u, respectively.

Theorem 10. *The problem represented by (6.4) is NP-complete.*

Proof. The number of constraints is polynomial in terms of the number of ground users, number of UAVs, and locations. Given any solution to our problem, we can check the solution's feasibility in polynomial time; then, the problem is NP.

To prove that the problem is NP-hard, we reduce the p-center problem which is NP-hard [77], to a special case of our problem. In the p-center problem, we are given a set of demand points m and a set of facilities p where each demand point receives its service from the closest facility. The objective is to determine the locations of $|p|$ facilities that minimize the maximal distance for all demand points [78]. The reduction steps are as follows.

- The p-th facility in the p-center problem is mapped to the u-th UAV in our problem, where the set of demand points m is mapped to the set of ground users I.
- In the special case of our problem that we map to, all wireless devices have the same residual energy $E_i = E, \forall i \in I$.
- In the special case of our problem that we map to, $P_{max} = \infty$ and $\tau_{th} = 0$.

Now, minimizing the the maximal distance in the p-center problem is equivalent to maximizing the lifetime in the special case of our problem. □

Due to the intractability of our problem, we start by considering the case where there is only one UAV. Based on this, we propose an efficient algorithm to solve the problem for the general case of multiple UAVs.

6.4 The Single UAV Case

For the special case of a single UAV. Our problem can be formulated as:

$$\max_{(X_u,Y_u,Z_u),\tau_{iu}} \min_{i\in I} \tau_{iu}$$

$$subject\ to$$

$$\begin{aligned}
&\left(2^{\frac{R.|I|}{B}}-1\right) NL_{iu} \leq P_{max} && \forall i \in I \quad (6.5.a)\\
&\tau_{iu} \geq \tau_{th} && \forall i \in I \quad (6.5.b)\\
&\tau_{iu}\left(2^{\frac{R.|I|}{B}}-1\right) NL_{iu} \leq E_i && \forall i \in I \quad (6.5.c)\\
&x_{\min} \leq X_u \leq x_{\max} && (6.5.d)\\
&y_{\min} \leq Y_u \leq y_{\max} && (6.5.e)\\
&z_{\min} \leq Z_u \leq z_{\max} && (6.5.f)
\end{aligned} \tag{6.5}$$

From equation (6.1), we can notice that the optimal altitude of the UAV that maximizes the lifetime of wireless devices is equal to $z_{\min}$, which could correspond to the minimum altitude due to safety consideration [25]. Now, our objective becomes finding the optimal 2D placement of the UAV such that the lifetime of wireless devices is maximized. Even though the problem has a number of nonlinear constraints, we can transform (6.5) to a convex optimization problem with two variables by proving that the constraint sets (6.5.a-6.5.c) can be represented by the intersection of half spheres and the region formed by this intersection is a convex set in terms of (X_u, Y_u).

Theorem 11. *The constraint sets (6.5.a-6.5.c) can be represented by the intersection of half spheres and the region formed by this intersection is a convex set in terms of* (X_u, Y_u).

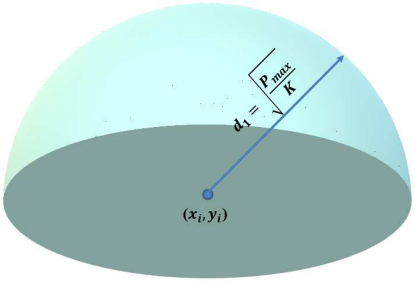

Figure 6.2 Range of distances that satisfies constraint set (6.5.a).

Proof. From (6.1) and (6.3), the transmit power of ground user i is given by:

$$p_{iu} = \left(2^{\frac{R_i|I|}{B}} - 1\right) N \left(\frac{4\pi d_{iu} f}{c}\right)^2 = K d_{iu}^2 \tag{6.6}$$

where K is a constant and equals $\left(2^{\frac{R_i|I|}{B}} - 1\right) N \left(\frac{4\pi f}{c}\right)^2$. Now, to satisfy constraint set (6.5.a), p_{iu} must be less than P_{max}. From (6.6), the range of distances d_1 that satisfies the constraint set (6.5.a) is given by:

$$d_1 \leq \sqrt{\frac{P_{max}}{K}} \tag{6.7}$$

The range of distances d_1 represents a half sphere with radius $\sqrt{\frac{P_{max}}{K}}$ as shown in Figure 6.2. To satisfy constraint sets (6.5.b) and (6.5.c), p_{iu} must be less than $\frac{E_i}{\tau_{th}}$. From (6.6), the range of distances d_2 that satisfies constraint sets (6.5.b) and (6.5.c) is given by:

$$d_2 \leq \sqrt{\frac{E_i}{\tau_{th} K}} \tag{6.8}$$

The range of distances d_2 also represents a half sphere with radius $\sqrt{\frac{E_i}{\tau_{th} K}}$ as shown in Figure 6.3. For each ground user i, the range of distances that satisfy the constraint sets (6.5.a)-(6.5.c) can be represented by a half sphere with radius:

$$min \left\{ \sqrt{\frac{P_{max}}{K}}, \sqrt{\frac{E_i}{\tau_{th} K}} \right\} \tag{6.9}$$

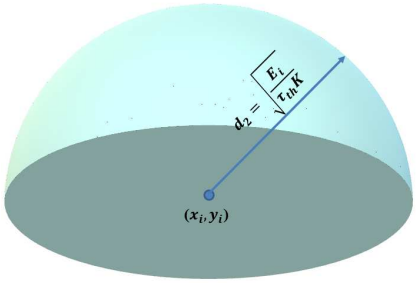

Figure 6.3 Range of distances that satisfies constraint sets (6.5.b) and (6.5.c).

The half sphere is a convex set and the intersection of convex sets is also a convex set [79].

□

From Theorem 11, we restrict the $2D$ placement of UAV (X_u, Y_u) to be in V. The convex feasible region V is given by:

$$
\begin{aligned}
V &= V_1 \bigcap V_2 \\
V_1 &= \bigcap_{i=1}^{|I|} \{(x, y, z) \in \mathbf{R}^3 | \sqrt{(x - x_i)^2 + (y - y_i)^2 + z^2} \leq \min\{\sqrt{\frac{P_{\max}}{K}}, \sqrt{\frac{E_i}{\tau_{th} K}}\}\} \\
V_2 &= \{(x, y) \in [x_{min}, x_{max}] \times [y_{min}, y_{max}] | z = z_{min}\}
\end{aligned}
\tag{6.10}
$$

where V_1 represents the convex set that satisfies the constraint sets (6.5.a)-(6.5.c) and V_2 represents the optimal altitude of the UAV z_{min}.

In the next theorem, we prove that the objective function is concave under a restriction on the coverage angle of ground user θ. The coverage angle is shown in Figure 6.4 and depends on the 3D placement of the UAV and the 2D location of ground user. This theorem enables us to find the optimal placement for the UAV.

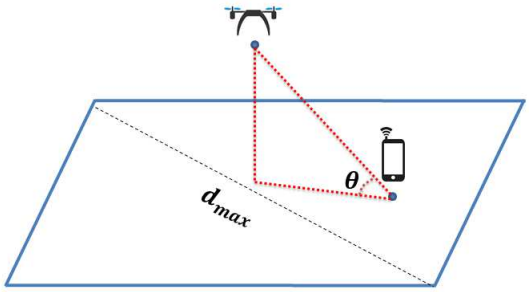

Figure 6.4 Coverage angle θ.

Theorem 12. *The objective function of (6.5) is concave if the coverage angle θ of each wireless device is greater than 60^o.*

Proof. Proving that the time duration of uplink transmission of wireless device τ_{iu} is concave implies that the objective function is concave where minimizing concave functions is concave [80] and concave maximization preserves concavity [79]. Now, we only need to prove that (6.11) is a concave function:

$$\tau_{iu} = \frac{E_i}{p_{iu}} = \frac{E_i}{(2^{\frac{R.|I|}{B}} - 1)NL_{iu}} = \frac{E_i}{(2^{\frac{R.|I|}{B}} - 1)N(\frac{4\pi d_{iu}F}{c})^2} = \frac{E_i}{Kd_{iu}^2} \tag{6.11}$$

Since $\frac{E_i}{K} > 0, \forall i \in I$, we need to prove that f is a concave function:

$$f = \frac{1}{(X_u - x_i)^2 + (Y_u - y_i)^2 + z_{\min}^2}, \forall i \in I \tag{6.12}$$

Using the second order condition, the function f is concave if the Hessian is negative semidefinite [79]. Now, the Hessian is negative semidefinite if these conditions are satisfied:

$$\begin{aligned}
&(a)\frac{d^2f}{dX_u^2} \leq 0, \quad \forall i \in I \\
&(b)\frac{d^2f}{dY_u^2} \leq 0, \quad \forall i \in I \\
&(c)\frac{d^2f}{dX_u^2}\frac{d^2f}{dY_u^2} - \left(\frac{d^2f}{dX_u dY_u}\right)^2 \geq 0, \quad \forall i \in I
\end{aligned} \tag{6.13}$$

To check the first condition, we need to find $\left(\frac{d^2f}{dX_u^2}\right)$:

$$\begin{aligned}
\frac{df}{dX_u} &= \frac{-2(X_u - x_i)}{((X_u - x_i)^2 + (Y_u - y_i)^2 + z_{\min}^2)^2} \\
\frac{d^2f}{dX_u^2} &= \frac{-2((X_u - x_i)^2 + (Y_u - y_i)^2 + z_{\min}^2)^2}{((X_u - x_i)^2 + (Y_u - y_i)^2 + z_{\min}^2)^4} + \\
&\quad \frac{8(X_u - x_i)^2((X_u - x_i)^2 + (Y_u - y_i)^2 + z_{\min}^2)}{((X_u - x_i)^2 + (Y_u - y_i)^2 + z_{\min}^2)^4} \\
&= \frac{-2((X_u - x_i)^2 + (Y_u - y_i)^2 + z_{\min}^2) + 8(X_u - x_i)^2}{((X_u - x_i)^2 + (Y_u - y_i)^2 + z_{\min}^2)^3} \\
&= \frac{6(X_u - x_i)^2 - 2(Y_u - y_i)^2 - 2z_{\min}^2}{((X_u - x_i)^2 + (Y_u - y_i)^2 + z_{\min}^2)^3}
\end{aligned} \tag{6.14}$$

From (6.14), $\frac{d^2f}{dX_u^2} \leq 0, \forall i \in I$ if:

$$z_{\min}^2 \geq 3(X_u - x_i)^2 - (Y_u - y_i)^2, \forall i \in I \tag{6.15}$$

Similarly, $\frac{d^2f}{dY_u^2} \leq 0, \forall i \in I$ if:

$$z_{\min}^2 \geq 3(Y_u - y_i)^2 - (X_u - x_i)^2, \forall i \in I \tag{6.16}$$

To check the third condition, we need to find $\frac{d^2f}{dX_u^2}\frac{d^2f}{dY_u^2} - \left(\frac{d^2f}{dX_u dY_u}\right)^2$:

$$\frac{d^2f}{dX_u dY_u} = \frac{8(X_u - x_i)(Y_u - y_i)}{((X_u - x_i)^2 + (Y_u - y_i)^2 + z_{\min}^2)^3} \tag{6.17}$$

From (6.17), we get:

$$\begin{aligned}
\frac{d^2f}{dX_u^2}\frac{d^2f}{dY_u^2} - (\frac{d^2f}{dX_u dY_u})^2 &= \frac{-2((X_u-x_i)^2+(Y_u-y_i)^2+z_{\min}^2)+8(X_u-x_i)^2}{((X_u-x_i)^2+(Y_u-y_i)^2+z_{\min}^2)^3}\cdot \\
&\quad \frac{-2((X_u-x_i)^2+(Y_u-y_i)^2+z_{\min}^2)+8(Y_u-y_i)^2}{((X_u-x_i)^2+(Y_u-y_i)^2+z_{\min}^2)^3} - \\
&\quad \frac{64(X_u-x_i)^2(Y_u-y_i)^2}{((X_u-x_i)^2+(Y_u-y_i)^2+z_{\min}^2)^6} \\
&= \frac{4((X_u-x_i)^2+(Y_u-y_i)^2+z_{\min}^2)^2}{((X_u-x_i)^2+(Y_u-y_i)^2+z_{\min}^2)^6} - \\
&\quad \frac{16(Y_u-y_i)^2((X_u-x_i)^2+(Y_u-y_i)^2+z_{\min}^2)}{((X_u-x_i)^2+(Y_u-y_i)^2+z_{\min}^2)^6} - \\
&\quad \frac{16(X_u-x_i)^2((X_u-x_i)^2+(Y_u-y_i)^2+z_{\min}^2)}{((X_u-x_i)^2+(Y_u-y_i)^2+z_{\min}^2)^6} + \\
&\quad \frac{64(X_u-x_i)^2(Y_u-y_i)^2}{((X_u-x_i)^2+(Y_u-y_i)^2+z_{\min}^2)^6} - \\
&\quad \frac{64(X_u-x_i)^2(Y_u-y_i)^2}{((X_u-x_i)^2+(Y_u-y_i)^2+z_{\min}^2)^6} \\
&= \frac{4((X_u-x_i)^2+(Y_u-y_i)^2+z_{\min}^2)}{((X_u-x_i)^2+(Y_u-y_i)^2+z_{\min}^2)^5} + \\
&\quad \frac{-16(X_u-x_i)^2-16(Y_u-y_i)^2}{((X_u-x_i)^2+(Y_u-y_i)^2+z_{\min}^2)^5} \\
&= \frac{-12(X_u-x_i)^2-12(Y_u-y_i)^2+4z_{\min}^2}{((X_u-x_i)^2+(Y_u-y_i)^2+z_{\min}^2)^5}
\end{aligned} \tag{6.18}$$

From (6.18), $\frac{d^2f}{dX_u^2}\frac{d^2f}{dY_u^2} - \left(\frac{d^2f}{dX_u dY_u}\right)^2 \geq 0, \forall i \in I$ if:

$$z_{\min}^2 \geq 3(X_u-x_i)^2 + 3(Y_u-y_i)^2, \forall i \in I \tag{6.19}$$

From (6.15), (6.16) and (6.19), the Hessian is negative semidefinite if the following conditions are satisfied:

$$\begin{aligned}
&(a) z_{\min}^2 \geq 3(X_u - x_i)^2 - (Y_u - y_i)^2, \forall i \in I \\
&(b) z_{\min}^2 \geq 3(Y_u - y_i)^2 - (X_u - x_i)^2, \forall i \in I \\
&(c) z_{\min}^2 \geq 3(X_u - x_i)^2 + 3(Y_u - y_i)^2, \forall i \in I
\end{aligned} \tag{6.20}$$

From the three conditions in (6.20), we can notice that if condition (c) is satisfied, then conditions (a) and (b) are also satisfied. Let us define $d_{\max}$ as a maximum possible 2D distance in the geographical area (i.e., if the users are distributed in a circular geographical area, then $d_{\max}$ is equal to the diameter of circle). From condition (c), if $z_{\min} \geq \sqrt{3} d_{\max}$ then the objective function of (6.5) is concave where $d_{max} \geq \sqrt{(X_u - x)^2 + (Y_u - y)^2}, \forall i \in I$. Then, the coverage angle θ must be greater than $tan^{-1} \frac{\sqrt{3} d_{\max}}{d_{\max}} = 60^o$. □

Here, we can notice that the altitude of UAV z_{min} controls the concavity of the objective function. Theorem 12 enables us to find the optimal placement for the UAV, when the coverage angle θ of each wireless device is greater than or equal to 60^o.

In this chapter, we assume that the wireless channel between a ground user and a UAV is line of sight dominated. To verify that the coverage angle that we characterize it in Theorem 12 guarantees a line of sight path, we utilize line of sight (LOS) probability models for downlink scenarios.

Table 6.1 Parameters for Air-to-Ground Path Loss Model Using HAP and LAP

Environment	Platform type	a_1	a_2	a_3	a_4	a_5	a_6
Suburban	HAP	101.6	0	0	3.25	1.241	0
Urban	HAP	120	0	0	24.3	1.229	0
Suburban	LAP	0.1	750	0	0	0	8
Urban	LAP	0.3	500	0	0	0	15

For low altitude aerial platforms (LAP), the probability of having a LOS connection in downlink scenario is given by [81]:

$$P(LOS) = \prod_{n=0}^{m} \left[1 - exp\left(- \frac{\left[Z_u - \frac{(n+\frac{1}{2})(Z_u - z)}{m+1} \right]^2}{2{a_6}^2} \right) \right] \tag{6.21}$$

where $m = \lfloor r\sqrt{a_1 a_2} - 1 \rfloor$, r is the ground distance between the UAV and ground user, Z_u and z are the UAV and ground user heights, and the parameters a_1, a_2 and a_6 are constant values that depend on the environment (see Table 6.1).

For high altitude aerial platforms (HAP), the probability of having a LOS connection in downlink scenario is given by [82]:

$$P(LOS) = a - \frac{a_1 - a_2}{1 + \left(\frac{\theta - a_3}{a_4} \right)^{a_5}} \tag{6.22}$$

where a_1, a_2, a_3, a_4 and a_5 are empirical parameters given in Table 6.1 for two different environments.

In Figure 6.5, we plot the probability of having a LOS wireless connection in suburban and urban environments using LAP and HAP. We can notice that the coverage angle that we characterize in Theorem 12 gives us more than 0.9 LOS probability.

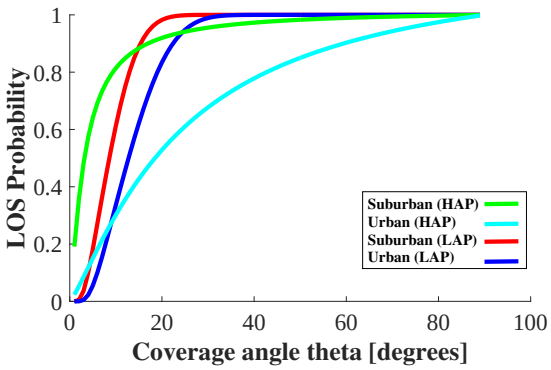

Figure 6.5 LOS probability for LAP and HAP in different environments.

Therefore, our assumption that a wireless channel is a line of sight dominated is a realistic assumption.

Now, we propose to use the Gradient Projection Algorithm [83] to find the optimal placement of a UAV, when the UAV's altitude satisfies the condition in Theorem 12. The gradient projection algorithm is given by:

$$(X_u, Y_u)^{n+1} = [(X_u, Y_u)^n + \delta \nabla \Psi((X_u, Y_u)^n))]^+ \tag{6.23}$$

where n is the iteration number, δ is a positive step size, $\nabla \Psi$ is the gradient of the objective function in (6.5) and $[q]^+$ denotes the orthogonal projection of vector q onto convex set Q. In particular, $[q]^+$ is defined by:

$$[q]^+ = arg \min_{w \in Q} ||w - q||_2 \tag{6.24}$$

The pseudo code of the gradient projection algorithm is shown in Algorithm 8.

Also, we can use the PSO algorithm [59] to find an efficient 3D placement of a UAV, when the altitude of a UAV does not satisfy the condition in Theorem 12.

Algorithm 8 The Gradient Projection Algorithm

1: **Input:**
2: The step tolerance ϵ.
3: The step size δ.
4: The maximum number of iterations $n_{\max}$.
5: **Initialize** (X_u, Y_u)
6: **For** n=1,2,..., $n_{\max}$
7: $(X_u, Y_u)^{n+1} = [(X_u, Y_u)^n + \delta \nabla \Psi((X_u, Y_u)^n))]^+$
If $\| (X_u, Y_u)^n - (X_u, Y_u)^{n+1} \| < \epsilon$
8: **Return:** $(X_u, Y_u)_{opt} = (X_u, Y_u)^{n+1}$
9: **End for**

6.5 Clustering Algorithm for Multiple UAVs Case

Due to the intractability of the general problem represented by (6.4), we consider clustering of ground users. The pseudo code of clustering users is shown in Algorithm 9 and it is inspired by the k-means clustering algorithm [62]. In the k-means clustering algorithm, we are given a set of points I, and want to group the points into k clusters such that each point belongs to the cluster with the nearest mean. The main step in our algorithm is to choose the number of clusters $|U|$ (step 4) and then randomly initialize $|U|$ clusters centroids (step 6). In each iteration, the algorithm will do two things: 1) cluster assignment step, 2) move centroids step (step 7). In cluster assignment step, the algorithm goes through each point and chooses the closest centroid and assigns the point to it. In move centroids step, the algorithm calculates the mean point of each cluster (the mean point minimizes the sum of squared Euclidean distances between itself and each point in the cluster) and moves the centroids there. The algorithm repeats these two steps until it converges. It converges when the assignments no longer change. After it finishes

clustering the users, it applies the Gradient Projection Algorithm or PSO Algorithm to find the placements of UAVs (steps 8-12) within each cluster.

Algorithm 9 Maximizing the Lifetime of Wireless Devices.

1: **Input:**
2: The residual energy of each wireless device E_i, $i \in I$.
3: The locations of $|I|$ ground users.
4: The number of UAVs $|U|$.
5: **START:**
6: Initialize the placements of the UAVs $\gamma_1, \gamma_2, ..., \gamma_{|U|}$ randomly.
7: Repeat until convergence:
For every user $i \in I$, set
$c^{(i)} = arg \min_{u \in U} ||(x_i, y_i) - \gamma_u||^2$
For each UAV $u \in U$, set
$$\gamma_u = \frac{\sum_{i \in I, c^{(i)} = u} (x_i, y_i)}{\sum_{i \in I, c^{(i)} = u} 1}$$
8: **If** $\theta_i \geq 60^o, \forall i \in I$
9: Calculate the optimal placements of UAVs using the
Gradient Projection Algorithm.
10: **else**
11: Calculate the efficient placements of UAVs using the
PSO Algorithm.
12: **endif**
13: **Output:**
14: $|U|$ Clusters.
15: The lifetime of wireless devices $\min_{i \in I, u \in U} \tau_{iu}$.
16: The placements of UAVs.

6.6 Finding the Minimum Number of UAVs

In this section, we consider the problem of minimizing the number of UAVs required to serve the ground users such that the time duration of uplink transmission of each wireless

device τ_{iu} is greater than or equal to τ_{th}. Our problem can be formulated as:

$$\begin{aligned} &\min_{(X_u,Y_u,Z_u),w_{iu},\tau_{iu}} |U| \\ &\quad subject\ to \\ &\qquad (6.4.a) - (6.4.g). \end{aligned} \tag{6.25}$$

Theorem 13. *The problem represented by (6.25) is NP-complete.*

Proof. The number of constraints is polynomial in terms of the number of ground users, number of UAVs, and locations. Given any solution to our problem, we can check the solution's feasibility in polynomial time; then, the problem is NP.

To prove that the problem is NP-hard, we reduce the set cover problem, which is NP-hard [84], to a special case of our problem. In the set cover problem, we have a set of elements $G = \{1, 2, ..., N\}$, called the universe, and a family S of subsets of G whose union equals the universe G. The objective is to find the smallest subfamily of sets $A \subseteq S$ whose union equals the universe. The reduction steps are as follows.

- The set of elements G in the set cover problem is mapped to the set of ground users I in our problem.
- The family S of subsets of G in the set cover problem is mapped to the subsets of covered ground users from all possible UAV placements, where a user i is covered by the UAV u located at (X_u, Y_u, Z_u) if $\tau_{iu} \geq \tau_{th}$.

If and only if, there exists a solution to the set cover problem with number of subsets C, then the minimum number of UAVs in our problem is C. □

Next, we propose to use two efficient methods to determine the minimum number of UAVs required to serve the wireless devices.

Method 1. *Minimizing the number of UAVs using clustering:* Due to the intractability of the problem, we consider clustering of ground users. The pseudo code of clustering users is shown in Algorithm 10. In our algorithm, we assume that each cluster will be covered by only one UAV. We start the algorithm with two UAVs $|U| = 2$ (step 5) and after it finishes clustering the users, it applies the Gradient Projection Algorithm or PSO Algorithm to find the placements of UAVs (steps 9-13) within each cluster. Then, it checks if the time duration of uplink transmission of each wireless device satisfies the constraint $\tau_{iu} \geq \tau_{th}$ (steps 14-15) , if not, the number of UAVs $|U|$ is incremented by one and the previous steps are repeated until it converges.

Method 2. *Minimizing the number of UAVs using matrix reduction method:* In Section 6.4, we prove that the constraint sets (6.5.a-6.5.c) can be represented by the intersections of half spheres. We also show that the optimal altitude of a UAV that maximizes the lifetime of wireless devices is equal to z_{min}. In this method, we represent the constraint sets of problem (6.25) by intersections of multiple circles when each user $i \in I$ satisfies this condition:

$$z_{min} \leq \min\{\sqrt{\frac{P_{\max}}{K}}, \sqrt{\frac{E_i}{\tau_{th}K}}\} \leq \min\{\Delta x_i, \Delta y_i\} \tag{6.26}$$

where Δx_i equals $\min\{|x_i - x_{min}|, |x_i - x_{max}|\}$ and Δy_i equals $\min\{|y_i - y_{min}|, |y_i - y_{max}|\}$. Here, we can find the minimum number of UAVs and their placements using the matrix reduction method [85]. The reduction method begins with a matrix representing which wireless devices are within the critical distance of every potential UAV placement. In our problem, the potential UAV placement is any point in the circle intersection region. The method then eliminates any row(s) (wireless device(s)) such that all of its entries

Algorithm 10 Minimizing the number of UAVs.

1: **Input:**
2: The residual energy of each wireless device E_i, $i \in I$.
3: The locations of $|I|$ ground users.
4: The threshold time duration of uplink transmission τ_{th}.
5: The number of UAVs is two $(|U| = 2)$.
6: **START:**
7: Initialize the placements of the UAVs $\gamma_1, \gamma_2, ..., \gamma_{|U|}$ randomly.
8: Repeat until convergence:
For every user $i \in I$, set
$c^{(i)} = arg \min_{u \in U} ||(x_i, y_i) - \gamma_u||^2$
For each UAV $u \in U$, set

$$\gamma_u = \frac{\sum_{i \in I, c^{(i)} = u} (x_i, y_i)}{\sum_{i \in I, c^{(i)} = u} 1}$$

9: **If** $\theta_i \geq 60^o, \forall i \in I$
10: Calculate the optimal placements of UAVs using the
Gradient Projection Algorithm.
11: **else**
12: Calculate the efficient placements of UAVs using the
PSO Algorithm.
13: **endif**
14: **For** $i = 1\ to\ |I|$
15: **If** ($\tau_{iu} < \tau_{th}$)
16: $|U| = |U| + 1$
17: **go to START**
18: **End**
19: **Output:**
20: $|U|$ Clusters.
21: The placements of UAVs.

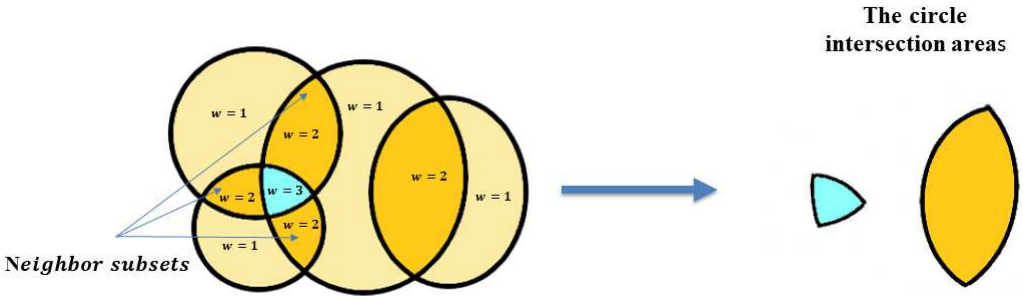

Figure 6.6 Computing circle intersection areas using Algorithm 11.

are greater than or equal to the corresponding entries of another row. The second step of the method eliminates any column(s) (potential UAV placement(s)) such that all of its entries are less than or equal to the corresponding entries of another column. The matrix reduction method repeats these two steps until it converges. It converges when no more columns or rows are eliminated. Now, the question is how to find the circle intersection areas. Unfortunately, when more than three circles are considered, the number of configurations grows exponentially. The authors in [1] present an algorithm, Computing Circle Intersection Areas (CCIA) Algorithm, to find the circle intersection areas. The overall complexity of this algorithm grows as $N_c^2 2^{N_c}$ where N_c is the number of circles and each circle represents the wireless coverage of base station. They apply their algorithm to compute the total coverage of ten base stations. In our problem, each circle represents the feasible region that satisfies the constraint sets of each wireless device. Due to the large number of wireless devices, it will be impractical to apply the CCIA algorithm.

In problem (6.10), we show that the constraint sets of wireless devices can be represented by the intersection of circles and the region formed by this intersection satisfies the constraint sets of wireless devices. It is obvious that finding at least one point in each circle intersection area is sufficient to solve our problem, where any point in the

circle intersection area will satisfy the constraint sets of wireless devices. In Algorithm 11, we divide the plane into equal sized grids and present a method that can find the points in the circle intersection areas in polynomial time in terms of the number of points in plane K and the number of circles $|I|$. The algorithm aims to find some points in each intersection region instead of finding all points as done in CCIA algorithm. It starts by giving each 2D point in $[x_{min}, x_{max}] \times [y_{min}, y_{max}]$ a weight w based on the number of circles that are covering a 2D point (step 4). It then finds each family G_w of subsets of $[x_{min}, x_{max}] \times [y_{min}, y_{max}]$ that has a weight w, where $w \in \{2, 3, ..., |I|\}$ (steps 5-6). After that, if there is a subset $g \in G_w$, it eliminates all neighboring subsets that have weights less than w (steps 7-8), as shown in Figure 6.6. Finally, it finds the points in the circle intersection areas (steps 9-11). The overall complexity of this algorithm grows as $|I|K^2$ where $|I|$ is the number of circles and K^2 is the grid size. It will be a critical issue to choose the appropriate grid size K^2 when algorithm 5 is applied. When increasing the grid size, the probability to detect the feasible regions of wireless devices will increase. We iteratively increase the grid size until we detect the feasible regions that satisfy the constraint sets of all wireless devices.

6.7 Numerical Results

6.7.1 Simulation Results for Single UAV

We first verify the results of Theorem 12. Then we use the Gradient Projection Algorithm and the PSO Algorithm. Table 6.2 lists the parameters used in the numerical analysis.

To verify the results of Theorem 12, we assume that 900 ground users are uniformly distributed in a geographical area of size $500m \times 500m$, then we plot the objective function

Algorithm 11 Computing Circle Intersection Areas.

1: **Input**
2: $|I|$ circles where the center of each circle is given by (x_i, y_i), $i \in I$.
3: **START**
4: Give a weight w for each 2D point $(x, y) \in [x_{min}, x_{max}] \times [y_{min}, y_{max}]$, where w represents the number of circles that are covering a 2D point (x, y).
5: **For** $w = |I|$ to 2
6: Find a family G_w of subsets of $[x_{min}, x_{max}] \times [y_{min}, y_{max}]$ that has a weight w.
7: **For** $w = |I|$ to 3
8: **For** each subset $g \in G_w$ that has weight w, remove neighbor subsets that have weights less than w.
9: **Output**
10: The circle intersection areas are given by:
11: $G_w \cup G_{w-1} \cup ... \cup G_2$.

Table 6.2 Parameters in Numerical Analysis

Maximum transmit power $P_{\max}$	0.5 watt
Energy of each wireless device E_i	Uniformly distributed between 4500 and 18000 Joule
Data rate R	1 Mbps
Total bandwidth B	50 MHz
The noise power N	1×10^{-17}
The carrier frequency F	2 Ghz
(κ, ϕ_1, ϕ_2)	(1, 2.05, 2.05)

in (6.5) without any constraints at two different altitudes of the UAV. The first value for altitude $z_{\min}$ is 1300 meters, which satisfies the condition in Theorem 12. The second

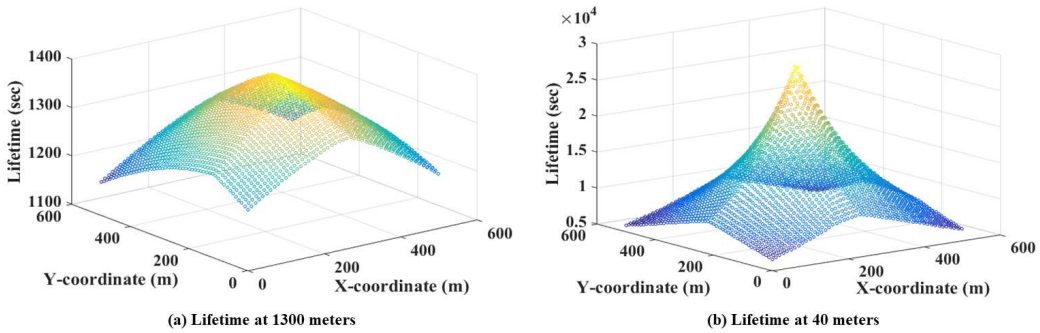

Figure 6.7 Lifetime of wireless devices at different altitudes.

value for altitude is 40 meters and it does not satisfy the condition in Theorem 12. In Figure 6.7.a, we can notice that the objective is concave when the altitude of UAV is equal to 1300 meters. On the other hand, the objective function becomes non-concave at 40 meters as shown in Figure 6.7.b.

In Figures 6.8 and 6.9, we place the UAV at altitude 1225 meters and use the gradient projection algorithm when the ground users are uniformly and non-uniformly distributed. The optimal placement are (244, 187, 1225) and (298, 251, 1225), respectively. In Figures 6.10 and 6.11, we place the UAV at altitude 500 meters. This altitude does not satisfy the condition in Theorem 12 and therefore we propose to use the PSO [59] when the ground users are uniformly and non-uniformly distributed. The efficient placements are (254, 212, 500) and (260, 255, 500), respectively. In order to verify the efficiency of PSO algorithm, we use a search-based algorithm. Both of the algorithms converge to the same 3D placement. A simple way to maximize the lifetime of wireless devices is to place the projection of a UAV placement at the center of deployment region regardless of the users distribution, let us call this method as the center projection method. In Table 6.3, we show the simulation results for single UAV. We can notice that our proposed UAV placement algorithms can improve the lifetime of

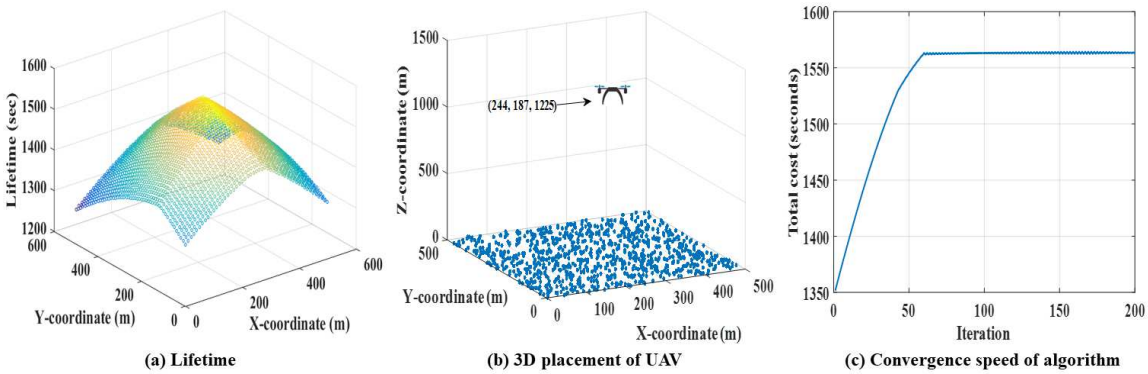

Figure 6.8 Simulation results of the uniform distribution case using gradient projection algorithm.

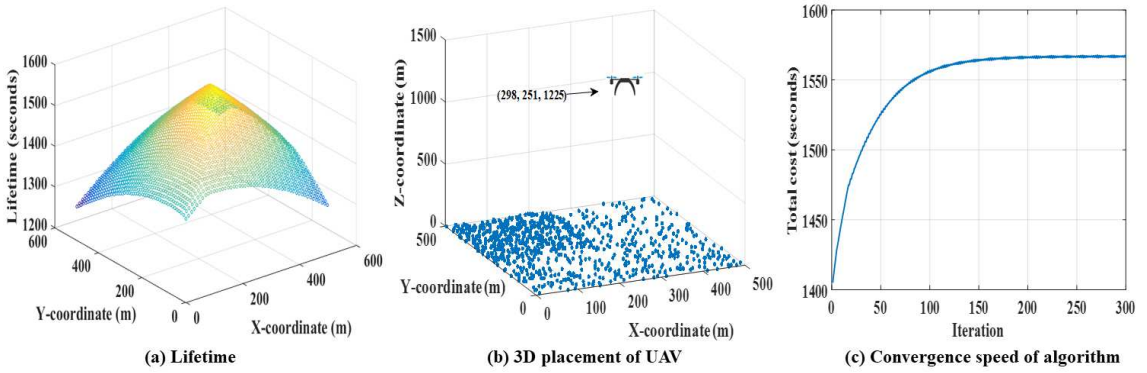

Figure 6.9 Simulation results of the non-uniform distribution case using gradient projection algorithm.

wireless devices by only 10% compared with center projection method. This is because the efficient placements of UAVs are near the center of the deployment region due to the uniformly distributed of residual energies of the wireless devices. For the multiple UAVs scenario, we show that our proposed UAV placement algorithms can improve the lifetime of wireless devices by 90%-122%.

6.7.2 Simulation Results for Multiple UAVs

For the multiple UAVs scenario, we assume that 1250 ground users are uniformly distributed in a geographical area of size $1000m \times 1000m$ and four UAVs are used to serve

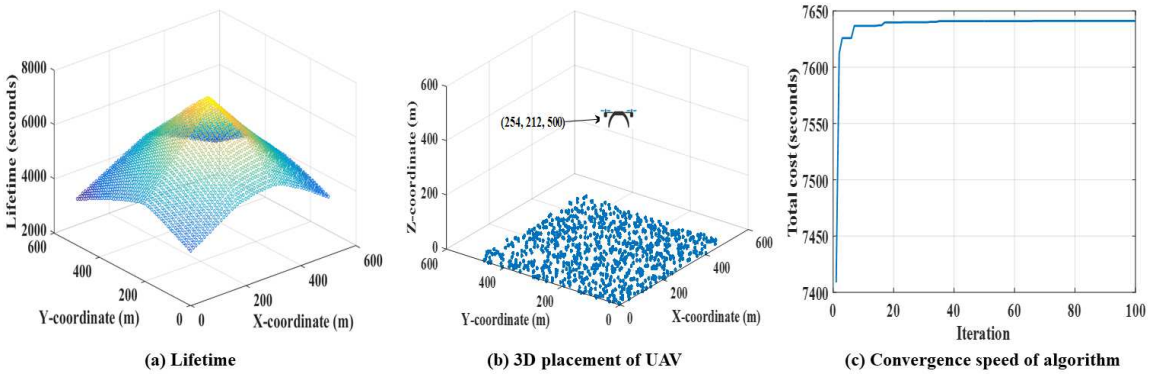

(a) Lifetime (b) 3D placement of UAV (c) Convergence speed of algorithm

Figure 6.10 Simulation results of the uniform distribution case using PSO algorithm.

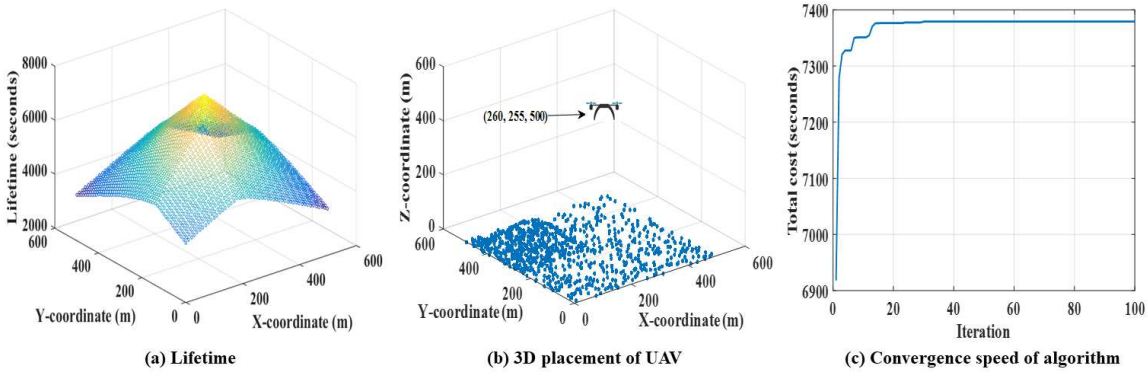

(a) Lifetime (b) 3D placement of UAV (c) Convergence speed of algorithm

Figure 6.11 Simulation results of the non-uniform distribution case using PSO algorithm.

the ground users. We apply Algorithm 9 to cluster the wireless devices into four clusters as shown in Figure 6.12, where each cluster is served by one UAV. After that, we utilize the UAV placement algorithms. In Table 6.4, we place each UAV at altitude 1500 meters and use the gradient projection algorithm to find the optimal placement in each cell. The optimal placements for the first, second, third and fourth UAVs are (753, 245, 1500), (915, 634, 1500), (263, 395, 1500) and (408, 980, 1500), respectively. We also place each UAV at altitude 500 meters and use the PSO algorithm to find an efficient placement in each cell. The efficient placements for the first, second, third and fourth UAVs are (733, 201, 500), (881, 749, 500), (207, 308, 500) and (298, 797, 500), respectively. We can notice that our proposed UAV placement algorithms can improve the lifetime of wireless devices

Table 6.3 Simulation Results for Single UAV

Algorithm	Distribution of users	3D placement of UAV	Lifetime
The gradient projection algorithm	Uniform	(244, 187, 1225)	1563 sec
The center projection method	Uniform	(250, 250, 1225)	1549 sec
The gradient projection algorithm	Non-uniform	(298, 251, 1225)	1566 sec
The center projection method	Non-uniform	(250, 250, 1225)	1548 sec
The PSO algorithm	Uniform	(254, 212, 500)	7641 sec
The search-based algorithm	Uniform	(254, 212, 500)	7641 sec
The center projection method	Uniform	(250, 250, 500)	6937 sec
The PSO algorithm	Non-uniform	(260, 255, 500)	7379 sec
The search-based algorithm	Non-uniform	(260, 255, 500)	7379 sec
The center projection method	Non-uniform	(250, 250, 500)	6819 sec

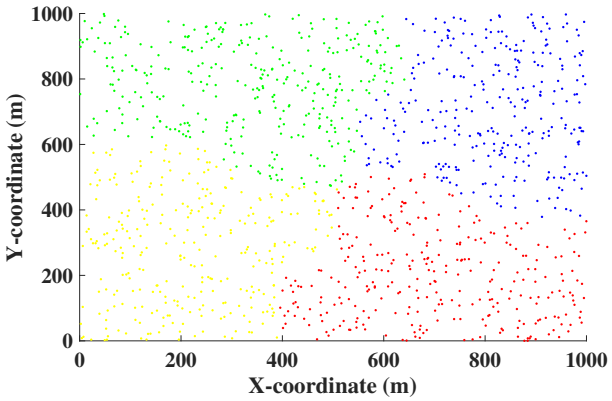

Figure 6.12 Clustering the wireless devices using Algorithm 9.

by 90%-122% compared with center projection method. This is because our proposed algorithms minimize the distances between the ground users and a UAV in each cluster.

Table 6.4 Simulation Results for Multiple UAVs Using Algorithm 9

Altitude of UAV	UAV index	Algorithm	3D placement of UAV	Lifetime
1500 meters	1	Gradient projection	(753, 245, 1500)	861 seconds
		Center projection	(501, 499, 1500)	793 seconds
	2	Gradient projection	(915, 634, 1500)	864 seconds
		Center projection	(501, 501, 1500)	780 seconds
	3	Gradient projection	(263, 395, 1500)	856 seconds
		Center projection	(499, 499, 1500)	827 seconds
	4	Gradient projection	(408, 980, 1500)	861 seconds
		Center projection	(499, 501, 1500)	777 seconds
500 meters	1	PSO algorithm	(733, 201, 500)	6613 seconds
		Center projection	(501, 499, 500)	3349 seconds
	2	PSO algorithm	(881, 749, 500)	6660 seconds
		Center projection	(501, 501, 500)	2995 seconds
	3	PSO algorithm	(207, 308, 500)	6351 seconds
		Center projection	(499, 499, 500)	3288 seconds
	4	PSO algorithm	(298, 797, 500)	5909 seconds
		Center projection	(499, 501, 500)	3095 seconds

In Figure 6.13, we assume that 1250 ground users are uniformly distributed in a geographical area of size $10000m \times 10000m$ and the time duration of uplink transmission of each wireless device τ_{iu} must be greater than or equal to 5 minutes. We also assume that

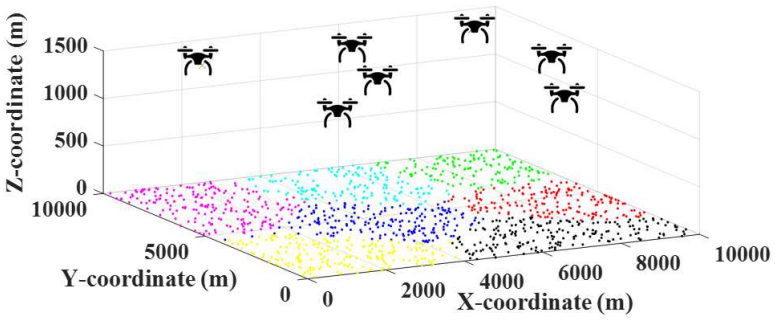

Figure 6.13 Minimizing the number of UAVs using Algorithm 10.

the UAVs have the same altitude 1500 meters. We utilize Algorithm 10 to minimize the number of UAVs required to serve the wireless devices. The algorithm converges when the number of UAVs is seven. The efficient placements of the UAVs and the lifetimes of the wireless devices are shown in Table 6.5.

Table 6.5 Simulation Results for Multiple UAVs Using Algorithm 10

Altitude of UAV	UAV index	Algorithm	3D placement of UAV	Lifetime
1500 meters	1	PSO algorithm	(8690, 4651, 1500)	448 seconds
	2		(4120, 4534, 1500)	377 seconds
	3		(1782, 1990, 1500)	391 seconds
	4		(8435, 8157, 1500)	521 seconds
	5		(1304, 7674, 1500)	338 seconds
	6		(7168, 1209, 1500)	330 seconds
	7		(5333, 8136, 1500)	503 seconds

In Table 6.6, we consider the case that each wireless device satisfies the condition in inequality (6.26) where the ground users are uniformly distributed in a geographical

Table 6.6 A Comparison Between CCIA Algorithm and Algorithm 11

Algorithm	Number of users	Step size	Optimal number of UAVs	Number of UAVs using algorithm	Total number of operations
CCIA Algorithm	1000	—	10	10	$1.07 * 10^{307}$
	2000		20	20	$4.59 * 10^{608}$
Algorithm 5	1000	100	10	10	$2.85 * 10^{9}$
		200		10	$2.2 * 10^{9}$
		300		10	$1.26 * 10^{9}$
	2000	100	20	20	$7.7 * 10^{9}$
		200		20	$4.4 * 10^{9}$
		300		20	$2.52 * 10^{9}$

area of size $10000m \times 10000m$. We apply algorithm 11 that iteratively increases the step size until it detects the feasible regions that satisfy the constraint sets of all wireless devices. The step size represents the number of points that the algorithm add to the grid size in each iteration. When increasing the step size, the probability to detect the feasible regions of wireless devices will increase. We find the number of operations (worst case) required to compute the circle intersection areas using CCIA algorithm and algorithm 11 for different number of users. We can notice that the number of operations of algorithm 11 is much lower than those in the CCIA algorithm. This is because the overall complexity of algorithm 11 grows as $|I|K^2$ (polynomial time) where $|I|$ is the number of users and K^2 is the grid size. In order to verify the efficiency of Algorithm 11, we find the optimal

number of UAVs using a search-based algorithm. Both of the algorithms converge to the same number of UAVs.

CHAPTER 7

SUMMARY AND FUTURE DIRECTIONS

The problem of minimizing the number of UAVs required for a continuous coverage of a given area is first studied in Chapter 3. Due to its intractability, partitioning the coverage graph into cycles that start at the charging station is proposed and the minimum number of UAVs to cover such a cycle is characterized based on the charging time, the traveling time and the number of subareas to be covered by the cycle. Based on this analysis, an efficient algorithm is developed to solve the problem.

In Chapter 4, the problem of optimal placement of a single UAV is studied, where the objective is to minimize the total transmit power required to provide wireless coverage for indoor users. Three cases of practical interest are considered and efficient solutions to the formulated problem under these cases are presented. Due to the limited transmit power of a UAV, the problem of minimizing the number of UAVs required to provide wireless coverage to indoor users is studied and an efficient algorithm is developed to solve the problem.

In Chapter 5, the problem of maximizing the indoor wireless coverage using UAVs equipped with directional antennas is studied. The case that the UAVs are using one channel is considered, thus in order to maximize the total indoor wireless coverage, the overlapping in their coverage volumes is avoided. Two methods are presented to place the UAVs; providing wireless coverage from one building side and from two building sides. The results show that the upside-down arrangements of UAVs can improve the total coverage by 100% compared to providing wireless coverage from one building side.

In Chapter 6, the placement problem of UAVs is studied, where the objective is to determine the locations of a set of UAVs that maximize the lifetime of wireless devices. Due to the intractability of the problem, the number of UAVs is restricted to be one. Under this special case, the problem is formulated as a convex optimization problem under a restriction on the coverage angle of the ground users and a gradient projection based algorithm is proposed to find the optimal location of the UAV. Based on this, an efficient algorithm is proposed for the general case of multiple UAVs. The problem of minimizing the number of UAVs required to serve the ground users such that the time duration of uplink transmission of each wireless device is greater than or equal to a threshold value is also studied. Two efficient methods are proposed to determine the minimum number of UAVs required to serve the wireless devices.

Some of the future possible directions for this work are:

- Some path loss models are formulated based on simulation softwares such as Air-to-Ground path loss for low altitude platforms and Air-to-Ground path loss for high altitude platforms, therefore it is necessary to perform real experiments to model the statistical behavior of the path loss.
- Previous research works utilize a UAV as an aerial relay node to maximize the throughput of ground users under the assumption of free space propagation. This assumption could not be practical especially for urban environments. As future work, we aim to utilize practical path loss models to study this problem.
- The problem of minimizing the number of UAVs required for a continuous coverage of a given area can be extended by considering more realistic scenarios such as utilizing UAVs with different energy capacities and using multiple charging stations to recharge the batteries of UAVs.
- The problem of maximizing the lifetime of wireless devices can be extended by considering the indoor users.
- The problem of providing indoor wireless coverage using UAVs can be extended by considering more realistic scenarios such as providing indoor wireless coverage for multiple buildings.

- As future work, we will utilize UAVs to minimize the age-of-information in wireless sensor networks. The age of information is defined as the amount of time elapsed since the instant at which the freshest delivered update takes place.
- We will utilize UAVs to maximize the number of covered users when the cellular base station is unable to provide wireless coverage for all users due to 1) The high number of users inside a targeted cell and/or 2) The location of a user has a high blockage probability.

REFERENCES

[1] F. Librino, M. Levorato, and M. Zorzi, "An algorithmic solution for computing circle intersection areas and its applications to wireless communications," *Wireless Communications and Mobile Computing*, vol. 14, no. 18, pp. 1672–1690, 2014.

[2] S. Hayat, E. Yanmaz, and R. Muzaffar, "Survey on unmanned aerial vehicle networks for civil applications: A communications viewpoint." *IEEE Communications Surveys and Tutorials*, vol. 18, no. 4, pp. 2624–2661, 2016.

[3] M. Mozaffari, W. Saad, M. Bennis, and M. Debbah, "Wireless communication using unmanned aerial vehicles (UAVs): Optimal transport theory for hover time optimization," *IEEE Transactions on Wireless Communications*, vol. 16, no. 12, pp. 8052–8066, 2017.

[4] P. Bupe, R. Haddad, and F. Rios-Gutierrez, "Relief and emergency communication network based on an autonomous decentralized UAV clustering network," *IEEE SoutheastCon*, pp. 1–8, 2015.

[5] M. Mozaffari, W. Saad, M. Bennis, and M. Debbah, "Mobile internet of things: Can UAVs provide an energy-efficient mobile architecture?" *IEEE Global Communications Conference (GLOBECOM)*, pp. 1–6, 2016.

[6] AT&T Inc., "Flying COW Connects Puerto Rico." [Online]. Available: http://about.att.com/inside_connections_blog/flying_cow_puertori (Accessed on May 27, 2018).

[7] AT&T Inc., "When COWs Fly: AT&T Sending LTE Signals from Drones."[Online]. Available: http://about.att.com/innovationblog/cows_fly (Accessed on May 27, 2018).

[8] Wikipedia, "Mobile cell sites." [Online]. Available: https://en.wikipedia.org/wiki/Mobile_cell_sites (Accessed on April 18, 2018).

[9] M. Mozaffari, W. Saad, M. Bennis, Y.-H. Nam, and M. Debbah, "A tutorial on UAVs for wireless networks: Applications, challenges, and open problems," *arXiv preprint arXiv:1803.00680*, 2018.

[10] Y. Zeng, R. Zhang, and T. J. Lim, "Wireless communications with unmanned aerial vehicles: opportunities and challenges," *IEEE Communications Magazine*, vol. 54, no. 5, pp. 36–42, 2016.

[11] I. Jawhar, N. Mohamed, J. Al-Jaroodi, D. P. Agrawal, and S. Zhang, "Communication and networking of UAV-based systems: Classification and associated architectures," *Journal of Network and Computer Applications*, vol. 84, pp. 93–108, 2017.

[12] J. Zhao, F. Gao, Q. Wu, S. Jin, Y. Wu, and W. Jia, "Beam tracking for UAV mounted satcom on-the-move with massive antenna array," *IEEE Journal on Selected Areas in Communications*, vol. 36, no. 2, pp. 363–375, 2018.

[13] M. Mozaffari, W. Saad, M. Bennis, and M. Debbah, "Optimal transport theory for power-efficient deployment of unmanned aerial vehicles," *IEEE International Conference on Communications (ICC)*, pp. 1–6, 2016.

[14] M. Mozaffari, W. Saad, M. Bennis, and M. Debbah, "Drone small cells in the clouds: Design, deployment and performance analysis," *IEEE Global Communications Conference (GLOBECOM)*, pp. 1–6, 2015.

[15] M. Alzenad, A. El-Keyi, F. Lagum, and H. Yanikomeroglu, "3-d placement of an unmanned aerial vehicle base station (UAV-bs) for energy-efficient maximal coverage," *IEEE Wireless Communications Letters*, vol. 6, no. 4, pp. 434–437, 2017.

[16] M. Mozaffari, W. Saad, M. Bennis, and M. Debbah, "Unmanned aerial vehicle with underlaid device-to-device communications: Performance and tradeoffs," *IEEE Transactions on Wireless Communications*, vol. 15, no. 6, pp. 3949–3963, 2016.

[17] R. I. Bor-Yaliniz, A. El-Keyi, and H. Yanikomeroglu, "Efficient 3-d placement of an aerial base station in next generation cellular networks," *IEEE International Conference on Communications (ICC)*, pp. 1–5, 2016.

[18] M. Mozaffari, W. Saad, M. Bennis, and M. Debbah, "Efficient deployment of multiple unmanned aerial vehicles for optimal wireless coverage," *IEEE Communications Letters*, vol. 20, no. 8, pp. 1647–1650, 2016.

[19] E. Kalantari, M. Z. Shakir, H. Yanikomeroglu, and A. Yongacoglu, "Backhaul-aware robust 3d drone placement in 5g+ wireless networks," *IEEE International Conference on Communications Workshops (ICC Workshops)*, pp. 109–114, 2017.

[20] M. Alzenad, A. El-Keyi, and H. Yanikomeroglu, "3d placement of an unmanned aerial vehicle base station for maximum coverage of users with different qos requirements," *IEEE Wireless Communications Letters*, 2017.

[21] S. A. W. Shah, T. Khattab, M. Z. Shakir, and M. O. Hasna, "A distributed approach for networked flying platform association with small cells in 5g+ networks," *IEEE Global Communications Conference (GLOBECOM)*, pp. 1–7, 2017.

[22] E. Kalantari, H. Yanikomeroglu, and A. Yongacoglu, "On the number and 3d placement of drone base stations in wireless cellular networks," *IEEE Vehicular Technology Conference*, pp. 18–21, 2016.

[23] M. Zhu, Z. Cai, D. Zhao, J. Wang, and M. Xu, "Using multiple unmanned aerial vehicles to maintain connectivity of manets," *International Conference on Computer Communication and Networks (ICCCN)*, pp. 1–7, 2014.

[24] J. Lyu, Y. Zeng, R. Zhang, and T. J. Lim, "Placement optimization of UAV-mounted mobile base stations," *IEEE Communications Letters*, vol. 21, no. 3, pp. 604–607, 2017.

[25] D. Yang, Q. Wu, Y. Zeng, and R. Zhang, "Energy trade-off in ground-to-UAV communication via trajectory design," *IEEE Transactions on Vehicular Technology*, 2018.

[26] D. Alejo, J. A. Cobano, G. Heredia, J. R. Martínez-de Dios, and A. Ollero, "Efficient trajectory planning for wsn data collection with multiple UAVs," *Cooperative Robots and Sensor Networks*, pp. 53–75, 2015.

[27] C. Wang, F. Ma, J. Yan, D. De, and S. K. Das, "Efficient aerial data collection with UAV in large-scale wireless sensor networks," *International Journal of Distributed Sensor Networks*, vol. 11, no. 11, p. 286080, 2015.

[28] C. Zhan, Y. Zeng, and R. Zhang, "Energy-efficient data collection in UAV enabled wireless sensor network," *IEEE Wireless Communications Letters*, 2017.

[29] H. Shakhatreh, A. Khreishah, J. Chakareski, H. B. Salameh, and I. Khalil, "On the continuous coverage problem for a swarm of UAVs," *IEEE Sarnoff Symposium*, pp. 130–135, 2016.

[30] R. Miller, "Hurricane katrina: Communications & infrastructure impacts," *National Defense University*, 2006.

[31] F. F. Townsend *et al.*, "The federal response to hurricane katrina: Lessons learned," *The White House, Washington, D.C.*, 2006.

[32] E. M. Noam, "What the world trade center attack has shown us about our communications networks," *Global Economy and Digital Society*, pp. 375–378, 2004.

[33] I. Dalmasso, I. Galletti, R. Giuliano, and F. Mazzenga, "Wimax networks for emergency management based on UAVs," *IEEE European Conference on Satellite Telecommunications (ESTEL)*, pp. 1–6, 2012.

[34] T. Ha, "The UAV continuous coverage problem," *Defense Technical Information Center Document*, 2010.

[35] J. Wu, "Collaborative mobile charging and coverage," *Journal of Computer Science and Technology*, vol. 29, no. 4, pp. 550–561, 2014.

[36] L. D. P. Pugliese, F. Guerriero, D. Zorbas, and T. Razafindralambo, "Modelling the mobile target covering problem using flying drones," *Optimization Letters*, pp. 1–32, 2015.

[37] D. Zorbas, T. Razafindralambo, F. Guerriero *et al.*, "Energy efficient mobile target tracking using flying drones," *Procedia Computer Science*, vol. 19, pp. 80–87, 2013.

[38] E. T. Ceran, T. Erkilic, E. Uysal-Biyikoglu, T. Girici, and K. Leblebicioglu, "Optimal energy allocation policies for a high altitude flying wireless access point," *Transactions on Emerging Telecommunications Technologies*, 2016.

[39] L. Gupta, R. Jain, and G. Vaszkun, "Survey of important issues in UAV communication networks," *IEEE Communications Surveys and Tutorials*, vol. 18, no. 2, pp. 1123–1152, 2016.

[40] R. E. Korf, "A new algorithm for optimal bin packing," *National Conference on Artificial Intelligence and Innovation Applications of Artificial Intelligence (AAAI/IAAI)*, pp. 731–736, 2002.

[41] D. S. Johnson and L. A. McGeoch, "The traveling salesman problem: A case study in local optimization," *Local search in combinatorial optimization*, vol. 1, pp. 215–310, 1997.

[42] M. Wannberg, "The quadrotor platform: from a military point of view," *Swedish Defense Material Administration*, 2012.

[43] R. D'Andrea, "Guest editorial can drones deliver?" *IEEE Transactions on Automation Science and Engineering*, vol. 11, no. 3, pp. 647–648, 2014.

[44] Sentinel, "SENTINEL+ Drone." [Online]. Available: http://www.airbornedrones.co/ (Accessed on May 12, 2016).

[45] H. Shakhatreh, A. Khreishah, and I. Khalil, "Indoor mobile coverage problem using UAVs," *IEEE Systems Journal*, 2018.

[46] H. Shakhatreh, A. Khreishah, and B. Ji, "Providing wireless coverage to high-rise buildings using UAVs," *IEEE International Conference on Communications (ICC)*, 2017.

[47] H. Shakhatreh, A. Khreishah, A. Alsarhan, I. Khalil, A. Sawalmeh, and N. S. Othman, "Efficient 3d placement of a UAV using particle swarm optimization," *IEEE International Conference on Information and Communication Systems (ICICS)*, pp. 258–263, 2017.

[48] A. Al-Hourani, S. Kandeepan, and A. Jamalipour, "Modeling air-to-ground path loss for low altitude platforms in urban environments," *IEEE Global Communications Conference (GLOBECOM)*, pp. 2898–2904, 2014.

[49] Ericsson, "Ericsson report Optimizing the indoor experience." [Online]. Available: https://www.ericsson.com/res/docs/2013/real-performance-indoors.pdf (Accessed on October 23, 2016).

[50] Nokia, "In-Building Wireless: One Size does not fit all." [Online]. Available: https://insight.nokia.com/infographic-building-wireless-all (Accessed on October 23, 2016).

[51] Cisco, "Cisco Service Provider Wi-Fi: A Platform for Business Innovation and Revenue Generation." [Online]. Available: https://www.cisco.com/c/en/us/solutions/collateral/service-provider/service-provider-wi-fi/solution_overview_c22_642482.html (Accessed on October 23, 2016).

[52] H. R. Facilities, “Using High-Power DAS in High-Rise Buildings.” [Online]. Available: highrisefacilities.com/using-high-power-das-in-high-rise-buildings/ (Accessed on August 18, 2017).

[53] Amplitic, “Coverage Solution for High-rise Building.” [Online]. Available: https://www.amplitec.net/products-2-coverage-solution-for-high-rise-building.html (Accessed on October 23, 2016).

[54] S. Zhang, Z. Zhao, H. Guan, and H. Yang, “Study on mobile data offloading in high rise building scenario,” *IEEE Vehicular Technology Conference (VTC Spring)*, pp. 1–5, 2016.

[55] M. Series, “Guidelines for evaluation of radio interface technologies for imt-advanced,” *International Telecommunication Union Report*, no. 2135-1, 2009.

[56] T. Imai, K. Kitao, N. Tran, N. Omaki, Y. Okumura, and K. Nishimori, “Outdoor-to-indoor path loss modeling for 0.8 to 37 ghz band,” *IEEE European Conference on Antennas and Propagation (EuCAP)*, pp. 1–4, 2016.

[57] J. L. Bentley and R. Sedgewick, “Fast algorithms for sorting and searching strings,” *ACM-SIAM symposium on Discrete algorithms*, pp. 360–369, 1997.

[58] R. S. Sutton and A. G. Barto, “Reinforcement learning: An introduction,” *MIT Press, Cambridge, MA*, vol. 1, no. 1, 1998.

[59] J. Kennedy and R. Eberhart, “Particle swarm optimization,” *IEEE International Conference on Neural Networks*, vol. 4, pp. 1942–1948, 1995.

[60] M. Clerc and J. Kennedy, “The particle swarm-explosion, stability, and convergence in a multidimensional complex space,” *IEEE transactions on Evolutionary Computation*, vol. 6, no. 1, pp. 58–73, 2002.

[61] R. Feick, M. Rodríguez, L. Ahumada, R. A. Valenzuela, M. Derpich, and O. Bahamonde, “Achievable gains of directional antennas in outdoor-indoor propagation environments,” *IEEE Transactions on Wireless Communications*, vol. 14, no. 3, pp. 1447–1456, 2015.

[62] J. A. Hartigan and M. A. Wong, “Algorithm as 136: A k-means clustering algorithm,” *Journal of the Royal Statistical Society. Series C (Applied Statistics)*, vol. 28, no. 1, pp. 100–108, 1979.

[63] H. Shakhatreh, A. Khreishah, N. S. Othman, and A. Sawalmeh, “Maximizing indoor wireless coverage using UAVs equipped with directional antennas,” *IEEE Malaysia International Conference on Communications (MICC)*, pp. 175–180, 2017.

[64] A. Ö. Kaya and D. Calin, “On the wireless channel characteristics of outdoor-to-indoor lte small cells,” *IEEE Transactions on Wireless Communications*, vol. 15, no. 8, pp. 5453–5466, 2016.

[65] E. G. Birgin, J. Martınez, and D. P. Ronconi, "Optimizing the packing of cylinders into a rectangular container: a nonlinear approach," *European Journal of Operational Research*, vol. 160, no. 1, pp. 19–33, 2005.

[66] M. Hifi and R. M'hallah, "A literature review on circle and sphere packing problems: Models and methodologies," *Advances in Operations Research*, vol. 2009, 2009.

[67] H. Shakhatreh and A. Khreishah, "Optimal placement of a UAV to maximize the lifetime of wireless devices," *IEEE International Wireless Communications and Mobile Computing Conference*, 2018.

[68] Y. Zeng, R. Zhang, and T. J. Lim, "Throughput maximization for mobile relaying systems," *IEEE Globecom Workshops (GC Wkshps)*, pp. 1–6, 2016.

[69] A. Kwasinski, P. L. Chapman, P. Krein, W. Weaver *et al.*, "Hurricane katrina: damage assessment of power infrastructure for distribution, telecommunication, and backup." *Grainger Center for Electric Machinery and Electromechanics. Technical Report.*, 2006.

[70] T. Taniguchi, Y. Karasawa, and N. Nakajima, "Effect of coordinated base station in uplink transmission under disaster cells," *International Conference on Selected Topics in Mobile and Wireless Networking (iCOST)*, pp. 83–88, 2012.

[71] T. Simon, A. Goldberg, and B. Adini, "Socializing in emergencies: A review of the use of social media in emergency situations," *International Journal of Information Management*, vol. 35, no. 5, pp. 609–619, 2015.

[72] H. He, S. Zhang, Y. Zeng, and R. Zhang, "Joint altitude and beamwidth optimization for UAV-enabled multiuser communications," *IEEE Communications Letters*, vol. 22, no. 2, pp. 344–347, 2018.

[73] M. Mozaffari, W. Saad, M. Bennis, and M. Debbah, "Mobile unmanned aerial vehicles (UAVs) for energy-efficient internet of things communications," *IEEE Transactions on Wireless Communications*, vol. 16, no. 11, pp. 7574–7589, 2017.

[74] A. Fotouhi, M. Ding, and M. Hassan, "Dynamic base station repositioning to improve spectral efficiency of drone small cells," *IEEE International Symposium on A World of Wireless Mobile and Multimedia Networks (WoWMoM)*, pp. 1–9, 2017.

[75] P. Scerri, R. Glinton, S. Owens, D. Scerri, and K. Sycara, "Geolocation of rf emitters by many UAVs," *Aerospace Conference (AIAA)*, p. 2858, 2007.

[76] M. Hasanzade, O. Herekoglu, N. K. Ure, E. Koyuncu, R. Yeniceri, and G. Inalhan, "Localization and tracking of rf emitting targets with multiple unmanned aerial vehicles in large scale environments with uncertain transmitter power," *International Conference on Unmanned Aircraft Systems (ICUAS)*, pp. 1058–1065, 2017.

[77] O. Kariv and S. L. Hakimi, “An algorithmic approach to network location problems. i: The p-centers,” *SIAM Journal on Applied Mathematics*, vol. 37, no. 3, pp. 513–538, 1979.

[78] A. Suzuki and Z. Drezner, “The p-center location problem in an area,” *Location science*, vol. 4, no. 1-2, pp. 69–82, 1996.

[79] S. Boyd and L. Vandenberghe, “Convex optimization,” *Cambridge University Press, Cambridge*, 2004.

[80] V. Krishnamurthy, “Partially observed markov decision processes,” *Cambridge University Press, Cambridge*, 2016.

[81] A. Al-Hourani, S. Kandeepan, and S. Lardner, “Optimal lap altitude for maximum coverage,” *IEEE Wireless Communications Letters*, vol. 3, no. 6, pp. 569–572, 2014.

[82] J. Holis and P. Pechac, “Elevation dependent shadowing model for mobile communications via high altitude platforms in built-up areas,” *IEEE Transactions on Antennas and Propagation*, vol. 56, no. 4, pp. 1078–1084, 2008.

[83] D. P. Bertsekas and J. N. Tsitsiklis, “Parallel and distributed computation: numerical methods,” *Prentice hall Englewood Cliffs, NJ*, vol. 23, 1989.

[84] R. M. Karp, “Reducibility among combinatorial problems,” *Complexity of computer computations*, pp. 85–103, 1972.

[85] G. Rushton *et al.*, “Optimal location of facilities,” *COMPress Wentworth, NH*, 1979.